School of Mines: Minerals, Energy and Chemical Engineering

Detection of Solids in a Flow Stream Using Ultrasonics and Advanced Algorithms

Hossein Seraj
0000-0003-4580-2026

This thesis is presented for the Degree of
Doctor of Philosophy
of
Curtin University

October 2021

Declaration

To the best of my knowledge and belief this thesis contains no material previously published by any other person except where due acknowledgment has been made. This thesis contains no material which has been accepted for the award of any other degree or diploma in any university.

Name: Hossein Seraj

Signature: Date: Oct. 2021

Abstract

Sand production is one of the most commonly encountered issues in gas wells. Production of sand from a gas reservoir can cause several problems to the downhole equipment, well head equipment and downstream facilities. The problems range from erosion issues in various components, to damage to the reservoir, reduction of production, and risk of leakage from the pipelines. In extreme cases, the erosion caused by the sand can put the integrity of the pipelines and equipment in jeopardy (exemplified by the explosion on Varanus Island).

In order to mitigate side effects of sand production from gas wells, various sand control techniques are considered by industry to eliminate production of sand as much as possible. Alternatively, different sand management techniques might be used to limit the sand production and to reduce/manage the effects.

In order to be able to apply sand control/sand management techniques, proper measurement of sand is vital. Nowadays, Acoustic Sand Detectors (ASDs) are widely used for sand measurement purposes. Operators of ASDs have several concerns about the accuracy of sand flow rate measurement using these devices. Therefore this research was conducted to find a way to both improve the accuracy of commercial ASDs and find an alternative approach to measure sand flow rate.

The first aim of this research was to improve the accuracy of sand flow rate measurement using ASD devices and their test results obtained from an experimental flow loop test facility at Curtin University. In the flow loop test, sand production along a gas pipeline was used to mimic different gas-sand mixtures in a pipeline, simulating various fluid velocities and sand flow rates. An ASD sensor and temperature/velocity sensors were installed in the flow loop and their information was gathered by the computer system for further processing and analysis. By comparing the results obtained from various tests using this flow loop, it was initially observed that one method of analysis demonstrated much more accurate results for predicting the sand flow rate using a commercial ASD, so an algorithm was developed to accurately estimate the sand flow rate using its raw data. It is shown that the suggested algorithm improves the accuracy of sand flow rate at least ten times greater than other algorithms suggested by the suppliers of ASDs as well as those suggested by other researchers.

The second aim of this research was to use ultrasonic sensors for sand flow rate measurement and to apply various signal processing methods to this data to obtain a methodology to measure sand flow rate. In this research, an ultrasonic sensor and a suitable data acquisition (DAQ) system were also installed in the flow loop test facility and the sampled signal collected on a PC. Then, the Fast Fourier Transform (FFT) method was applied to the signals and the FFT curves then smoothed using a Savitzky-

Golay filter. This research shows that the peak value of the FFT curve at 10-50 kHz has a relationship with the sand flow rate. Since this method uses a peak value in a defined frequency range, the interference from noise in other frequency ranges can be minimised. Using the frequency domain instead of the time domain to measure sand flow rate is a new approach.

To further analyse the ultrasonic signals, a discrete wavelet transform (DWT) was used. The transform converts ultrasonic signal in the time domain to a series of coefficients. Each coefficient represents the strength of the signal over a certain frequency range. In this research, it is shown that the strength of the signal in the frequency range from 15.625 kHz to 62.5 kHz has a linear relationship with the sand flow rate.

I also used the Welch method to analyse the signal from ultrasonic sensors. The Welch method divides the signal into various segments and then calculates the average of the squared FFT for the various segments. It was found that there was a linear relationship between the Power Spectral Density (PSD) obtained using the Welch method and the sand flow rate.

This research improves the operation of gas facilities by improving the accuracy of sand flow rate measurement using an ASD. Since the ASD used in this experiment is commonly used in a wide range of gas facilities worldwide, applying this new algorithm can improve the accuracy within many global gas processing installations. Since applying this algorithm only requires minor modifications to the control system where the sand flow rate is calculated, so the application of this algorithm is expected to greatly enhance the operation of gas facilities without demanding major changes to the system.

Consequently this research provided three different techniques (i.e., using FFT, DWT and Welch methods) with greater accuracy to estimate the sand flow rates using simple ultrasonic sensors, which is new knowledge.

Acknowledgements

First of all, I would like to express my gratitude to my supervisors Prof. Brian Evans and Dr. Mohammad Sarmadivaleh for their continuous support for this research. Prof. Brian has continuously supported me during this research and provided valuable advice. Dr. Mohammad Sarmadivaleh has also supported me a lot in the recent years.

Also I acknowledge the support of my previous supervisor Prof. Mohammad Serkat Masoum in the early stages of this research.

I am thankful to Dr. Masood Mostofi for his support during my lab experiments.

To

My parents

My wife

My children

Publications

The following publications were developed from this research:

1- H.Seraj and B.Evans, *Improving Sand Flow Rate Measurement using Ultrasonic Spectral Analysis and filtering.* IET Science, Measurement & Technology, 2020, https://10.1049/iet-smt.2019.0479

2- H.Seraj, B.Evans, M.Sarmadivaleh, *Improving Sand Flow Rate Measurement Using the Wavelet Transform*, International Journal on Smart Sensing and Intelligent Systems, 2021, https://doi.org/10.21307/ijssis-2021-001

It can be noted that the Journal of IET Science, Measurement & Technology (where the first paper is published) has an impact factor of 1.975 (IET Digital Library: IET Science, Measurement & Technology (theiet.org)). Also the International Journal on Smart Sensing and Intelligent Systems (where the second paper is published) has an impact factor of 1.24 (International Journal on Smart Sensing and Intelligent Systems Impact Factor | Resurchify).

Contents

List of Figures

List of Tables

Nomenclature

Greek letters

M	Reading from Acoustic Sand Detector (ASD)
h	Erosion rate
V	Fluid velocity
Z	Factor representing background noise
M	ASD reading
W	Sand mass flow rate
D	Mean diameter of sand particles
D_p	Diameter of the pipe/equipment
ρ_m	Fluid density
V_p	Particle Velocity
Q	Sand volumetric flow rate
P	Peak value of smoothed FFT curve
f_{max}	Maximum frequency of sending laser pulses through fiber optic cable
v_{fiber}	Velocity of light in the fiber optic cable
$l_{up/down}$	Total length of light travel in the fiber optic cable
l_{fiber}	Length of fiber optic cable
v_{light}	Velocity of light in vacuum (3 x 10^3 m/s)
n_{index}	Refractive index of fiber optic cable

Abbreviations

AFG	Arbitrary Function Generator
ASD	Acoustic Sand Detector
A/D	Analog to Digital
DA	Data Access
DAQ	Data Acquisition
DAS	Distributed Acoustic Sensing
DFT	Discrete Fourier Transform
DWT	Discrete Wavelet Transform
EP	Erosion Probe
FFT	Fast Fourier Transform
GUI	Graphic User Interface
HWS	Hierarchical Waveform Storage
OPC	Open Platform Communication
PC	Personal Computer
PSD	Power Spectral Density
VSD	Variable Speed Drive

1 Introduction

1.1 Problem statement

When gas and condensate is produced from an offshore or land-based gas reservoir, some sand may also be produced from the reservoir. Production of such solid particles creates many problems, which affect both downhole/subsea equipment and surface/topside equipment.

Problems in downhole/subsea equipment due to sand production can be in the form of formation damage, a decrease in the production due to well sand-up, erosion of downhole/subsea equipment and damage to the sand controlling equipment (e.g. sand screen), higher corrosion rate, an increased demand for inhibitors (e.g. corrosion inhibitor), higher safety risks due to erosion/equipment damage, increased cost/demand for work-overs, etc. [1, 2].

Damage to a formation can for example be caused by creation of a cavity behind the casing of a sand screen due to sand production from the reservoir and subsequent collapse of the formation after this cavity expands [2]. Sand production from a formation section can also cause formation “sanding-up” of the well in which the sand accumulates in the wellbore and stops production of the well which in the worse cases, may cause abandonment of the well [3].

Issues in the topside/surface equipment can result from a high corrosion rate, increasing the maintenance and operation costs (e.g. for sand removal/disposal) [4][2], plugging of the equipment, increased demand for inhibitor (e.g. corrosion inhibitor to protect against extra corrosion due to sand production), extra capital costs to install sand removal facilities (e.g. de-sander, etc.), reduced production (e.g. due to inefficiencies in separator handling, etc.), damage to pipe/equipment due to higher erosion rates, and increased safety risks caused by erosion/damage from sand production [1]. Also the production of solid particles can cause plugging/fouling of surface production equipment such as separators. The sand can also deposit in the pipelines, which may also reduce or stop production.

In subsea applications, due to the high cost of completion/etc., any damage due to sand production is of major concern [5].

Currently Acoustic Sand Detectors (ASD) are used widely in the industry. The output data from an ASD is affected by noise from mechanical equipment (e.g. pumps, compressors) and also noise created due to the passage of the gas through pipes/valves (e.g. the noise produced from the choke valve in the wellhead). Also the reading of an ASD depends on other factors such as installation location.

Consequently, an accurate reading from an ASD is highly dependent on its correct calibration [6]. There are a lot of concerns about the accuracy of commercial ASDs on the market. Therefore this research was conducted to find a way to both improve the accuracy of the commercial ASDs in the market and find an alternative approach to accurately measuring the sand flow rate.

Since commercial ASDs provide a limited amount of useful data (since they have an embedded microprocessor which performs preliminary calculations in the ASD), it is not possible to apply various signal processing techniques to their output. Therefore in addition to the research for improving the accuracy of commercial ASD, I have used ultrasonic sensors to measure sand flow rate. So an ultrasonic circuit including an ultrasonic sensor, amplifier, data acquisition system and computer was used to obtain the acoustic signal received from the impact of sand particles on a pipe wall. Then various signal processing methods were used to analyse these signals.

1.2 Objectives

The following were the objectives of this research:

1- Literature review of related research in the area of sand flow measurement.
2- Establish a laboratory setup of the flow loop test facility by connecting the ASD to a respective laptop and connecting this laptop to a main PC. Then read the output signal of an ASD using Matlab software. Also connect the temperature/velocity sensor to the main PC using a *National Instruments* data acquisition unit (USB-6009) and collect the temperature/velocity data on the main PC.
3- Perform flow loop tests at various sand flow rates, sand particle sizes and air velocities in order to obtain the signals from the ASD, and temperature/velocity sensors under these test conditions.
4- Analyse the data from each flow loop test. The aim was to obtain a relationship to improve the prediction of sand flow rate using an ASD. Such a relationship must have a lower standard deviation between the actual sand flow rate and the sand flow rate prediction compared with any relationship proposed by other researchers.

5- Setup a new test measurement method using *National Instruments* data acquisition hardware and ultrasonic sensor and to obtain the reading of an acoustic sensor at various sand flow rates, air velocities and sand particle sizes.
6- Perform these experiments at various sand flow rates and fluid velocity to obtain ultrasonic sensor data using mentioned data acquisition system.
7- Apply FFT signal processing methods to ultrasonic data and find any relationship between the FFT signal and the sand flow rate.
8- Apply other data analysis methods such as the Discrete Wavelet Transform (DWT) and the Welch signal processing techniques. Also to find any relationship between the discrete wavelet transform coefficients (obtained by the DWT method) or the Power Spectral density (obtained by the Welch method) and the sand flow rate.

It should be noted that the original objectives of this research were those of items 1 to 4 above (which used an ASD to measure sand flow rate). Due to progress in this research, objectives 5 to 8 (using ultrasonic sensors to measure sand flow rate) were added as the research developed.

In brief, the original objective of the research was to improve the accuracy of sand measurement using a commercial ASD, which in turn could improve estimation of sand flow rate passing along pipelines from a gas field. It could help operators to follow sand control/sand measurement strategies more precisely and make better decisions about sand production.

Also the overall objective of the additional steps (items 5 to 8) was to measure sand flow rate using ultrasonic sensors. This would help to understand the relationship between the ultrasonic sensor output and the sand flow rate. Three different signal processing techniques (i.e., FFT, DWT and Welch) were eventually tested.

1.3 Significance of study

Due to various concerns with sand production causing erosion of equipment, several operating companies have a comprehensive procedure for sand control/sand management.

Conventionally in cases of sand control where the operator tries to prevent sand production using a suitable sand exclusion technique, there is a need to detect any sudden increase in sand production during field operations. This sudden increase can be a sign of the failure of sand control equipment. For example, in the case of a sand screen failure, the operator must quickly identify any increase in

sand production and reduce the production or shutdown the affected well in order to protect the wellhead equipment from excessive wear.

Also in the case of sand management techniques where small amounts of sand production are allowed in the field, it is vital to measure the sand flow rate to make sure that the produced sand rate is less than the maximum allowable sand rate as per the sand management philosophy.

In both of these cases, it is very important to have a trustworthy sand measurement device. As a commercial ASD is one of the most commonly used devices for sand measurement, this research focuses on improving the accuracy of sand measurement using a typical ASD device. As reported, there are many concerns with trusting the accuracy of a reading from an ASD [7]. Therefore improving the measurement using an ASD device can help to improve proper implementation of sand control/sand measurement techniques in order to prevent adverse effects caused by inaccurate readings of ASD devices.

In this research, I have tried to improve the accuracy of sand flow rate measurement using an ASD provided by a commonly used supplier, since an improved relationship to accurately estimate sand flow rate using such an ASD device would improve many situations where it is used.

In building this laboratory flow loop, I also setup a data acquisition system to read the ultrasonic signals created by the impact of sand particles in the pipeline. Using signal analysis methods (e.g. FFT), the data obtained from the ultrasonic sensors was analysed to find a relationship between the sand flow rate and ultrasonic signals.

Using ultrasonic sensors (instead of commercial ASDs) for measuring sand flow rate provides an economic option to the operator of any gas fields. In addition, using ultrasonic sensors enables engineers to apply various signal processing techniques for sand flow rate measurement (which is not typically possible with the commercial ASDs).

1.4 Overview

Production of gas from an unconsolidated formation or poorly consolidated formation may cause production of sand along with the gas. The production of sand is due to the drag force created by the gas fluid [8].

The gas which is produced from gas wells can consequently contain a large amount of sand, so that movement of sand from a gas reservoir through the downstream production facility can potentially create a lot of equipment issues. These issues include damage to the reservoir, erosion of well bore/well head/pipelines and the accumulation of sand in the well/downstream facilities.

Equipment erosion which is the major issue resulting from sand production occurs due to the repetitive impact of sand particles on the pipe/equipment internal walls. Higher level sand erosion may happen in the valves, chokes, pipe bends, reducers, etc. Erosion can cause leakage of gas and in extreme cases, it causes failure of the equipment/pipes [9]. Accumulation of the sand is another major issue resulting from sand production. In the case of sand accumulation in a wellbore, the gas/oil production may be reduced/stopped which may necessitate using expensive methods for sand removal.

Due to such difficulties with sand production, various methods of sand control and sand management are used. In order to identify whether a sand control method may work properly or to apply sand management techniques correctly, the sand flow rate in the gas field is measured. Such measurements are performed using various instruments such as an Acoustic Sand Detector (ASD). It is reported that measurement with such devices has a lot of uncertainties. For instance, it is reported that poor confidence in the accuracy of sand measurement devices is a major concern when applying sand management techniques [7]. In order to reduce such concerns, this research attempted to identify and improve the characteristics (e.g. accuracy) of sand flow measurement using an Acoustic Sand Detector.

1.5 Thesis Organization

The first chapter of this thesis serves as introductory to this thesis and includes the overview, problem statement, objectives, significance of the study, and thesis organisation.

The second chapter includes a background review of this thesis. In this chapter, previous research in the area of sand flow measurement is highlighted and the required background information for performing this research is mentioned.

The third chapter of the thesis is devoted to a methodology for performing tests using a flow loop test facility. Various parts of the flow loop are explained, and the efforts to repair a defunct existing flow loop to a level consistent with performing this research is explained. Then the procedure to sieve sand particles and develop a test matrix used for checking an ASD is specified.

The fourth chapter is devoted to explaining the use of an ultrasonic sensor and signal processing techniques. Attempts to use ultrasonic sensors to read the acoustic signal created by sand particles are mentioned in this chapter. Also various signal processing techniques to analyse the data collected from an ultrasonic sensor is explained. Three processing techniques being the Fast Fourier Transform (FFT), the Discrete Wavelet Transform (DWT) and the Welch method are explained. This chapter also explains the results obtained from applying these signal processing methods to measure sand flow rate.

The fifth chapter is devoted to the results of this research. In this chapter, first the results of using different relationships to predict sand flow rate from an ASD reading is mentioned. Then these results are compared and the best relationship to predict sand flow rate using an ASD is specified. Then the results of using an ultrasonic sensor for sand flow measurement is highlighted. The results of using the three different techniques (i.e., FFT, DWT and Welch methods) to analyse the ultrasonic signals are then provided. Also the accuracies of sand flow rate measurement using these three different techniques are compared.

The sixth chapter concludes the results obtained in this research, and provides recommendations for further research.

1.6 Summary of Chapter

At the end of each chapter, these is a summary of that chapter, which provides a final overview of that chapter's contents and discusses the next steps.

This first chapter is devoted to the introduction of this research in sand flow measurement. After providing the overview and problem statement, the objectives of this research were defined. The significance of this study is mentioned, and the chapter concludes with the thesis structure. In the next chapter, I present a review of literature associated with this research.

2 Literature review

2.1 Introduction

In this chapter, a background review of sand measurement is provided. Various issues with sand production in oil and gas pipelines are mentioned. Various methods to eliminate or reduce sand production in oil and gas wells are reviewed. Then various types of instruments to measure sand production are explained. Also ultrasonic sensors which are used in this research for measuring sand flow rate are discussed. In this research, I have applied various signal processing techniques for analysing the ultrasonic signal, which is the reason I review various signal processing methods. It should be noted that various topics mentioned in this chapter are provided as a background review for this research. This does not mean that all of the topics mentioned in this chapter are used in this research, but rather that they are provided in order to have a more comprehensive background review in the area of sand flow rate measurement.

2.2 Concerns associated with sand production

Production of sand from oil and gas wells may potentially cause various issues which can be in the following forms:

- Reducing output in oil and gas production: This happens in the case where the sand produced by oil and gas wells are not completely transported with the oil/gas, when some portion of the sand accumulates in the producing well causing reduction in the production of oil and gas [10]. In the worst case, it may block the production of oil and gas due to sand build-up in the well. To remove such blockages, wireline clearing may be needed [11].
- Operational issues with the downstream facility: When sand is transported to downstream facilities (e.g. refineries, gas/LNG processing facilities), it will create several operational issues. For example, in cases where it accumulates in the separators, it will adversely affect their functionality. In several cases where automated sand removal features are not considered for these separators, operators need to clean-up the separators by opening them and removing the sand. For doing such vessel cleaning, the operators need to temporarily take each

particular separator out of operation to open them. Therefore, such operations may increase economic cost or may reduce the up-time of the facility/separator. Also in several modern downstream facilities, more automated sand removal features are used for the incoming separators. Adding such sand removal features to separators can increase the capital cost of the plant. Figure 2-1 shows the case where sand has accumulated in a downstream vessel [12].

Figure 2-1: An example of accumulation of sand in downstream facility inside a vessel [12]

Also sand particles could settle in the production pipeline, especially when the velocity of the fluid is relatively low. In this case, there might be a need for frequent pigging of the pipelines to remove settled sands [13]. During the pigging process, a pig (a mechanical device) is inserted into the pipe. The pig travels with the fluid and can perform various activities such as cleaning, inspection, etc. Performing pigging will add operational costs. In addition, it necessitates using a pig launcher and a pig receiver in the facility which increases the CAPEX of the project.

- Collapse of the formation: Production of sand from a reservoir might increase the potential for reservoir or wellbore collapse [14]. For instance, it may cause collapse of the sand arches

in the reservoir. Arches are the hemispherical shape collection of sand grains which are created in the reservoir [15]. This may cause changes/issues in the reservoir (such as changing the permeability). Excessive sand production can create a cavitation in the reservoir. After this cavitation is getting bigger overtime due to further sand production, the same may collapse and the sand particles from surrounding area of the reservoir fill the cavity. Collapse of the reservoir near well bore may decrease the permeability of the reservoir, especially in the reservoirs with higher amount of fine sand particles (clay) or wide range of sand particle size [16]. The reduction in the permeability decreases the hydrocarbon production from the well [16]. Figure 2-2 shows the case where sand production causes creation of a void (cavitation) behind the casing [15].

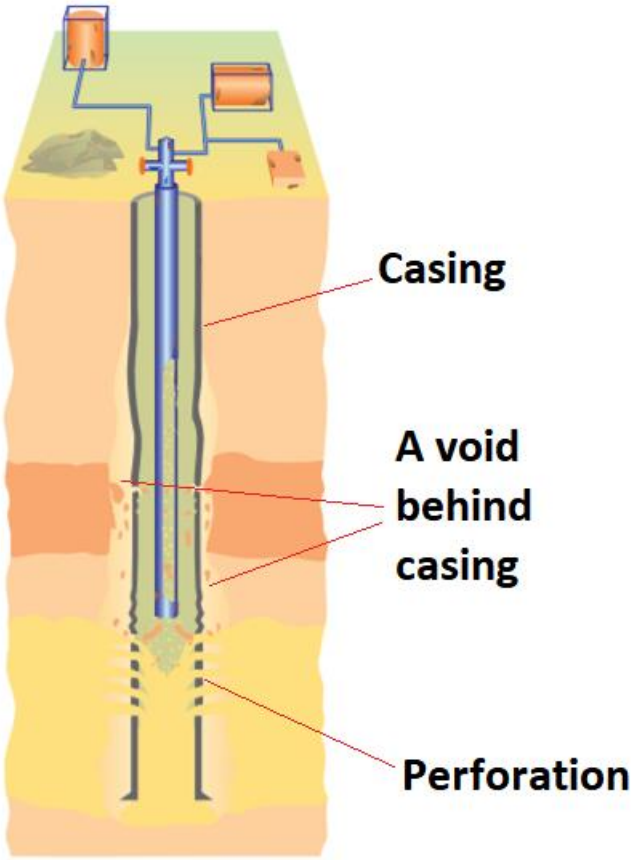

Figure 2-2: creation of a void due to sand production [15]

- Erosion: Sand production can cause erosion in the wellbore/wellhead and transportation pipelines. This erosion can cause malfunction of the equipment (e.g. a choke valve). Figure 2-3 shows an example of erosion in the internal parts of a choke valve [17].

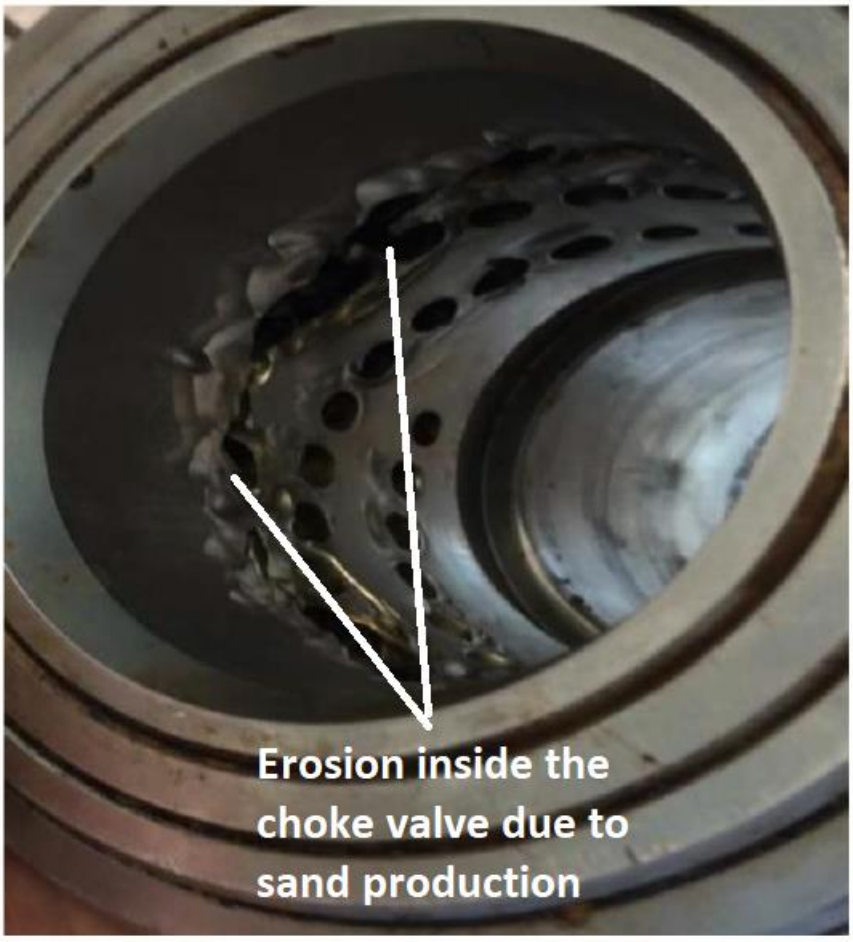

Figure 2-3: An example of erosion of internal part of choke valve due to sand production [17]

In extreme cases, severe erosion may cause rupture of the pipes which hold high pressure oil and gas products. In the industry, rupture of such equipment which hold high-pressure fluid is called a "*loss of containment*". This may cause a catastrophic event such as an explosion, as well as major damage to the environment, etc. Figure 2-4 shows an example of loss of containment where the pipe holding the pressure is eroded due to sand production [2]. This picture shows a weld neck flange which used to connect a pipe to an adjacent equipment. Due to sand production, a rupture is created in this pipe/weld neck flange.

Figure 2-4: An example of loss of containment due to sand erosion [2]

Figure 2-5 shows an example of failure of the downhole (wire-wrapped sand screen) equipment due to sand production [18].

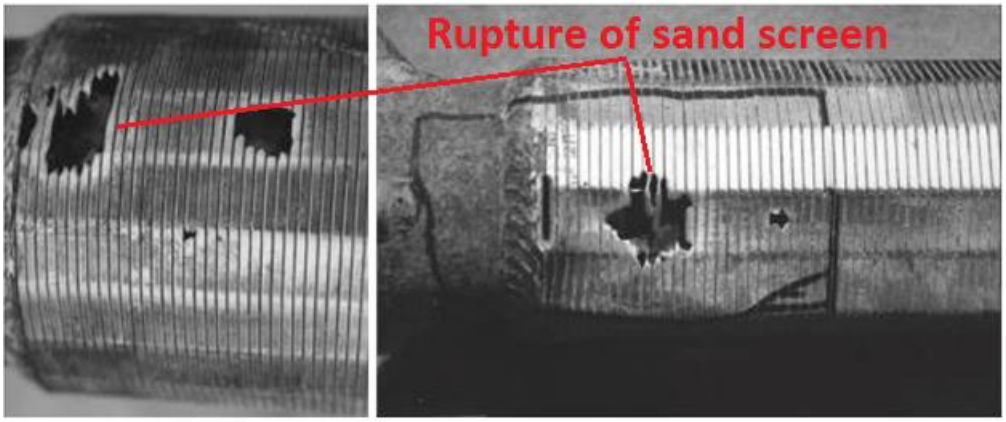

Figure 2-5: Failure of downhole (wire-wrapped sand screen) due to sand production [18]

2.3 Sand Control/Management philosophy

Since production of sand in gas wells creates several issues, this research focuses on sand production from gas wells. Various techniques are used to eliminate or minimize the production of sand or to reduce its adverse effects. These techniques can be divided into two main categories which are sand control/exclusion techniques and sand management techniques [19].

In the sand control/exclusion categories, the purpose is to eliminate or minimize the production of sand to the extent possible by using various well completion methodologies [20]. For doing so,

traditionally gravel packs or sand screens are used [21]. Furthermore, newer sand consolidation methodologies such as high energy resin placement can be used to reduce/eliminate the production of the sand from the gas reservoir [22].

The other technique to minimize the effect of sand production is the sand management technique [19]. In this group of methods, the operator allows a limited amount of sand to be produced from a gas well but tries to minimize the adverse effect of sand production to control it [23]. In this category, it is necessary to estimate/quantify various effects of the sand production in the wellbore and downstream facilities. Also, suitable precautions for sand production may be considered. For example, the amount of erosion is measured at a few points and a suitable thickness of pipe/equipment with an adequate amount of erosion allowance is considered in its physical thickness. Furthermore, a suitable method for separating and gathering sand from production fluid (e.g. de-sander [24] or a sand removal provision [25]) is considered in the downstream facilities.

When using sand prevention methods, signals obtained from different sand measurement instruments like an Acoustic Sand Detector (ASD) can be used to check whether the sand prevention devices are working perfectly [2]. For instance, if a sand screen is used as a sand prevention technique, then an abrupt increase in the signal in an acoustic sand detector might be a signal that the sand screen in the well has failed. Therefore, it is important for any sand measuring device to be able to identify small amounts of sand production to allow identification of any immediate probable failure in sand prevention techniques.

When using sand management techniques, accurate measurement of sand production is very important. The reason for this is that various sand management techniques are based on allowing a certain amount of sand production in the gas field so that any side-effect of sand production is under control. Therefore it is important to accurately know the current amount of sand production to make sure that it is less than the sand rate limit required by the sand management technique.

2.3.1 Sand control techniques

In sand control techniques, the industry tries to prevent sand production in the well [10] by using various sand control techniques. In the following sections, some common types of sand control methods are discussed.

2.3.1.1 Sand Screen

The use of sand screens is one of the common methods of sand prevention in which a circular shape forms of screen of various types may be placed in the wellbore to prevent production of sand particles at the reservoir level. Typical sand screens are as follows:

- Wire wrapped screen: where a wire is wrapped around a perforated layer with metal bars. Figure 2-6 shows a typical arrangement of a wire wrapped sand screen [26]. These screens can be used as a stand-alone or in combination with gravel packing as explained below.

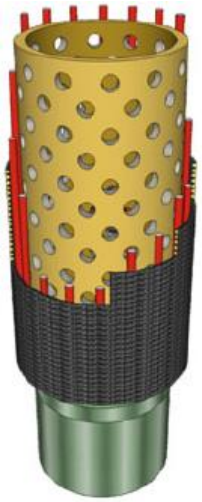

Figure 2-6: Typical make-up of a wire wrapped sand screen [26]

- Pre-packed screen: where gravels are filled between two layers of perforated or wire wrapped screen. Figure 2-7 shows a typical arrangement of a pre-packed sand screen [26].

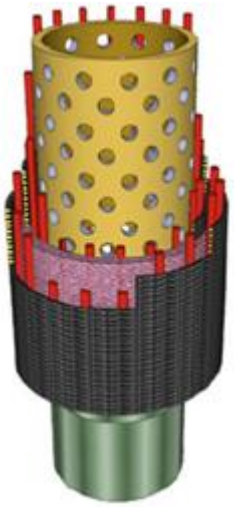

Figure 2-7: Typical make-up of pre-packed sand screen [26]

- Wool wrapped screen: where wool is wrapped between two perforated layers. Figure 2-8 shows a typical arrangement of a wire woollen wrapped screen [26].

Figure 2-8: Typical make-up of wool wrapped screen [26]

- Premium screen: where different layers are provided for sand filtration and protection.

Figure 2-9 shows a typical arrangement of a premium screen [26]. These types of screens are more expensive compared to other methods as various layers of synthetic material are used in this type of screens.

Figure 2-9: Typical make-up of premium screen [26]

2.3.1.2 Slotted liners

Slotted liners are pipes with parallel vertical cuts around their circumference. This type of slotted liner is mostly used for preventing sand production in unconsolidated reservoirs which produce oil with a high viscosity. Figure 2-10 shows different types of slots in a slotted liner plus the completion of a slotted liner along with its gravel pack [26].

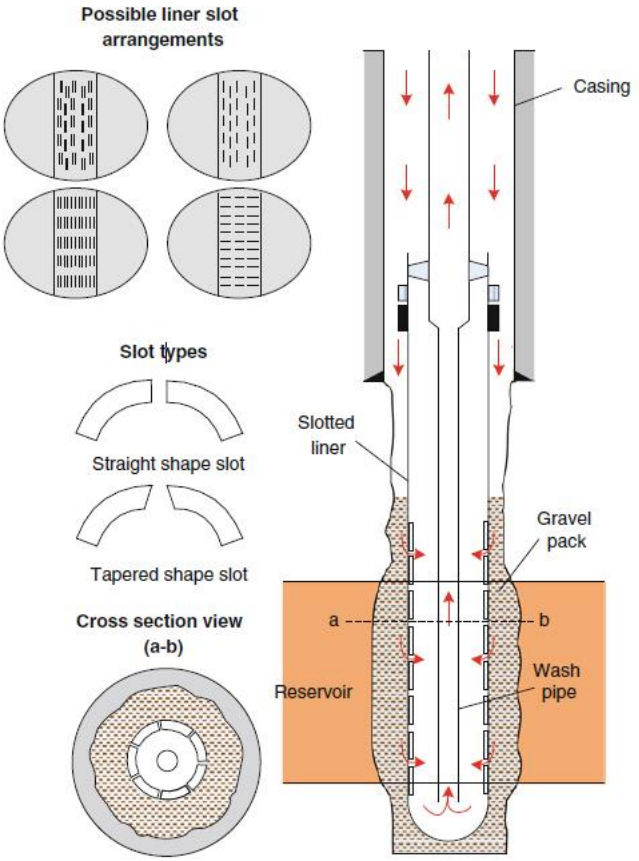

Figure 2-10: Typical make-up of slotted liner [26]

2.3.1.3 Gravel pack

The *Gravel pack* is one of the most commonly used sand control methods [26]. This method is typically used along with a sand screen/slotted liner. Also it can be used as inside-casing gravel packing or as open-hole gravel packing [27]. In the case of inside-casing gravel packing, a slurry with properly sized gravels is injected into the wellbore between the sand screen/slotted liner and the perforated casing. The gravel accumulates behind the sand screen or slotted liner. Also there will be some perforations in the casing. In this case, the production fluid travels through the perforation, *gravel packs* and *sand screen/slotted liner* and up the well. These gravels prevent production of large sand particles as the gravels filters and so hinder movement of the sand particles.

A *gravel pack* can also be of the open-hole type. In case of open-hole gravel packing, the well does not have casing and the gravels are located around the sand screen/slotted liner. In this case, the production fluid (e.g. gas) can enter the well through the gravel pack around the sand screen/slotted liner from all radial directions (360 degrees). Entering of production fluid from 360 degree angles

around the well (compared with narrower angles for inside-casing gravel packing) provides less pressure drop across gravel packing and therefore might assist productivity of gas from a well.

2.3.1.4 Expandable slotted liner

Expandable slotted liners are similar to slotted liners. After these slotted liners are lowered in the well along with drill pipes and placed in a suitable position, they are expanded using a cone shaped ring as shown in Figure 2-11 [26].

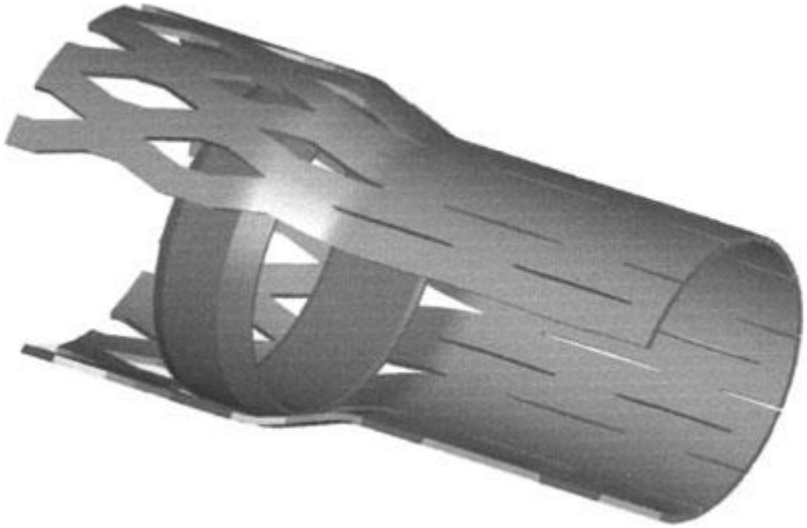

Figure 2-11: Typical slotted liner after expansion [26]

2.3.1.5 Frack and Pack

The *Frack and pack* method is the generic name used for a series of sand completion techniques. This method is used mostly for poorly consolidated reservoirs. The same technique comprises of two stages. First, during completion of the well, a fracture is created in the well bore by creating a pressure above the fracture pressure [8]. Then the same fracture is filled with a proppant component. Filling of the fracture can improve the reservoir stability (e.g. by preventing collapse of the reservoir around the fracture point) and also by preventing the sand production and arrival of sand particles at the wellbore [26].

2.3.1.6 Consolidation methods

During consolidation, cementation (consolidation) is attempted between sand grains in the reservoir around the gas well [8]. By creating such consolidation between sand grains in the reservoir, the sand production rate is reduced. Such consolidation must be performed in such a way that there is minimal effect on permeability, so that the production fluid can easily flow through the consolidated sand grains. Consolidation methods are divided into two main categories: *In-Situ* formation consolidation and *consolidated gravel*.

In *In-Situ* formation consolidation, typically a resin (such as epoxy resin) is used to cement the formation grains. In this case, a resin material is pumped into the well in order to make the sand particles bond together [28]. This resin will travel to the reservoir and then create a bond (consolidation) between sand grains near the well.

In the *consolidated gravel method*, the gravel-pack material which is coated with consolidating resin is placed in the wellbore at the reservoir level [8].

2.3.2 Sand management

In contrast to sand control techniques which try to eliminate sand production in gas wells, in sand management techniques, a limited amount of sand production is allowed in gas wells. In sand management, downhole equipment which excludes sand production (such as sand screens, gravel packs, etc.) are not used. Instead in the sand management method, a controlled amount of sand production is allowed from each gas well using various techniques such as adjusting the "*critical bottomhole flowing pressure"* [10]. The idea is to have a limited amount of sand production so that the side effect of sand production is within an acceptable range. Sand production may be controlled in such a way that the sand erosion rate is below a certain limit (e.g. 0.1 mm/year [29]). The maximum allowed rate of sand production is called the "*Acceptable Sand Rate*" [30]. The other consideration in applying sand management techniques could be that the fluid should have the correct properties so that it can carry the sand produced, so that the sand does not keep on settling and stagnating in the pipes and reduce/block the pipes. This condition is referred to as the "*Sand Minimum Transport Condition"* [31].

Applying sand management techniques instead of sand control methods can increase the production from the gas field [32]. In order to have proper sand management, it is necessary to have an accurate measurement of the sand flow rate and erosion rate in the pipe. Various types of instruments such as

those explained in section 2.5 are used for sand flow rate and erosion measurement. The accuracy of these instruments is vital for proper implementation of sand management.

In sand management techniques, mechanisms to confront sand accumulations may also be considered. For instance, separators can be equipped with a spray or cyclone jetting facility to remove the accumulated sand at the bottom of them [27].

There are three main issues which need to be considered in the sand management method [33]. The first issue is to have a proper sand erosion estimation. The main goal of this estimation is to insure that the integrity of the pipes/equipment are maintained. Various equipment such as an erosion probe (as described in section 2.5) can be used for such a purpose. Typically erosion probes are installed in '*hot spots*' where the amount of sand erosion is expected to be the most. Also the reading from an ASD can be used to predict the sand flow rate and then this sand flow rate can be used to predict the erosion rate.

The second issue to be considered in the sand management technique is sand settling [33]. To handle this issue, various strategies can be considered. For instance, pigging may be considered to remove the sand settlement. Also in cases where pigging is not possible (such as places where pig launcher/receiver are not available), then sand flow rate can be limited to a level where the sand settlement does not happen in the pipe.

The third issue to be considered in sand management is sand monitoring. Sand monitoring will provide a qualitative amount of sand production using various sensors such as an erosion probe and an Acoustic Sand Detector (ASD). Proper sand monitoring is needed for various reasons. For instance, while it is necessary to have a good estimation of sand erosion in a pipe, sand monitoring may also be used to find the effect of sand production on the gas reservoir.

2.3.3 Sources of solid particles

There are various sources of sand particles in gas wells. Solid particles can be generated from the reservoir formation or from other sources such as drilling mud (mud cake), fractionation solids, cementing solids, gravel pack filling sand, scale, etc. [3].

Typically, at the start-up of the production from a well, there is a period where a greater amount of solids are produced. The solids produced during start-up periods tend to be solids which are left in the well after drilling, fracturing, cementing, and/or completion work. Once all these left-over particles are removed by fluids during the start-up of the well, thereafter the solids production stabilizes at lower rate.

Other operations which affect the production of particles during the production life of a well are the quick opening/shutdown of the well, workover (e.g. tubing), stimulation (acidizing), etc.

In addition, injection of scale, corrosion, wax, hydrate inhibitors and the method of injection (e.g. injection location and injection flow rates) or lack of injecting such inhibitors can affect production of related solids due to scale, corrosion, wax and/or the hydrate phenomenon. Failure of the wellhead/wellbore equipment (such as failure of sand screens, choke valves, packers, and tubing) can also affect solids production. Specifically, failure of a sand screen or other sand control methods can lead to an increase in sand production [3].

Production of some types of solids is particularly more critical than others, as they might indicate damage to the reservoir/wellbore/etc. For example, the particles generated from a gravel pack or sand screen are more important than other types (such as those created from wax), as the particles generated from a gravel pack might show that the gravel pack has been eroded and therefore it might potentially show damage to the gravel pack and the completion system. In this case, necessary actions such as *choke-back* (i.e., reducing the opening percentage of choke valve) might be considered to reduce production of sand and its adverse effects.

In order to identify the source of the sand and take subsequent action, typically a sand sampling system is used. There are various types of sampling system such as *full production stream sampling, deposit sampling,* and *slip stream sampling.*

After taking a sample, various techniques can be used to identify the source of the sand. For example, sand particles can be checked using a digital microscope. An initial look at the particles in a microscope might give an idea of the sand source.

Also, particles can be examined using a hot probe to see whether they melt (which in this case, the particle would have a hydrocarbon source such as wax, as solid particles from hydrocarbon sources have a lower melting temperature).

2.4 Types of sand/erosion measurement

There are various types of sand/erosion detection and measurement equipment. Here, a list of various methods for sand/erosion detection is provided:

- Acoustic sand detector
- Active ultrasonic sand detector
- Erosion probe
- Distributed Acoustic sensing

These methods are now explained further:

2.4.1 Acoustic Sand Detector (ASD)

In Acoustic Sand Detectors (ASDs), an acoustic sensor is installed on the outside of a pipe, typically after a bend. When there are sand particles in the fluid which pass through this pipe, the sand grains impact upon the pipe wall. This causes small vibrations in the pipe. These small vibrations create the acoustic signals. These vibration/acoustic signals are generated by the kinetic energy of the sand particles arriving with momentum which is converted to vibration/acoustic signals. These acoustic signals pass through the pipe wall and reach the acoustic sensor ASD where the acoustic signals are converted to electrical signals [34]. Figure 2-12 shows a typical installation of an ASD after a bend in the pipe [35].

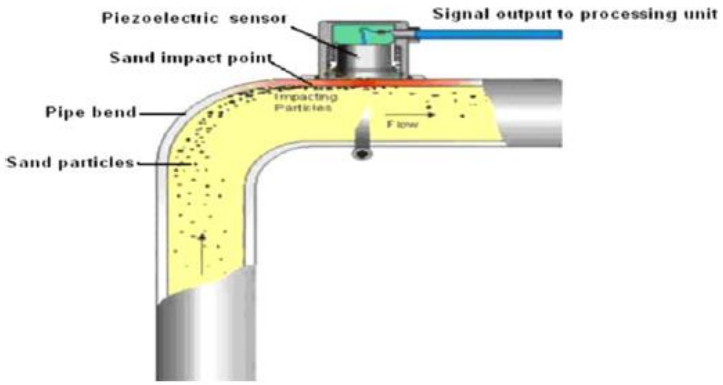

Figure 2-12: Installation of typical ASD after a pipe bend [35]

Since ASDs are sensitive to sound signals, therefore other sources of sounds can also affect their measurement. For example, the flow-induced and background noises created after adjusting the

choke valve can affect the readings of ASDs [6, 36]. Flow-induced signals are those which are generated due to structural vibration of the equipment (e.g. valves, pipes, vessels, etc.) due to the passage of the fluid [37]. Typically these noises are in the lower frequencies [36].

ASDs are frequently used in subsea oil and gas applications (e.g. in subsea wellheads). Since subsea structures (e.g. wellheads) are very remote and also any maintenance activities of such equipment is very costly, therefore the ASDs are typically used to monitor sand production in subsea applications. Using them, the operators can make sure that the subsea equipment is not exposed to excessive sand production. In subsea applications, the ASD is not fixed to the wellhead. Instead, the ASD is installed in an ASD funnel and the funnel is permanently fixed to the subsea structure. Thereafter the ASD can be removed using a Remotely Operated Vehicle (ROV). An ROV is an unmanned vehicle that can dive into deep water and do certain activities such as removal and installation of an ASD on subsea equipment. Figure 2-13 shows an ASD and the ASD funnel used in subsea equipment [34].

Figure 2-13: Typical ASD and ASD funnel in subsea applications [34]

In the case of subsea sensors, the ASD has a sensor head which includes the acoustic sensor. The sensor head in an ASD must have close contact with the pipe wall so that it can pick up the sound signals [38].

As per supplier's recommendations, ASDs are typically installed after a bend in the pipe. Due to the change in flow direction after the bend, more sand particles impact the pipe wall and therefore create more acoustic signals [39].

The signal created by an ASD depends on the location of the ASD. For instance, if there are multiple bends in the pipe, depending on the bend where the ASD is installed, the strength of the output from

the ASD might vary. Therefore it is important to calibrate these ASDs after being fixed onto a particular location on the pipe [40].

To convert these acoustic signals obtained from these ASDs to measure sand particle flow rate, there are various empirical approaches [41]. A number of these empirical methods use velocity of the fluid as an input to sand flow rate calculations. This velocity can be estimated by having a flow meter in the pipe and to convert the flow rate into velocity [39] (by dividing the volumetric flow rate by the area of the cross-section of the pipe).

A choke valve is typically installed on subsea wellheads along with ASD. A choke valve is a device which regulates the amount of fluid production from a gas and oil well, which is performed by throttling the choke valve to a certain opening degree (between 0 -100%). During throttling of the flow using a choke valve, a lot of acoustic signal is created by the choke valve. As the ASD is sensitive to the acoustic signals, therefore one must pay attention to the installation location of the ASD. The reason is that the sound created from the choke valve can adversely affect the reading of the ASD. Since the choke valve creates background/flow induced noise due to turbulent/transient conditions of the fluid after the choke valve, therefore it is advisable to install the ASD a certain minimum distance from the choke [38].

Once the raw signal value obtained from the ASD is recorded, then the flow rate of sand can be estimated using this signal. One supplier for an ASD (*Clamp-On*) has suggested using the following relationship to calculate sand flow rate [6]:

$$sand\ flow\ rate = \frac{ASD\ raw\ value - Zero}{Step} \tag{2.1}$$

where "*ASD raw value"* is the output from the ASD, "*Zero"* is the offset considered to compensate for the background noise, and "*Step"* is the gain between the ASD output and sand flow rate.

Other researchers have also proposed other relationships to convert the reading from the ASD to sand flow rate. For instance, Gao et al. [35] has suggested the following relationship in which the sand flow rate has a direct relationship with the reading from an ASD, minus the background noise. Also in this relationship, the sand flow rate has an inverse relationship with the square of flow velocity:

$$sand\ flow\ rate = \frac{ASD\ raw\ value - Background\ noise}{K\ V^2} \tag{2.2}$$

where V is the fluid velocity and K is a constant value.

Salama et al. [42] performed several experiments under single phase and wet gas conditions. He concluded that by considering a non-linear relationship, the accuracy of the sand flow rate

measurement might increase. Also they mention that considering a non-linear relationship to estimate sand flow rate may increase calibration requirements.

Odigies et al. [43] suggested the use of the following relationship for estimating sand flow rate:

$$sand\ flow\ rate = \frac{M^2 - Z^2}{C\ (C+2Z)} \tag{2.3}$$

where Z is the parameter showing the effect of background noise, M is the output of the ASD, and C is a constant value.

2.4.2 Active ultrasonic sand detector

There has also been some research in using active ultrasonic sand detectors where there is an active ultrasonic transmitter at one side of the pipe and an ultrasonic receiver at the other side of the pipe. however some researchers show that active ultrasonic sand detection is not very sensitive for measuring the sand rates [21]. It should be noted that using an active ultrasonic sand detector was not the original objective for this research, but only mentioned in this section in order to have a more comprehensive background review of the methods used for sand flow rate measurement.

In this method, ultrasonic waves are created using an ultrasonic sensor. Then the properties of the media (e.g. gas including sand particles) is measured using the characteristics of an ultrasonic signal (e.g. attenuation, phase shift, etc.) received by the other ultrasonic sensor. The properties of the solid particles can be identified using ultrasonic attenuation spectroscopy in which the frequency spectrum of the ultrasonic signals is analysed. Two methods are typically used for ultrasonic spectroscopy. The first method is the *Through Transmission* (TT) and the other is the *Pulsed Echo* (PE) type [44]. In the TT mode, there is a transducer which transmits ultrasonic signals and there is another receiver on the line. In the PE type, the same transducer is used for both transmitting and receiving the signal.

These techniques are heavily dependent on the ultrasonic propagation in the media. Therefore, it depends on parameters like temperature of the media, concentration of particles, etc.

2.4.3 Erosion Probe

Erosion probes are used for sand/erosion measurement. However, using an erosion probe was not an objective for this research, but only mentioned in this section to have a more comprehensive background review of the methods used for sand flow rate measurement.

Erosion probes (EP) are an intrusive type of erosion measuring device where a probe is inserted in the pipe where the sand rate/erosion is going to be measured. The impact of particles (sands) causes erosion in the sensing part of the probe element. This erosion changes the electrical resistance of the sensing element. Then, the electrical resistance of the probe is measured using an electronic device.

In addition to the change introduced by erosion of the EP surface of the signal, the variation in the temperature also affects the resistance of the EP sensing probe. Therefore the reading from the EP is also affected by the variation in the fluid temperature. In order to compensate for the sensitivity of the EP to temperature variation, some suppliers provide a reference element in the EP as well [45]. This reference element is not directly exposed to the fluid and therefore the element resistance is not affected by erosion caused from sand impact [46]. But this reference element is installed at a location in proximity to the fluid and therefore under the stable conditions (where process temperature does not change), and so the temperature of the fluid will be equal to the temperature of the reference element. Then in this stable condition, the temperature of both sensing element and reference element is equal to the fluid temperature. Therefore, by comparing the difference between the resistance in the sensing and reference elements, the electronic comparator in the EP can identify the erosion in the sensing element. The difference between the resistances is a good indicator of the erosion of the probe element in which the effects of the temperature change in the sensor probe (under stable conditions) is compensated. Therefore by introducing a reference element into the EP, the effects of the temperature change under stable conditions (where the fluid temperature is not varying) can be compensated [36].

Although using such a reference element in which the effects of temperature changes can be compensated under stable conditions, the EP probes are still sensitive to the temperature during transition periods between the two stable temperature conditions [47].

Also to differentiate between erosion and corrosion, the sensing element of some erosion probes is made of *Corrosion Resistant Alloys* (CRA) [3]. The advantage of using CRA is that the CRA material is not corroded due to any corrosive environment in the produced oil and gas (e.g. possibility of H2S in production fluid). The only issue regarding the CRA material is that it may not be eroded as fast as the material in the pipeline [3].

Erosion probes can be provided in many different shapes. For example, some suppliers provide probes with multiple erosion sensing sections in the probe bar [3]. This arrangement may help to perform an average measurement of the erosion in these sections and therefore make the erosion measurement less affected by how the sand is distributed in the cross-section of the pipe. Figure 2-14 is an example of these types of erosion probes [48].

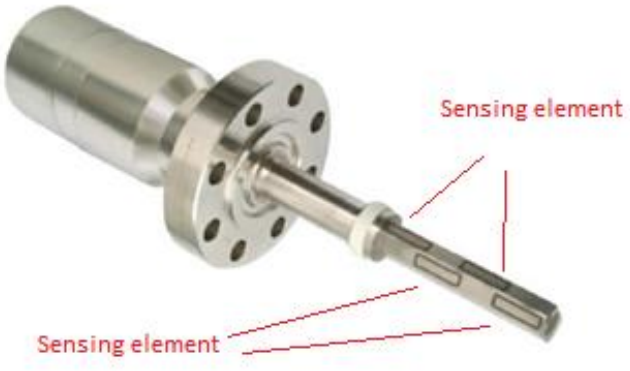

Figure 2-14: An example of Erosion Probe with multiple erosion sensing sections [48]

Also some suppliers provide erosion probes in which the sensing element has a 45 degree inclination with respect to the flow direction. They also provide good exposure of the probe to the sand particles. Figure 2-15 shows an example of these types of probes [48], which are commonly installed in the straight section of the pipe [49].

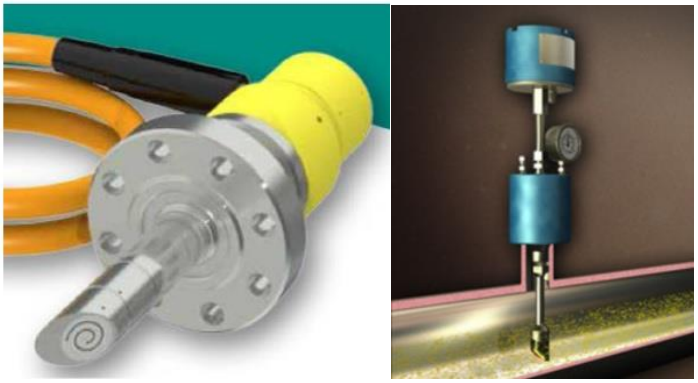

Figure 2-15: An example of Erosion probe with angled-head probe [49]

https://www.smsoilfield.com/blog/technology/item/36-why-sand-erosion-probes-don-t-work

While the ASD is affected by adjustment of the choke valve due to flow-induced/background noise, the EP probe is more immune to actual choke valve adjustment [50].

On the other hand, the ASD is providing an immediate response to changes in the sand flow rate, while the response from the EP to the changes in sand flow rate is very slow. The reason is that as soon as the sand flow rate increases, the acoustic signal created by the sand impact on the pipe wall increases and therefore the output of the ASD increases. But when the sand flow rate increases, the erosion

rate of the sensing element in the EP slowly increases, and it takes more time for erosion to happen before the EP output changes.

There are empirical methods which relate the amount of erosion in the sensing element of the EP to the amount of sand rate in the pipe [51].

2.4.4 Distributed Acoustic Sensing (DAS)

Distributed Acoustic Sensing (DAS) is a potential method for sand monitoring purposes. This method uses fiber optic cable along the pipe and an *Optical Time Domain Reflectometer* (OTDR). It should be noted that using a DAS to measure sand flow rate was not an objective in this research. The DAS method is mentioned in this section of the thesis just to have a more comprehensive background review of the various techniques used for sand flow measurement. This method is not investigated in this thesis, since using this method was not the focus of this research.

In the DAS method, short laser pulses are created by an *Interrogator Unit* and transmitted along the fiber optic. The optical signals are backscattered from different sections of the fiber optic and are then measured by an *Interrogator Unit* [52].

In the case of distributed acoustic sensing (DAS), the backscattered signal happens in the Rayleigh frequency band [53, 54]. DAS uses a coherent optical time-domain reflectometry technique in which a series of short length highly coherent signals are transmitted along the fiber and the backscattered signals from the inhomogeneity in the fiber are measured [55]. Various frequency bands in the received acoustic signal can be used to investigate different flow phenomena [56].

In the case of sand detection in a wellbore, the sand jet at a particular point (e.g. from a particular perforation) will cause sand to hit the opposite side of the tubing. This causes a high acoustic signal reading from this point using a DAS [57]. Also it is expected that the sand will travel in the middle of the pipe after about 20 diameters after each turn or impact on the pipe wall during wellbore monitoring [2]. It may also be noted that a DAS system is distributed, which means that it is reading the vibrations over a length (e.g. 10-20 meters) of the well, as opposed to the specific point locations that an ASD or EP reads.

The acoustic signal phase change along different sections of the fiber optic cable (gauge-length) depends on the strain in that part of the fiber optic cable [52]. These acoustic signals can then be measured along different sections of the fiber optic cable. The advantage of using this technique is that it can potentially be used to provide data about the location where more sand particles enters into the well. Especially with the introduction of advanced completion techniques, it is possible to

have gas wells which produce from different gas fields located at various depths of the wells. Such completion is called multi-zone completion. By using DAS, operators can identify which zone in a multi-zone well is producing more sand. The same data can be used to shut-off the production from a specific zone in the wellbore where too much sand is produced [58].

One of the recent applications of distributed sensing using fiber optics is when a fiber optic cable is installed in the wells. Traditionally, in-the-well sensing is limited to measurement of pressure/temperature in few points in the well, but providing in-the-well distributed sensing offers many more options. Distributed temperature/acoustic sensing in the well can be used for sand monitoring purposes, flow monitoring/production profiling [59], seismic [52], Electrical Submersible Pump (ESP) monitoring/surveillance [60], sand detection [58], hydraulic fraction monitoring [54], gas lift optimization [54], water injection profiling [61], fracture height monitoring, and stimulation monitoring [62].

One practice traditionally used for adjusting the choke valve opening is to increase choke opening until sand production starts (or reaches a certain threshold). In such cases, the sand production rate is measured by sand sensors in the wellhead (e.g. using an ASD). In this case, it takes some time for sand to reach from the production zone to the wellhead area, before the increased sand production can be sensed by an ASD. In the case of a well with high production rates, this practice has the potential for damaging the sand screen downhole, since by the time the increased sand production can be sensed by the sensing element at the wellhead and the operator reduces the choke valve opening, the sand screen has been subjected to increased sand production and probable damage. Using a DAS in this case can provide the early detection of sand production in the wellbore and therefore reduce the chance of sand screen damage [54].

The frequency of transmitting laser pulses along the line depends on the length of the fiber optic cable. The following relationship specifies the maximum frequency of transmitting laser pulses in the fiber optic cable [54]:

$$\mathrm{f_{max}} = \frac{\mathrm{v_{fiber}}}{\mathrm{l_{up/down}}} = \frac{{}^{\mathrm{v_{light}}}/_{\mathrm{n_{index}}}}{2\times \mathrm{l_{fiber}}} \qquad (2.4)$$

where f_{max} is the maximum frequency of transmitting laser pulses along the fiber optic cable, v_{fiber} is the velocity of light in the fiber optic cable. $l_{up/down}$ is the total length of light travelled in the fiber optic cable which (for reflections) is twice the length of fiber optic cable (l_{fiber}). v_{light} is the velocity of light in a vacuum (3 x 10^8 m/s). n_{index} is the refractive index of fiber optic cable.

Also there is a term called *spatial resolution* in the area of imaging and sensing. Spatial resolution is the distance between any two adjacent points along which the acoustic signal has been measured by

a DAS. The smaller the spatial resolution, the more precise the information offered by a DAS. Spatial resolution has a relationship with the length of the laser signal sent through the fiber. If the laser pulse has a shorter wave length, then the spatial resolution will be shorter [54].

There are two kinds of fiber optic cable, namely single mode and multi-mode. In single mode cables, the laser pulses can travel through the fiber in only one direction (i.e., along the axis of the fiber optic) while in multi-mode fiber, the laser pulse is allowed to travel in several forms (i.e., spiral, zig-zag, etc.) in the transverse direction to the fiber lay while it is moving along the axis of the fiber optic cable [54].

DAS in a borehole

When DAS is used in a gas wellbore, it can be used to identify the sand ingress zone (e.g. the zone in the reservoir which creates a lot of vibration) [63]. At the location where sand is produced and enters the tubing, the sand particle travel direction is perpendicular to the pipe while in other areas, the sand particle travel direction is along the pipe. Therefore in the sand ingress locations, sand particles actually strike the pipe while in other locations, they may scrape the pipe in a shear motion. As a result, the vibration signals created at the sand ingress zone are stronger than other areas. This vibration causes fibre optic cable strain and helps to identify the sand ingress zone using the in-the-well fiber optic DAS methods.

If "*1/3 octave"* frequency band is used, then it is possible to distinguish the sand produced noise from fluid-induced noise [63]. When the 1/3 Octave frequency band is used, then the upper frequency limit in each band is equal to the lower frequency in that band multiplied by the cube root of two ($\sqrt[3]{2}$). Using this Octave band method, the amount of acoustic energy may be calculated in each frequency band [64].

The DAS method can also be used for flow profiling in a wellbore. For example, the DAS method can be used for slug detection using thermal-slug modelling [56]. When a pipe carries two-phase gas-liquid mixture, then the dag and liquid fluids may travel in slug flow pattern. In *Slug flow*, batches of liquid followed by sections of gas travel in the pipe [65]. The DAS method can also be used for flow profiling by performing inflow-noise modelling [56].

2.5 Benefits of accurate measurement of sand flow rate

Accurate measurement of sand flow rate has several advantages. Some of the advantages of measuring sand flow rate are as follows:

1- When sand management techniques are applied in the field, it is vital to understand the sand flow rate. In sand management techniques, there is a limit on the allowable amount of sand flow rate, and therefore operators need to know the current sand flow rate in order not to exceed this limit. Proper application of sand management techniques is dependent on accurate measurement of the sand flow rate [32] [66].

2- In order to apply the sand control method (as described in section 2.6) properly, it is vital to know the early/sudden increase in sand production. Early indication of sand production using a sand measurement device and also the amount of produced sand can be used to identify any probable issues with the chosen sand control method [67, 68]. For example in the case of a sand screen not working correctly due to a rupture in it, then an accurate sand measurement device can identify any increase in sand production. This early detection can help the operator be aware of the issue and find the reason by further study (e.g. bringing a sample of the sand particles to the lab for examination) and take any further actions to prevent any damage to the downstream facilities due to increased sand production (e.g. by reducing/stopping the production from the respective well).

3- Where sand control/management provisions are not considered (e.g. there is no sand screen/gravel pack or other sand prevention facility in the well), the operator of these wells might be interested in obtaining maximum sand-free production [69] and to increase the production until the sand production is still negligible. In this case, it is important to have a sand measurement device which can identify a small amount of sand production within fluids.

Due to all of the above mentioned reasons, it is very important to measure sand flow rate accurately in gas fields. Therefore this research which tries to develop methods to improve the accuracy of sand flow rate measurement, will be helpful on these various occasions.

2.6 Ultrasonic signals

Acoustic signals are transmitted through the media using vibrating waves. Humans can hear acoustic waves in the frequency range from about 20 Hz to 20 kHz. Note that this range may differ from person to-person and in persons of various age groups. Acoustic signals above 20 kHz which cannot be heard by humans are typically referred to as *Ultrasonic signals*. Also the acoustic signals below 20 Hz (which again cannot be heard by human due to their low frequency) are called *Infrasonic signals* [70]. In this research, I have studied sand flow rate measurements using ultrasonic signals (with a frequency range above 20 kHz).

Ultrasonic signals travel through various media such as gases, liquids and solids. Travelling of the ultrasonic signals in the media is typically referred to as the "propagation of ultrasonic signals". There are various methods of propagation of ultrasonic signals in the media. One method is *longitudinal* wave propagation in which the oscillation of the particles in the media are in the same direction as the direction of wave propagation. The other method of sand production is the *transverse (Shear*) wave in which the oscillation of the sand particles are perpendicular to the direction of wave propagation. In gases and liquids, the ultrasonic wave propagation happens only in longitudinal form because the media has elasticity. In all solids, ultrasonic wave propagation occurs in both longitudinal and transverse forms [71].

For measuring the ultrasonic signal of each type (i.e., longitudinal or transverse), a suitable ultrasonic sensor is used, which means that when measuring longitudinal waves, an ultrasonic sensor suitable for measuring longitudinal waves is selected.

Piezoelectric sensors are commonly used for measuring ultrasonic waves [72]. Piezoelectric material creates a voltage when there is a mechanical displacement. Therefore when there is a displacement in a piezoelectric material due to the vibration provided by the ultrasonic signal, this sensor converts this movement into an electrical signal [71]. Piezoelectric sensors can often measure ultrasonic signals in a wide frequency range (up to about 10 MHz). Figure 2-16 shows the typical construction of a piezoelectric sensor [73].

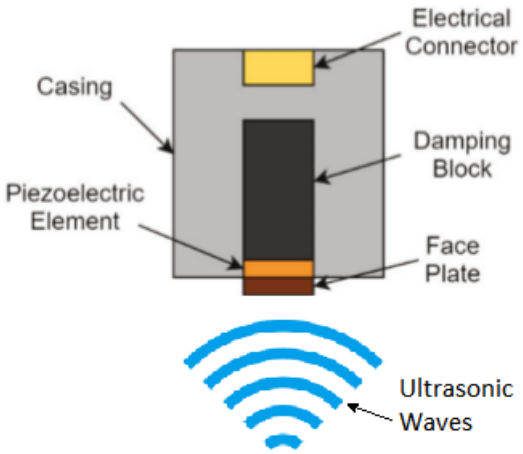

Figure 2-16: Typical construction of a Piezoelectric sensor [73]

In Figure 2-16, the casing provides the mechanical support for the sensor. It also provides electrical shielding for the piezoelectric element. The dampening block dampens the vibration of the piezoelectric element. The piezoelectric element creates an electrical signal as a result of the mechanical displacement of the element. The face plate provide protection for the piezoelectric sensor (as it is a fragile device) [73]. The face plate will also provide acoustic impedance matching with the product it is in contact with. For instance in this research, I put ultrasonic sensors in contact with the steel pipe through which the sand is passing, to measure the sand flow rate. Therefore in this case, the face plate should provide an acoustic match between the piezoelectric element and the pipe material. It should be noted that the acoustic impedance of a material is defined as the product of the density of the material multiplied by the velocity of acoustic signal in that material [74].

When the acoustic signal passes from one material to another material, then a portion of the acoustic signal reflects back to the first material while some portion of acoustic signal passes to the second material. When the difference between the acoustic impedances of these two materials are small, then more of the acoustic signal passes from one material to the other one. Therefore by having a better impedance match between the ultrasonic sensor face plate and the material it is in contact with, more ultrasonic signals can reach the piezoelectric element of the ultrasonic sensor.

Capacitance type acoustic sensors are also occasionally used for acoustic measurement. These sensors are typically used to measure the acoustic signal in the audible frequency range. Therefore these types of sensors are mostly suitable for the lower frequency range (with maximum frequency of 20 kHz) [71].

2.7 Signal processing methods used in sand flow rate measurement

One of the methods used in this project for measuring sand flow rate is the ultrasonic sensor. As has been explained, to measure sand flow rate using an ultrasonic sensor response, suitable signal processing needs to be performed to analyse the output signal from the ultrasonic sensor. This section is a background review of signal analysis methods used in this application.

Many signal processing methods can be classified as being one of the following two main categories:

- Frequency domain
- Time-Frequency domain

Since these signal processing techniques are used in this research, a brief description of these methods is provided in this section.

2.7.1 Fast Fourier Transform

In the frequency domain category, typically a *Fourier Transform* is used to convert the signal from the time-domain to the frequency domain. In this research, the frequency domain is used to analyse the signal from ultrasonic sensors. Typically the signal which needs to be analysed (e.g. the output of an ultrasonic sensor/amplifier) consists of samples using a suitable Analog to Digital (A/D) convertor. In cases where signal is converted to a discrete value using an A/D convertor, then the *Discrete Fourier Transform* (DFT) can be used to convert the discrete signal to the frequency domain using the following relationship [75]:

$$F_k = \sum_{n=0}^{N-1} f_n \, e^{-\frac{2\pi jk}{N}nk} \qquad k = 0, \dots, N-1 \qquad (2.5)$$

In this relationship, f_n is the magnitude of the ultrasonic signal sample in the time domain, N is the number of samples, and F_k is their DFT values in the frequency domain.

To calculate the DFT values using the above relationship, the *Fast Fourier Transform* (FFT) method can be used. FFT provides a method to calculate the DFT values with a minimum amount of calculation. Therefore by using an FFT, DFT calculation can be performed faster [76]. In this research, the FFT method is used to estimate the sand flow rate using ultrasonic signals.

The other category of signal processing is that of the time-frequency domain. This category is used when the signal in the time domain is non-stationary. Non-stationary signals are those signals for which their characteristics (e.g. frequency content) changes over time. Therefore they are converted

into the time-frequency domain. The frequency content can be determined at certain time intervals in the time-frequency domain.

2.7.2 Short Term Fourier Transform

The *Discrete Short Term Fourier Transform* (STFT) is one of the popular signal processing methods in time-frequency space. The Discrete STFT is defined as follows [77]:

$$Y(n,w) = \sum_{-\infty}^{\infty} y(m)\, a(n-m) e^{-jwm} \qquad (2.6)$$

where $Y(n,w)$ is the STFT in the time and frequency domain, $y(m)$ is the signal in the time domain, $a(n-m)$ is the window function which is shifted by m steps, w is the frequency and n is the index in discrete time.

There are various types of windows. Some of the popular windows are the *Hamming* window, the *Hanning* window, and the *Rectangular* window [77]. Using the STFT, I can identify the frequency content of the signal at various times intervals. The problem with the STFT is the dilemma of resolution between time and frequency. This means that if for instance the resolution in the time domain is adequate, then the resolution in frequency domain may be poor. Figure 2-17 shows an example of an STFT with adequate time resolution and poor frequency resolution [78]. In this figure, it is not easy to find the frequency content of the signal (when seen as the curve expands in the frequency scale), but it is obvious how the frequency is presented in which time window.

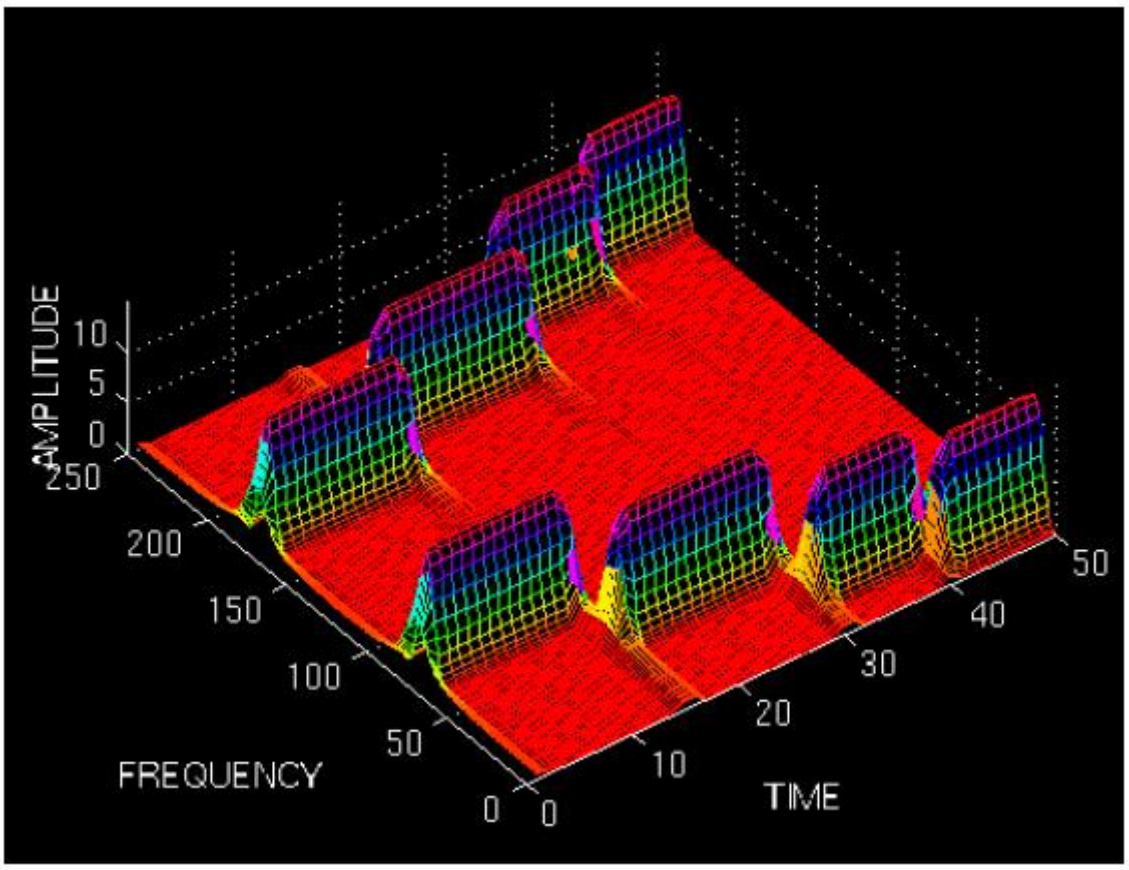

Figure 2-17: An example of STFT with good time resolution but poor frequency resolution [78]

When the resolution in the frequency domain is good, then the time resolution is poor. Figure 2-18 shows an example of the STFT with poor time resolution and good frequency resolution [78]. In this figure, the frequency content of the signal is well defined, but it is difficult to determine the time values when specific frequencies occur (as the frequency values overlay each other in time scale). For instance, it is very clear that there is a frequency content of 50 in this Figure (good frequency resolution). But for the frequency value of 50, the associated time is somewhere between 10 and 35, so it is not very clear that this frequency value is occurring at which specific time (i.e., poor time resolution).

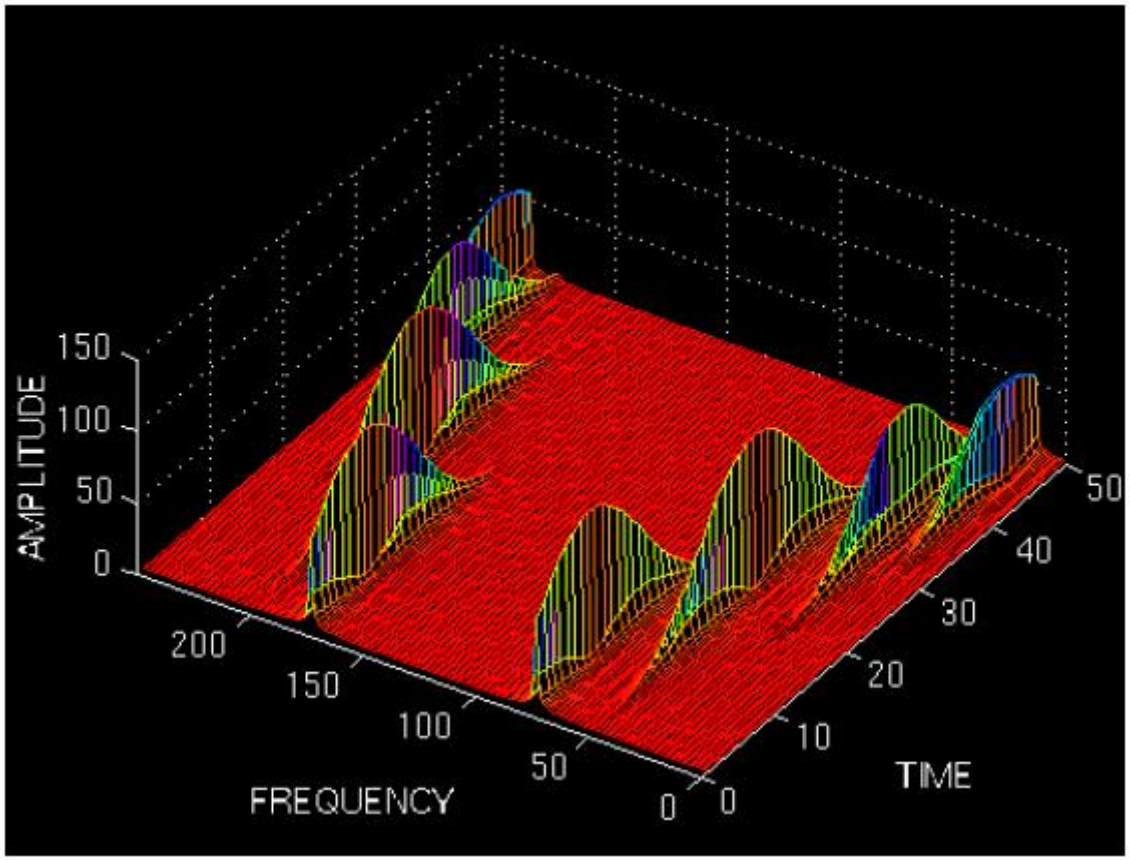

Figure 2-18: An example of STFT with poor time resolution but good frequency resolution [78]

2.7.3 Discrete Wavelet Transform

To resolve the resolution issue of the STFT method, an improved signal analysis method is typically used which is called the *wavelet transform*. Similar to the STFT method, the wavelet transform method converts a time domain signal to the time-frequency domain.

As I have used the wavelet transform method to analyse the signal data from an ultrasonic sensor, therefore the wavelet transform will be described in more details. Also the wavelet approach to improve the time-frequency resolution is explained.

It should be noted that there are two types of wavelet transform. The first type is the *Continuous Wavelet Transform* (CWT) and the other one is the *Discrete Wavelet Transform* (DWT). CWT is defined as:

$$CWT_x^{\Psi}(\tau, s) = \Psi_x^{\Psi}(\tau, s) = \frac{1}{\sqrt{|s|}} \int x(t)\ \Psi^*\left(\frac{t-\tau}{s}\right) dt \qquad (2.7)$$

where the $\psi(t)$ is the transform function. The CWT is a function of two parameters namely τ and s. τ is called the *translation* and s is called the *scale*.

Translation corresponds to the time information of the CWT and scale corresponds to the inverse of frequency of the signal. So as can be seen, there is an indefinite number of choices for τ and s, and so a long calculation is needed to calculate the CWT. To find a reasonable number of choices for τ and s and get a good balance between the amount of calculation and the useful outcome of the wavelet transform for data analysis, there are a few methods. One of the most well-known methods in selecting the time-frequency resolution is multi-resolution analysis. Burt et al. [79] were among the first researchers who worked on multiresolution analysis. This technique was developed further by other researchers. Finally applying multi-resolution analysis to the wavelet transform resulted in the development of the *Discrete Wavelet Transform* (DWT). DWT has been widely used in various applications such as image processing, data compression, de-noising, etc. [80]

With the *Discrete Wavelet Transform* (DWT), the signal passes through a series of high frequency and low frequency filters [78]. For example, a signal with frequencies up to 1 MHz is passed through frequency filters of 0-500 kHz and 500 kHz - 1 MHz. Then the lower band portion will go through another set of low pass and high pass filters. In this example, the 0-500 kHz signal goes through 0-250 kHz and 250 kHz-500 kHz filters. To pass a discrete signal through a digital filter, a convolution operation is used. This relationship shows how the signal is passing through a low pass filter using convolution:

$$x[n] * h[n] = \sum_{-\infty}^{\infty} x[k].h[n-k] \qquad (2.8)$$

where $h[n-k]$ is the impulse response of the low pass filter (shifted by k samples in time). Also $x[n]$ is the signal in the time domain. Similarly, the signal is passed through a high pass filter. The output of high pass filter constitutes the first level of DWT coefficients.

Then the output signals from the low pass and high pass filters are sub-sampled by 2. That means that every other sample is discarded. Then the subsampled output of the low pass filter will again be filtered by another low pass and high pass filter as follows:

$$y_{high}[n] = \sum_{-\infty}^{\infty} z[n].g[2n-k]$$
$$y_{low}[n] = \sum_{-\infty}^{\infty} z[n].h[2n-k] \qquad (2.9)$$

In this relationship, $h[n]$ is the impulse response of the low pass filter and $g[n]$ is the impulse response of the high pass filter. Also $z[n]$ is the output of the low pass filer from the previous stage which is subsampled by 2. The output from the high pass filter in this stage is actually the level 2 DWT coefficients.

This procedure to sub-sample the outputs from low/high pass filters by 2, and pass the subsampled signals of low pass filter through low/high pass filters continues until the DWT coefficients are obtained up to the required level. Figure 2-19 shows the procedure to obtain DWT coefficients [78]:

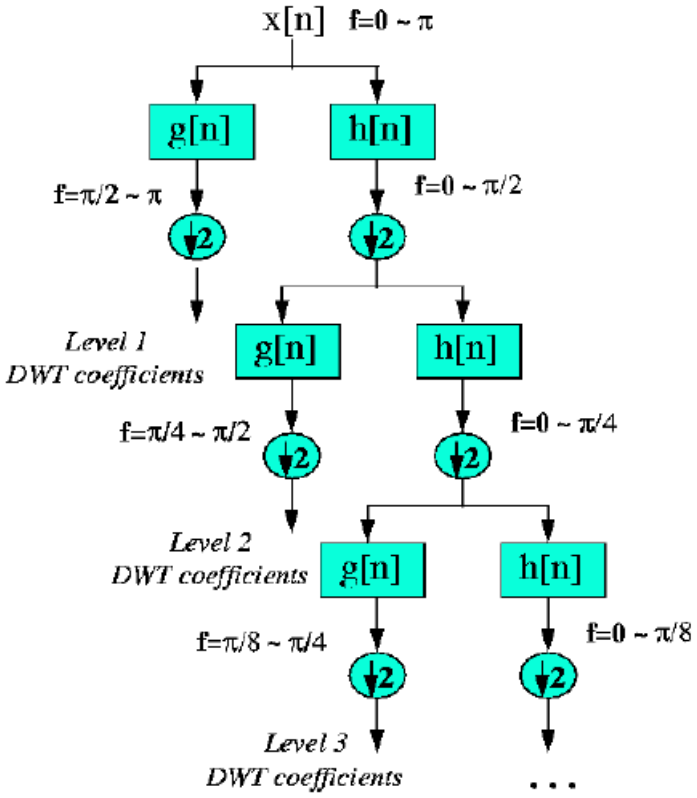

Figure 2-19: Illustration of DWT calculation method [78]

The *Discrete Wavelet transform* (DWT) is used for various applications. For instance, it is used for de-noising purposes in sand measurement applications [35]. In this research, I use the DWT to estimate sand flow rate using ultrasonic sensors.

The DWT method is superior to the STFT method for processing non-stationary signals. The reason is that the STFT provides equal resolution in the time-frequency domain while the DWT provides variable resolution.

2.7.4 The Welch method

The Welch method is another signal processing method used to transfer a signal from the time domain to the time-frequency domain, and is used to analyse non-stationary signals. The Welch method is used to calculate the *Power Spectral Density* (PSD) of the signal.

PSD shows the power of the signal against the frequency axis. In other word, it shows how the power of the signal is distributed across various frequency ranges.

The Welch method used the *windowed periodogram* and FFT methods to calculate the spectral power density of the signal [81]. The idea is to divide the signal into smaller blocks. Then the signal in each block is tapered. The tapering is used to reduce or taper the signal to become zero at the edge of any block, so that there are no computational edge effect.

Then the FFT method is applied to the tapered signal for each block and the squared FFT for that block can be calculated. Figure 2-20 shows how the segmenting is performed by the Welch method [81].

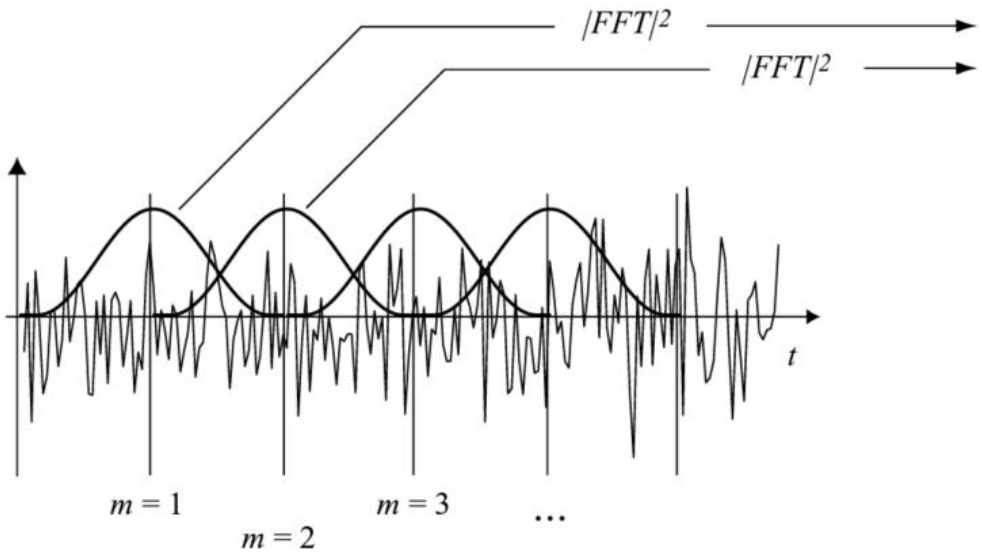

Figure 2-20: Segmenting of the signal in order to calculate PSD using the Welch method [81]

As can be seen in this figure, the segments have overlap. In this case, they have an overlap of 50%. That means that for instance, 50% of the segment identified by m=2 in the above figure is overlapping the segment identified by m=1. In this figure, the tapering signal is identified by the solid sinusoidal shaped line. As can be seen, the tapering signal is equal to zero at the edge of each block. Therefore the multiplication of the tapering signal and the actual signal results in a signal which has zero value at the boundary of each block.

Once the FFT of tapered signal is calculated for each block, then there will be no unwanted high frequency spectrum in the FFT due to any sudden change at the edge of the block. Therefore tapering of the signal eliminates edge effects which distort the output data.

The square of the FFT for each block is then calculated. These square FFTs for various blocks are averaged. The average value represents the output of the Welch method which is the Power Spectral density (PSD) of the signal. By averaging the square FFTs of the signals for various blocks, the effect of noise is minimized. Therefore the Welch method is suitable for analysing stochastic signal which includes a lot of noise. In this research, I use the Welch method to analyse the ultrasonic signal created by sand particles. Since the ultrasonic signal is created by the impact of various sand particles of different shape, velocity, etc. to the pipe wall, therefore the ultrasonic signal has some stochastic nature. Therefore the Welch method is a suitable technique to reduce the effect of such noise. This will be discussed in the following chapters.

Below, the steps to calculate Welch method is provided [82].

1) Divide the data into various segments:
   Assuming the discrete data as follow (N sample of data):
   $x[0], x[1], \ldots., x[N-1]$

   Then the segments are as follow:

   Segment 1: $x[0], x[1], \ldots., x[M-1]$
   Segment 2: $x[S], x[S+1], \ldots., x[M+S-1]$
   ⋮
   Segment K: $x[N-M], x[N-M+1], \ldots., x[N-1]$

   Where
   M is the number of data points in each segment
   S is the number of overlapping points between two adjacent segments
   K is the number of segments

2) For each segment, calculate the DFT of the data tapered using a window function. The calculation is performed as follow:

$$X_k(\vartheta) = \sum_m x[m]\, \omega[m]\, e^{-j2\pi\vartheta m} \qquad (2.10)$$

where ϑ is the frequency of DFT calculated for multiple frequencies of $\vartheta = {}^{i}/_{M}$ in which $-(M/2-1) \leq i \leq (M/2)$. Also m is calculated as follow:

$$m = (k-1)S, \dots, M + (k-1)S - 1 \tag{2.11}$$

Also $\omega[m]$ is the window function which perform tapering of the signal as explained before.

3) Then calculate the periodogram value as follow:

$$P_k(\vartheta) = \frac{1}{W}|X_k(\vartheta)|^2$$
$$W = \sum_{m=0}^{M} w^2[m] \tag{2.12}$$

4) Calculate the Welch value by averaging the periodogram as follow:

$$S_k(\vartheta) = \frac{1}{K}\sum_{k=1}^{K} P_k(\vartheta) \tag{2.13}$$

2.8 Summary of the chapter

This chapter focussed on a literature review for this research. First, various concerns in sand production from gas wells were reviewed. Then the two main strategies to mitigate the side effects of sand production (i.e., sand control and sand management methods) were introduced. Then various methods for sand control were elaborated, followed by the various sources of the generation of solid particles in the gas fields.

Afterwards, various types of sand/erosion measuring devices (i.e., acoustic sand detectors, active ultrasonic sensors, erosion probes, distributed acoustic sensing) were discussed and their merits reviewed. The benefits of having accurate sand flow rate measurement was discussed.

The two types of ultrasonic wave propagation were explained, and the ultrasonic sensor used to measure such ultrasonic wave propagation was reviewed.

Finally, various signal processing techniques which are used in this research were explained. Specifically four signal processing techniques (i.e., *Fast Fourier Transform*, *Short term Fourier Transform*, *wavelet transform* and *Welch* methods) were explained in more detail.

3 Methodology for using an ASD

In this chapter, the methodology and test facility used for research in the area of ASD is discussed. In particular, the description of the flow loop test which was used for this research is provided. First the overall test facility is described and the schematic diagram of the flow loop is presented. Then the details of various components in the flow loop is provided. Finally the details of the software programming and the analysis used to improve sand flow measurement using an ASD is provided. It should be noted that as part of this research, ultrasonic sensors were also used to measure sand flow rate. The methodology to use ultrasonic sensors to measure sand flow rate is explained in the next chapter of this thesis.

3.1 Introduction

In order to perform research in the area of sand flow measurement, the flow loop test facility at Curtin University building 619 was used. In this flow loop, air flow was created in a pipe where sand could be injected. Various instruments for measuring sand flow rate (e.g. an Acoustic Sand Detector (ASD) from *Clamp-on* Company, and an Erosion Probe (EP) From *Cosasco* Company) were installed in the flow loop. Consequently, this facility could be used to simulate gas pipes which carry some sand particles. The velocity of the air and the sand injection rate could be controlled in this flow loop, which was an open loop type. That is, the air and sand passing through this flow loop did not recirculate in the flow loop. Consequently, the sand particles were injected at some point and collected at the end of the flow loop. Also the air which was taken from the surrounding environment was expelled to the atmosphere.

3.2 Schematic diagram of the flow loop facility

Figure 3-1 shows the original block diagram of the flow loop facility at Curtin University. Note that as part of this research, some extra equipment (e.g. ultrasonic sensors) were added to this flow loop. This additional equipment will be discussed in Chapter 4. Also the revised schematic diagram after adding this additional equipment is provided in Chapter 4.

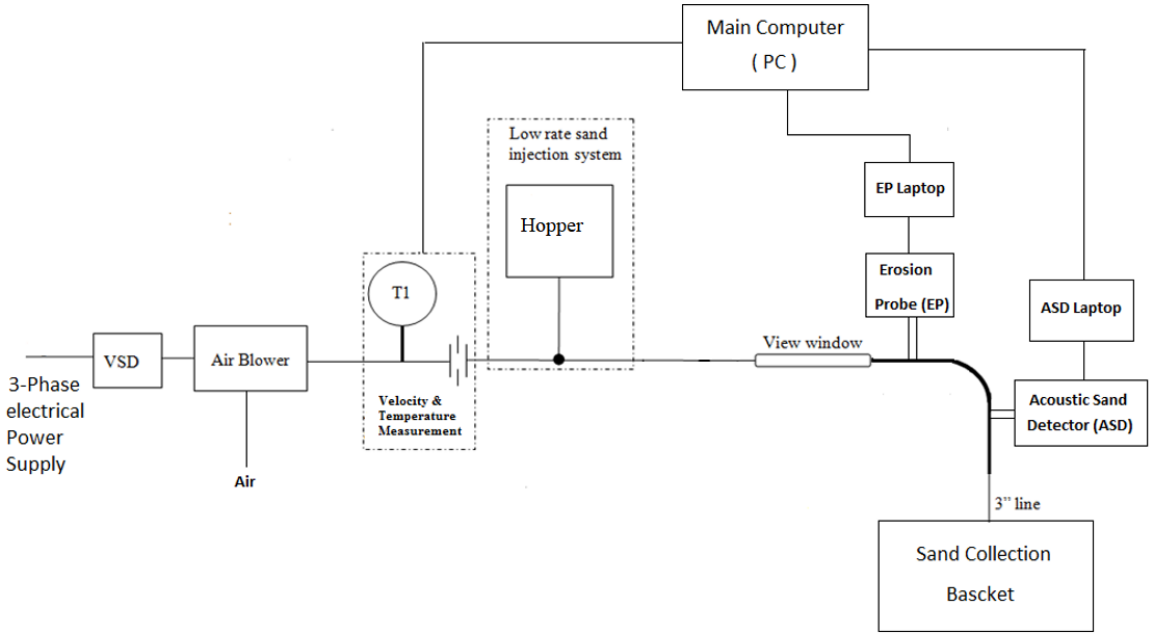

Figure 3-1: Schematic Diagram of flow loop test facility in Curtin University

As can be seen in this block diagram, an air blower is provided to create air flow in the flow loop. A Variable Speed Drive (VSD) was used to adjust the speed of the air blower. By adjusting the VSD, the velocity of the air flow could be controlled in the flow loop. Also a hopper (sand injection device) was installed on the pipe. This hopper could inject the sand at various doing levels into the pipe. The sand injected into the pipe was carried along by the moving air in the pipe.

An Erosion Probe was also installed in the horizontal straight section of the pipe. The sand carried by the air impacted the Erosion Probe head which was mounted in the pipe and caused erosion in the head. The Erosion Probe provided the data about the amount of erosion at its head.

Also the Acoustic Sand Detector (ASD) was installed after a bend in the pipe. The sand particles carried by the air impacted the pipe wall at the bend. This created acoustic waves which were measured by the ASD.

The data output from the ASD and Erosion probe were submitted to their respective laptops. Then the information from the ASD and erosion probe laptops was submitted to the main PC. The main PC was also connected to the hopper, in order to control the sand injection rate.

A temperature/velocity sensor was also installed on the pipe. The temperature/velocity information obtained from this sensor was passed to the main PC.

After passing by the Erosion probe and ASD, the air-sand mixture was routed to the sand collection basket placed at the end of the pipe. The sand was collected in this collection basket, while the air was released to atmosphere through mesh in this basket.

3.3 Elements in flow loop test facility

Various components of the flow loop are described in more detail below:

3.3.1 Hopper

The purpose of the hopper is to inject sand particles into the pipe. This hopper came with a glass container and a control unit installed on top of the glass container. Inside the glass container, there is a rotating shaft which was connected to the hopper control unit on top of glass container. The hopper control unit adjusts the rotational speed of this shaft. The faster the shaft rotates, the more sand that is injected into the pipe.

The hopper was connected to the computer using RS485 communication protocol. Suitable software provided by the supplier of the hopper was used to remotely control the hopper. This software provides the command for rotational speed of the hopper shaft. Since the sand injection rate depends on the shaft rotational speed, therefore the command indirectly defined the sand injection rate. Figure 3-2 shows the hopper used in this research.

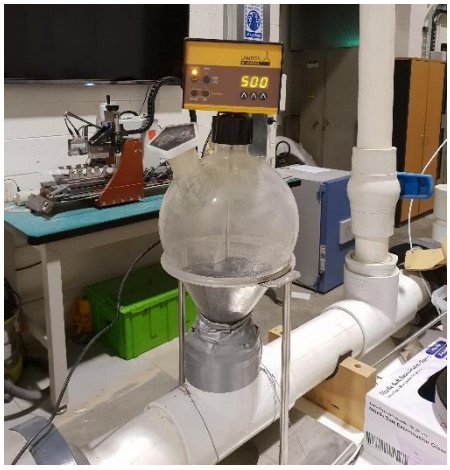

Figure 3-2: Sand dosing instrument in flow loop test facility

3.3.2 Air Blower

The air blower was used to create air flow in the flow loop. The air blower was model LTV-050 from Pneuvay Engineering Pty Ltd. Figure 3-3 shows this blower.

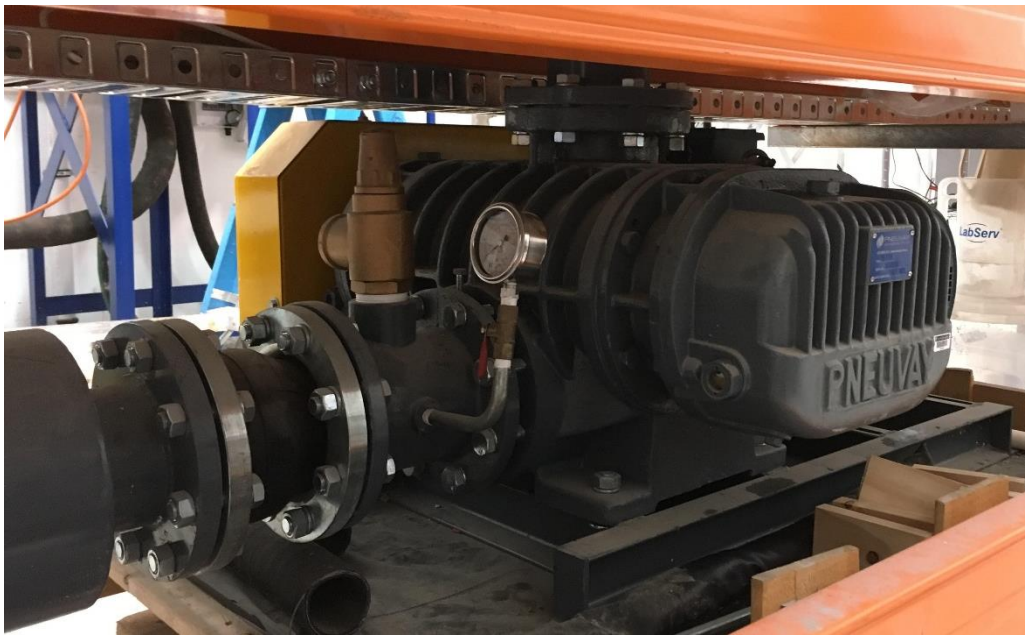

Figure 3-3: Air Blower used in flow loop test facility

The blower was installed below the table where various devices of the flow loop equipment (e.g. pipe, ASD, computer) were located. The blower was connected to a 3-phase electrical motor. The power supply to this motor was provided by a Variable Speed Drive (VSD). Therefore by adjusting the VSD, the rotational speed of the motor could be controlled. As a result, by adjusting the speed of the motor

connected to the blower, the velocity of the air in the pipes downstream of the blower could be controlled.

3.3.3 Variable Speed Drive (VSD)

The variable speed drive was provided by TECO Company and used to adjust the rotational speed of the air blower motor, and therefore controlled the velocity of the air in the flow loop.

Figure 3-4 shows the VSD drive used in the flow loop test facility.

Figure 3-4: Picture of the Variable Speed Drive (VSD) used in flow loop test facility

This VSD drive uses the current vector control method to adjust the speed. It has an LCD panel and a few control buttons. The buttons were used to configure the VSD and adjust the speed. Various parameters such as speed command can be seen on the LCD display of the VSD.

Considering the relatively complex process for configuration and adjustment of the VSD, it is important to follow the operating procedure of this device. Therefore, as part of this research, I reviewed the operating manual of this VSD and followed this manual to adjust the speed of the VSD.

3.3.4 Erosion probe

The Erosion Probe from *Cosasco* Company was used in the flow loop. Figure 3-5 shows a picture of this erosion probe and its related laptop.

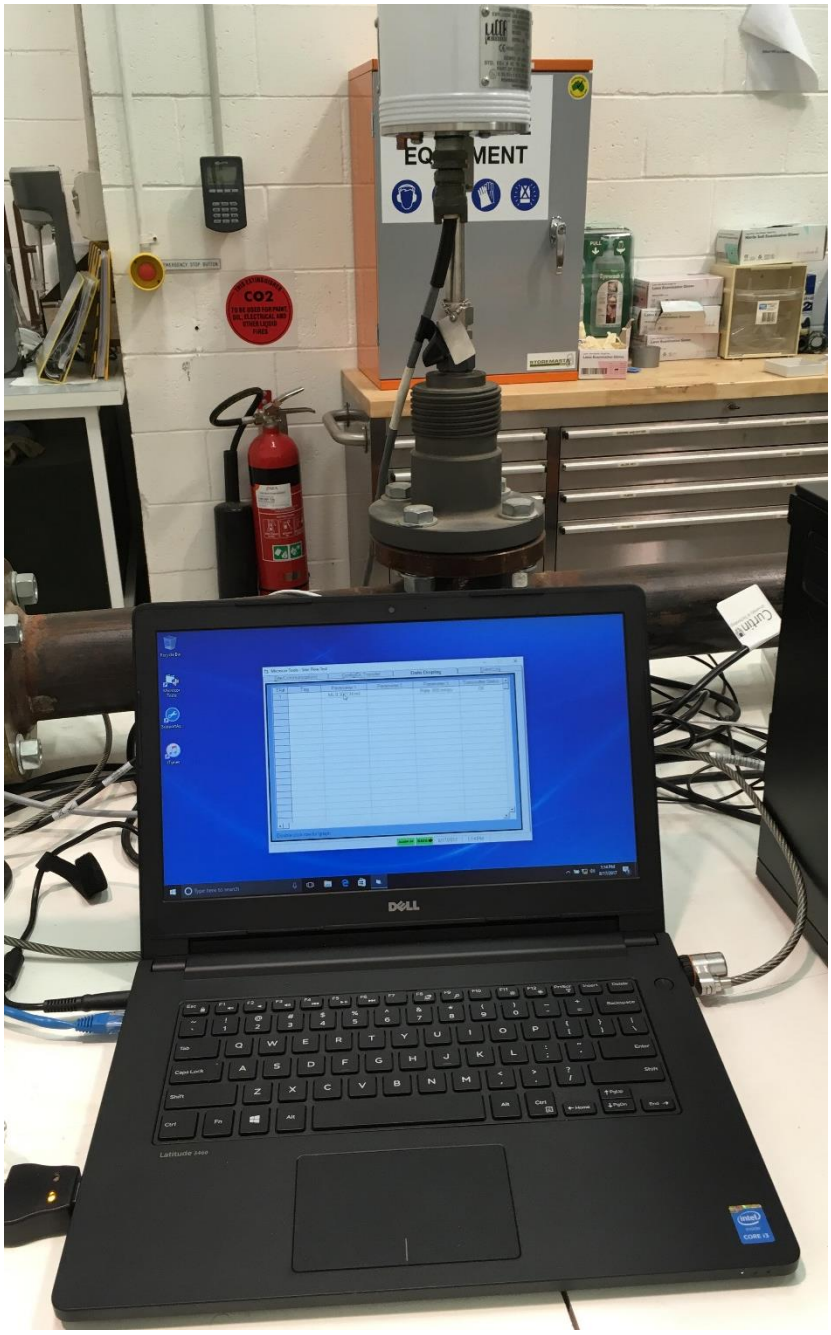

Figure 3-5: Picture of the Erosion Probe and related laptop used in flow loop test facility

This EP uses a combination of Electrical Resistivity (ER) and Linear Polarization (LP) methods to measure erosion [83]. The sensor is connected to the laptop using RS485 interface protocol with the following parameters:

Baud Rate: 2400, Data Bits: 8, Stop Bits: 1, Parity: None

The laptop of the erosion probe ran *Microcor* software provided by the supplier of the EP. This software collects data from the EP and reports this information to the main PC. Also this program provides the trend of the erosion over time.

This EP also performed temperature compensation using a reference element. The EP has two elements. One is in contact with the sand particle (called the “measuring element”) and one not in contact with the sand particles (called the “reference element”). The EP compares the measuring element with the reference element to measure the erosion of the measuring element.

3.3.5 Acoustic Sand Detector

An Acoustic Sand Detector (ASD) provided by *Clamp-On Company* was used in the flow loop test facility. This ASD was installed after a bend as per supplier recommendation. The ASP probe was connected to a receiving unit provided by the supplier. The ASD was also provided with a dedicated laptop and special software which was provided by *Clamp-on*. The signal from the ASD probe was transferred to the receiving unit. Then the data was transmitted by the receiving unit to the ASD laptop. Then the ASD signal was transferred from this ASD laptop to the main PC. Figure 3-6 shows the ASD, receiving unit and the ASD laptop.

Figure 3-6: Image of ASD, receiving Unit and the Laptop for the Clamp-On ASD used in Flow loop test facility

3.3.6 Velocity/temperature measurement

There was a sensor for measuring the Velocity and temperature of the air. This sensor was provided by *Omega Company*. The velocity/temperature sensor was connected to a receiver unit. Figure 3-7 shows this velocity/temperature sensor.

Figure 3-7: Picture of velocity/temperature sensor in flow loop test facility

Figure 3-8 shows the picture of the receiver unit for the velocity/temperature sensor.

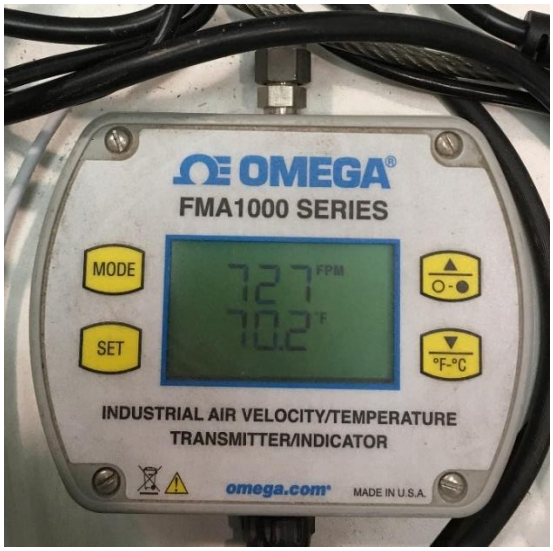

Figure 3-8: Picture of the receiver unit for velocity/temperature measurement in flow loop test facility

The signals from this velocity/temperature sensor were transmitted to a data acquisition unit from *National Instrument Company*, Model No "USB-8009". The USB-8009 has eight analogue input channels and has a resolution of 14-bits. Refer to Chapter 4 for more explanation about the resolution of data acquisition systems. The sampling rate of each channel is 48 kS/s (Kilo Samples per second). Figure 3-9 shows this data acquisition system. It should be noted that under Nyquist theory, the sampling rate should be at least 2 times the highest frequency rate of the signal. Practically the

sampling rate should be around 5-10 times the highest frequency rate of the signal. Therefore with a sampling rate of 48 kS/s, a signal with a maximum frequency content of 4.8 kHz can be easily sampled. Considering slow changes in the velocity and temperature and their low frequency content, such sampling rate is acceptable. Therefore using the USB-8009 was suitable for this application.

Figure 3-9: Picture of National Instrument Data Acquisition System in flow loop test facility

3.3.7 Sand Collection Basket

After the air/solid mixture passed through the pipe where various sensors were installed, it reached the sand collection basket. In the collection basket, the air passed through a mesh to the surrounding environment while the sand was collected in the basket.

Figure 3-10 shows the sand collection basket used in this research.

Figure 3-10: Sand Collection Basket

3.3.8 Main PC

The main PC collected the data from the following sources:

1- Erosion Probe (EP) Laptop
2- Acoustic sand Detector (ASD) laptop
3- Velocity/temperature information through National Instrument Data acquisition system
4- Hopper

Therefore the main PC was the main location where the data from the various instruments were collected and recorded.

The user of the flow loop could give the command to the hopper from the main PC. The user could also record the information from various sensors (EP, ASD, and velocity/temperature measurement) in the main PC. The main PC used Matlab software to collect data from the various sensors.

3.4 Renovation activities performed on the flow loop

Since the flow loop had not been used for several years, several pieces of equipment did not work properly or the respective instruments/units were not available in the beginning of this research. Also the computer systems related to measurement and control of the flow loop (comprising main PC, laptops for EP and ASD) were not functioning at the beginning of this research.

As part of this research, I expended a lot of effort on renovating various pieces of equipment of this flow loop and brought them to an operating condition. Here below, various activities are discussed which I performed to bring the flow loop to working conditions.

3.4.1 Resolving issues with the Erosion probe

The laptop for the EP probe did not boot-up due to internal issues. Under this project, several attempts had been made to start-up this laptop. However, since this laptop was very old and due to internal issues in this laptop, it could not be turned on. First, Curtin Information Technology (IT) department tried to fix it, but despite several attempts, the problem with this laptop could not be fixed. Since this computer was procured from non-university sources, Curtin IT was not officially responsible to support this laptop.

A replacement laptop was procured from the supplier of the EP probe (*Cosasco Company*). Extended discussion occurred with the supplier about the hardware/software requirements. It took several months to finalise the procurement process and to receive the laptop. Special software from the supplier of the EP probe (Microcor software) was installed on the laptop.

Following this, much effort was made to connect the laptop to the main PC and to pass the information from the EP probe software (Microcor) to the MATLAB software on the main PC. The Windows operating system has a strong firewall system which put strict restrictions for exchanging the data to/from the operating system. These restrictions are there to prevent unauthorized access to the information on the PCs and to prevent various Virus/malware software gaining access while the PC is connected to a network or the internet. Therefore in order to pass the data between the computers, appropriate settings on Windows were made to allow the software to pass the information through the computer network. Consequently as part of this research, a lot of effort was made to adjust the settings of the windows on the main PC and the ASD and EP laptops.

3.4.2 Resolving issues with the Main PC

As mentioned earlier, the main PC is supposed to collect the data from EP and ASD laptops. At the beginning of this research, the main computer was not working properly and no signal was submitted to the monitor for display. Consequently, a new graphics card was procured and installed. By doing this the hardware issue of this PC was resolved.

Also after a while working with the main PC, it was recognised that the performance of the same was very low. Therefore as part of this research, a new PC was sourced from the stock items at Curtin University. Also various software was then installed on the main PC (such as MATLAB, Labview, etc.).

3.4.3 Establishing Communications between the main PC, ASD laptop and EP laptop

After the hardware issue was resolved with the main PC, an attempt was made to connect it with the EP and ASD laptops.

A communication network was established between the main PC and the EP and ASD laptops which used an Ethernet Switch to establish the interface between these computers. The IP address settings of the computer and the laptops were set appropriately to enable communication through the Ethernet network. After installing the switch and adjusting the IP addresses, necessary checks were performed to make sure that the Ethernet communication worked properly. These checks were performed using the Windows command prompt.

The ASD laptop sent data to the PC using Modbus on the Ethernet protocol. Therefore although the Ethernet communication was established between the ASD laptop and the main PC, the Modbus communication over Ethernet needed to be established using suitable functions in the MATLAB software.

The EP laptop sent the data to the main PC using OPC over the Ethernet protocol, which is an “Open Platform Communication”. OPC is a collection of standards and methods for industrial communication. OPC includes various types of communication. The OPC DA (OPC data access) is used for real-time communication. The OPC DA protocol was used in this research to transfer the data from the EP laptop to the main PC. Setting the OPC communication between the EP laptop and the main PC was a very tedious task, with many details for OPC communication needing to be considered. The Windows setting and firewall settings were adjusted to enable OPC communication. Suitable scripting was performed in Matlab to transfer the data between the EP laptop and the main PC using OPC protocol.

For testing the OPC communication, some effort was made to find suitable software. As a result, *Matrikon* software was chosen. This software is able to recognise OPC client in computer networks and is typically used to check the OPC connection across computer networks. Then some trials were made to get familiar with the software. This software was used to check whether the main PC can recognise the Microcor software in the EP laptop which worked as an OPC client in the computer network in this project. During the first trials, Matrikon software was not able to recognise the Microcor software. There was much discussion with the supplier of the EP laptop/Microcor software to resolve this issue. A lot of work was performed on the OPC protocol, setting the OPC communication, and adjusting the Windows setting to allow OPC communication. Finally after all these efforts, Matrikon software was able to recognise the Microcor software in the EP Laptop as an OPC Client. This showed proper OPC communication between the EP laptop and the main PC.

While establishing the virtual private network between the main PC, ASD laptop and EP laptop, I faced another problem. The problem was that in order for the Matlab software on the main PC to run, the main PC must be connected to the Curtin intranet (i.e., Curtin computer network), in order for the Matlab software to obtain the necessary licence/authentication. In addition, the main PC should be connected to the Virtual Private Network to get data from ASD and EP laptops. These two different connections did not work simultaneously at first. I focussed a lot of time on this issue and finally I was able to resolve this using proper settings in Windows.

3.4.4 Procurement and Installation of the hopper

At the beginning of this research, the glass container of the existing hopper was broken and therefore the hopper could not be used. Therefore as part of this research, a new hopper was procured from a German Company '*Lambda*'. To perform this procurement, I performed many engineering activities to make sure that the new hopper would suit the purpose. For instance, installation requirements for the glass container of the hopper, the connection of the hopper with the computer, and the software for remote control of the hopper were considered. After performing all engineering activities and procurement of the hopper, the hopper was successfully installed on the flow loop. I installed the software for remote control of the hopper. Establishing communication between the hopper and the main PC took a lot of effort. Finally I was able to remotely control the hopper from the main PC using the software provided by the hopper supplier.

3.4.5 Installation of the data acquisition system for velocity/temperature sensor

At the early stage of this research, the data acquisition system was not connected to the velocity/temperature sensor. I installed this data acquisition system, and reviewed the velocity/temperature sensors and data acquisition system documentation. Also several trials were done to connect the data acquisition system to the main PC. It took some effort to read the information of the velocity/temperature sensor in Matlab software within the main PC.

3.4.6 Installation of the ASD sensor, laptop and receiving unit

At the early stage of this research, the ASD circuit (including ASD receiver, and laptop) was not installed. An understanding of how the software on the laptop was configured to read the data from the ASD was required. Also the ASD laptop must be connected to the main PC, via Modbus over Ethernet (i.e., MODBUS TCP/IP) communication between the main PC and the ASD laptop. Also the parameters on the Modbus communication need to be set in both the ASD laptop and main PC.

3.5 Selection, and preparation of sand particles

Since solid particles (which are typically referred to as *sand particles*) need to be used during any experiment with the sand flow loop, suitable solid particles need to be provided for such experiments. In this section, various details and selections to provide such solid particles were explained.

3.5.1 Selection of sand particles for experiment

For performing experiments with a sand flow loop, a suitable type of sand is needed. After doing some research, the sand from *Sibelco Company* was selected. *Sibelco* supplies sand particles for various purposes such as sand blasting and water filtration. The sand particles procured from this company were mostly composed of silica, which is one of the main components of the solids that pass along a gas production pipeline.

Table 3-1 shows the composition of the chosen sand particles from this company. The percentage of each composition is provided according to the supplier data sheet:

Table 3-1: Composition of the sand particles

Serial No	Component	Composition	Percentage
1	Silica	Sio_2	99.8
2	Ferric oxide	Fe_2O_3	0.01
3	Titanium dioxide	TIO_2	0.02
4	Alumina	Al_2O_2	0.02
5	Calcium oxide	CaO	0.01
6	Magnesium oxide	MgO	0.02
7	Sodium oxide	Na_2O	0.01
8	Others		0.11

In order to investigate the effect of particle sizes on ASD readings, sand particles need to be categorized into different particle size ranges. Since the sand particles provided by *Sibelco Company* has a wide range of sizes, they had to be sieved in order to separate them into different sizes.

To perform sieving, sieves with various mesh sizes are placed in a column. Then this sieve column is placed in the sieve machine. The bigger the sieve size range, the higher it should be placed in the sieve column. This ensures that the particles with smaller sizes than a particular sieve mesh size pass through. Then, these particles will be retained in the sieves below this particular sieve depending on their size. After performing sorting using the sieve machine, the particles were categorized according to their mean diameter. Table 3-2 shows the average particle size in each category.

Table 3-2: Average particle sizes

category	Average Particle diameter (in micron, µm)
1	350
2	450
3	550
4	655

The sieve mesh sizes used in this project were 710 µm, 600 µm, 500 µm, 400 µm, and 300 µm. These sieve mesh sizes are in accordance with ISO 565/3310-1 standard.

The medium size of the sand collected in each sieve was the average of the mesh sizes of the same sieve and the sieve on top of this sieve. For instance, the average size of the sand collected in a sieve with mesh size 300 µm was the average between 300 µm and 400 µm (as sieve with a 400 µm mesh size was installed above the sieve with a 300 µm mesh size). The same led to the segregation of the sand particles into different groups with the average sizes mentioned in Table 3.2.

3.6 Test Matrix

To understand the behaviour of the ASD under various conditions, it is required to record readings of the ASD at various sand flow rates and air velocities. A test matrix used to test the ASD in this research is explained in this section. The test matrix is a list of various conditions at which each experiment is performed. In the experiments for checking the behaviour of the ASD, sand flow rate, velocity of the air, and sand particle size are the varying conditions in the test matrix. Sand flow rate is controlled by giving various commands to the hopper. This command is used to adjust the speed of the internal motor in the hopper. Changing the speed of this internal motor causes a change in the sand flow rate.

To find out how the rotational speed of the hopper correlates to the sad flow rate, a series of tests were conducted. In each test, a known amount of sand (e.g., 1 kg) was placed in the hopper container. Then the hopper was started with a known rotational speed command. Then I measured the time period from the start of the hopper to the time the container is emptied. Since I knew the amount of sand in the container (i.e., 1 Kg) and the time period it took to inject this amount of sand, I measured the injected sand flow rate (by dividing the known sand weight into the time period). This way, I knew the actual sand flow rate (i.e., injected sand flow rate) for this particular rotational speed. I repeated this test for several other rotational speeds of the hopper. Therefore, I established the command to give to the hopper in order to get a specific sand flow rate. So by controlling the rotational speed of the hopper, I was able to change the actual sand flow rate in the pipe. I used this information for all other tests during this research where I needed to have various amount of actual sand flow rate in the pipe. It should be noted that the injected sand flow rate was the “actual” sand flow rate (as there was only one source of sand injection to the pipe which was the hopper). Therefore these two terms (i.e., actual sand flow rate and injected sand flow rate) is used throughout this thesis to show the actual sand flow rate in the pipe. In some case, I simply use the term “sand flow rate” to refer to the “actual sand flow rate” (in order not to constantly repeat the word “actual”).

In addition, the velocity of the air fluid is a varying condition in this experiment to simulate changes in gas production flow rate. The velocity of the air is adjusted by giving various commands to the VSD. The VSD changes the rotational speed of the air blower based on the command provided to the VSD. Changes in the rotational speed of the air blower also vary the velocity of the air fluid in the sand flow loop.

The sand particle size was also changed by putting the sand with various particle sizes in the hopper container. Table 3-3 shows the test matrix used in this research in which the ranges of air velocity and sand flow rates were specified.

The sand flow rate specified in Table 3-3 is the actual sand flow rate in the pipe obtained by giving suitable rotational speed commands to the sand hopper. Then I have used the signal from the ASD and ultrasonic sensor (as discussed in more detail in the following chapters) and applied various techniques to estimate the sand flow rate (as if I did not know actual sand flow rate at this stage, since in typical applications of gas wells, the operators do not know the actual sand flow rate and I tried to simulate the industrial conditions here). Then I compared the estimated sand flow rate obtained by the ASD or ultrasonic sensor with the actual sand flow rate (as in this experimental facility, we know the actual sand flow rate, since we purposely injected sand with the known sand flow rate). By comparing the estimated sand flow rate and actual sand flow rate, I understood how various techniques/sensors can accurately estimate the actual sand flow rate. The same is also discussed in other sections of this thesis.

Table 3-3: List of various air velocities and sand flow rates during flow loop test

Air velocity versus sand flow rate	5 g/s	10 g/s	15 g/s	20 g/s	25 g/s
2 m/s	X	X	X	X	X
4 m/s	X	X	X	X	X
6 m/s	X	X	X	X	X
8 m/s	X	X	X	X	X
10 m/s	X	X	X	X	X

In this table, the rows show air velocity in meters per second (m/s) and the columns show the sand flow rate in grams per second (g/s).

Also as mentioned in Table 3.2, the sand particle sizes used in these experiments were 350 µm, 450 µm, 550 µm and 655 µm.

Therefore considering there were five (5) options for air velocity, five (5) options for sand flow rate and four (4) options for sand particle size, there were 100 different conditions for the experiment. In this research, tests at all these conditions were performed and the reading of the ASD and EP stored in an Excel spread sheet for each condition. These test results were used for data analysis. The same will be further explained in Chapter 5 of this thesis.

It should be noted that several other tests were also performed to test the ultrasonic sensors used in this flow loop. Those tests were discussed in Chapter 5 of this research. Also many other trial tests were performed to make sure that the system was working properly and the data stored correctly. Those trial tests were used to check the operation of the VSD, ASD, EP, hopper, etc. Also several trial tests were performed to check the Matlab program in the main PC which collected data from the ASD, EP and velocity/temperature sensors. Altogether, a few hundred tests were performed during this research.

It should be noted that this section provides the test matrix used for research performed on the ASD. As part of this study, separate tests were performed using ultrasonic sensors to measure sand flow rates. This will be explained in Chapter 4.

3.7 Software programming of the main PC

As mentioned earlier, the main PC was used to gather all the information from the EP, ASD and velocity/temperature sensor. Also, it provided the ability to monitor the signals from these sensors and to store the data collected for each experiment. IN order to perform all these activities, MATLAB software was used in this research. MATLAB has many options to establish an interface with various pieces of hardware, and it has the capability to monitor the information, to store data, plus many other features for matrix calculation.

One of the most challenging parts of this research was establishing the interface with various pieces of hardware (EP, ASD, velocity/temperature sensor) and the main PC. As mentioned before, the ASD and EP are connected to their respective laptops and then the information is transferred from these laptops to the main PC. In brief, establishing an interface with these devices involved various aspects such as the following activities:

- Setup an appropriate computer network using suitable Ethernet switch
- Configure the IP address of Laptops and main PC
- Testing the Ethernet communication between the laptops and main PC
- Configuring the OPC setting of EP laptop

- Installing the Matrikon software on main PC and checking the OPC communication of EP laptop over Ethernet network
- Establishing an interface between the Matlab on main PC and EP laptop via OPC over Ethernet protocol
- Establishing an interface between Matlab on main PC and ASD laptop via Modbus over Ethernet protocol
- Installing the data acquisition unit from *National Instruments Company* to read the data from velocity/temperature sensor.
- Providing an interface between Matlab software and the National Instrument data acquisition unit to read the data from velocity/temperature sensor

Also the data had to be monitored to have a better understanding of the trend of the data from various sensors. Matlab would start/stop the recording of test results from various sensors. In order to provide a suitable user interface for monitoring the data and giving start/stop commands and other user interface activities, a Graphical User Interface (GUI) was developed in the Matlab environment. This creates a faceplate on the monitor including various graphical tool such as push buttons, graphs, selector switches, etc. Then the information is shared between this user interface and the rest of the program in the Matlab software. Figure 3-11 shows the user interface developed for the flow loop test facility:

Figure 3-11: Matlab GUI used in sand flow loop test

As can be seen, there are various graphs in this user interface. These graphs shows the trend of the changes in the readings from the EP, ASD and velocity/temperature sensors. These graphs provide interactive visual indications which help to understand the output of the sensors. It can also be used for troubleshooting and testing the functionality of the sensors.

Also some buttons are presented in the user interface to start/stop recording the signals from sensors. Users can provide the path (directory) of the Excel file in which the results are stored.

After the start button is pressed on the GUI user interface, the results are recorded in a matrix every second. The matrix has multiple rows and columns. Each column in this matrix shows the results for one particular sensor. For instance, there are some columns for the ASD, ER, velocity and temperature sensors. Each row in this matrix shows the test result at a certain time during each experiment. Once the stop button is pressed, recording of the test results are stopped and the data in this matrix is transferred to the Excel sheet. Each Excel sheet is stored in the path specified in the GUI user interface. Also the file name of the Excel file shows the date and the time an experiment has been performed.

Also the main PC interfaces with the hopper. The communication was established using RS485 protocol. Therefore in this research, the user works with both MATLAB software using the GUI interface and the software linked to the hopper.

As mentioned before, the results of each test at a particular test condition (i.e., articular sand flow rate, velocity of the air, and sand particle size) were recorded in one Excel spread sheet. Therefore after performing tests at various conditions (various air velocities, sand sizes and sand flow rates), several Excel sheets are generated. The next step in this research was to analyse the data provided in these excel sheets. Considering the advanced capabilities of Matlab software in a matrix operation and also its superior data analysis capabilities, Matlab software was also chosen for data analysis.

For this purpose, first the data in various Excel sheets needs to be read by the Matlab software. During this operation, the data from these Excel sheets were transferred to the variables defined in the Matlab code. This activity was performed by writing a suitable script (program) in Matlab software. Considering there were large amounts of data for each test and the number of tests performed, the total amount of data was huge. Therefore during scripting in Matlab to read data from the Excel sheets, an error was encountered during running the script. This error was created as the amount of data was larger than the default maximum amount of data which can be read in Matlab software. After some investigation, it was understood that the data limit in Matlab could be adjusted to enable dealing with large data. Therefore the default Matlab setting was adjusted to increase the amount of data which could be uploaded. Also the virtual memory in Windows was increased to enable Matlab to store big data in the memory of the main PC during running the Matlab program. After adjusting

the Matlab data limit and increasing Windows virtual memory, the issue with handling large amounts of data was rectified.

After the test results were uploaded to the Matlab environment, it was necessary to find a way to predict sand flow rate from the signal provided by the ASD. The supplier of the ASD suggested to use a relationship to convert this raw signal to sand flow rate. This relationship was explained in Chapter 2 and for ready reference, it is provide below [84]:

$$sand\ flow\ rate = \frac{ASD\ raw\ value - Zero}{Step} \tag{3.1}$$

In this relationship, it is assumed that the sand flow rate has a linear relationship with the ASD raw signal. “Zero” in this relationship is a bias to compensate for any background noise effect. The “Step” in this relationship represents the gain between the ASD raw signal and sand flow rate.

Many operators have raised concern with the accuracy of sand flow measurement with available ASDs on the market [7]. To improve the accuracy of sand flow rate measurement, it is necessary to find an improved relationship to predict sand flow rate from the raw signal provided by the ASD. To do this, various hypothesis can be considered to relate the raw signal from the ASD and sand flow rate. For instance, it is assumed that the relationship between the ASD raw signal and sand flow rate could be a non-linear relationship. Various forms of linear and non-linear relationship were considered, then optimised. This optimisation was performed by choosing the parameters in these relationships in such a way that predicting the sand flow rate using that relationship had a minimum error with the actual sand flow rate. Note that I measured the error by comparing the actual sand flow rate (which I knew beforehand, as I have given suitable command to hopper to inject the sand with required flow rate in the pipe) with the estimated sand flow rate (obtained by calculation in Matlab software).

After optimization of each of these relationships, various relationships were compared against each other. This comparison was performed by comparing the error in predicting the sand flow rates using them. The relationship with the minimum error represents the best relationship to predict sand flow rate. Table 3-4 shows various relationships considered for predicting sand flow rate from ASD raw signal. These relationships are also mentioned in the paper by Seraj and Evans [85] which we published during this research. The paper shows some of the results obtained during this research.

Table 3-4: Various relationships considered for predicting sand flow rate from ASD raw value

1	$Q = \frac{M - Z}{dV^b(1 + aD^c)}$
2	$Q = \frac{M - Z}{dV^b(1 + aD + cD^2)}$
3	$Q = \frac{M - Z}{d(1 + bV + cV^2)}$
4	$Q = \frac{M - Z}{d(1 + aD + cD^2)}$
5	$Q = \frac{M - Z}{dV^b}$
6	$Q = \frac{M^2 - Z^2}{d(d + 2 * Z)}$
7	$Q = \frac{M^2 - Z^2}{d(d + 2 * Z)(1 + bV + cV^2)}$

In this table:

D represents the diameter of the sand particles.

V represents the velocity of air.

M represents the raw value of ASD.

Q indicates the sand flow rate.

Z is the parameter considered to compensate for background noise.

a, b, c and d are constant parameters used in each of the relationships.

The optimization of each relationship was performed by selecting these parameters in such a way that the overall error in predicting sand flow rate using that relationship was minimised. As can be seen, in relationships, 1, 2 and 4, the diameter of sand particles were considered in calculating sand flow rate. The hypothesis behind these relationships was that for predicting sand flow rate from ASD raw signal, the mean diameter of sand particles would also play a role. In relationships 1, 3 and 5 of this table, a non-linear dependency between the ASD raw value and velocity of air is considered. Relationship 4 is also similar to the one suggested by the supplier of ASD [84] but in this relationship, the diameter of sand particles was taken into account. Relationship 6 is the one suggested by Odigie et al. [43] for predicting sand flow rate from the ASD raw value. The reason this is considered in the table is to compare the results obtained in this research by the one provided by previous researchers in this field. Relationship 7 is also a generalised version of the relationship suggested by Odigie et al. [43]. In this

relationship, the effect of the fluid velocity is considered as a polynomial in the denominator of the relationship. The criteria to compare these relationships was to minimize the mean error and standard deviation in predicting sand flow rate.

The results of optimizing the parameters in these relationships are specified in Chapter 5 of this thesis. Also after optimising each relationship, the mean error and standard deviation in predicting sand flow rate using that relationship is estimated in the Matlab software. The mean error and standard deviation in measuring sand flow rate using these relationships are specified in Chapter 5. Based on the mean error and standard deviation, the most accurate relationship is also explained in Chapter 5 of this thesis.

To perform optimization for each relationship, it is assumed that each parameter in this relationship can vary within a certain range. Then a matrix is considered for each parameter. This matrix has a certain number of rows (e.g. 100) and one column. The first element of the matrix is equal to the minimum value of the selected range for that parameter. The last element of the matrix is also equal to the maximum value of the selected range for that parameter. The interim elements of the matrix are selected so that it covers the range from the first element to the last element with equal increments between adjacent elements of the matrix. Similar matrices are considered for other parameters in this relationship. Consequently, a script was written in Matlab which estimated the mean error and standard deviation of predicting the sand flow rate in all elements of the matrices explained previously. This means that for all the combinations of the elements for various parameters in each relationship, the mean error and standard deviation could be calculated.

Then the sand flow rate prediction, mean error value and standard deviation were stored in a multi-dimensional matrix. After the same matrix was completed by considering all various combinations of parameter values, the minimum mean error value was found in the calculated matrix. Then the values of parameters related to this minimum mean error were obtained. These values represent the optimised selection of the parameters for this particular relationship. Then the selected parameters for the relationship (based on minimum mean error criteria) plus the mean error and standard deviation were stored for that particular relationship.

The same practice was repeated for all other relationships mentioned in Table 3-4. After optimisation was performed for all relationships, the optimised values for the parameters were obtained. Also the mean errors and standard deviations of sand flow rate measurement using the optimised parameters were obtained. These results are provided in Chapter 5 of this thesis. Using these results, I compared different relationships to find which one provided the smallest mean error.

As part of this research, the output signal from the Erosion Probe was also checked. The aim was to correlate the information from the Erosion Probe and the sand flow rate. As mentioned earlier in this thesis, a lot of activities were performed to restore the EP and related laptop. After obtaining the results from the EP and further analysis, it was realised that the reading from EP was changing very slowly. The reason for this slow change was the low amount of sand particles (less than one kilogram) injected in the flow loop test each time the experiment was conducted, which caused a low amount of erosion in EP. Since the test facility used for this research is an open loop system, it is not possible to recirculate the air-sand fluid for a long period and observe the behaviour of the Erosion Probe. Therefore it was decided not to pursue the recordings from the EP in this research any further. Instead, ultrasonic sensors were used to measure the sand flow rate. Ultrasonic sensors provide a much faster response compared with the Erosion Probes. The details of using Ultrasonic sensors for sand flow rate measurement are further discussed in the next chapter.

3.8 Summary of the chapter

In this chapter, the flow loop test facility used for this research was explained. Various components of the flow loop were explained. Also since the flow loop was not operational at the beginning of this research, various efforts were made to make this flow loop test operational. In addition, the size/material of the sand particles used for this research was explained. Furthermore, the software I developed for collecting the information from various components of the flow loop test were reviewed. Finally, the relationships used to improve the sand flow rate estimate using the ASD were explained.

4 Ultrasonic sensors and signal processing

In the previous chapters, it was explained that the reading from the Clamp-on ASD was used for measuring the sand flow rate. Since the Clamp-on ASD is widely used in the oil and gas industry especially in subsea facilities, improving the measurement of the sand flow rate using a Clamp-on ASD will have a positive impact on the operation of the gas fields.

In this research, further study was performed in using ultrasonic sensors to measure the signal created by sand particles in a gas pipe. Having the possibility of measuring a raw signal from ultrasonic sensors provides several opportunities for research. After obtaining the signals from ultrasonic sensors using a suitable data acquisition system, it is possible to apply various signal processing methods to the data obtained. For instance, the Fast Fourier Transform (FFT) of an ultrasonic signal can be obtained, to examine the relationship between the frequency content of ultrasonic signal and sand flow rate.

In the following sections, I explain the various activities I performed to obtain the ultrasonic signals. Also the various equipment used for sensing, data acquisition and signal processing of ultrasonic signal is discussed. Afterwards, the tests conducted using this equipment is mentioned. Then various analyses performed on these data are explained, and finally, the results obtained from the analysis are presented.

4.1 Revised schematic of flow loop after adding ultrasonic measuring technique

The schematic diagram of the flow loop is provided in Chapter 3 in which the ASD and EP are used to measure sand/erosion flow rates. As part of this research, the ultrasonic technique was added to the flow loop as a secondary method to measure sand flow rate. Figure 4-1 shows the schematic of the flow loop facility after adding the ultrasonic technique.

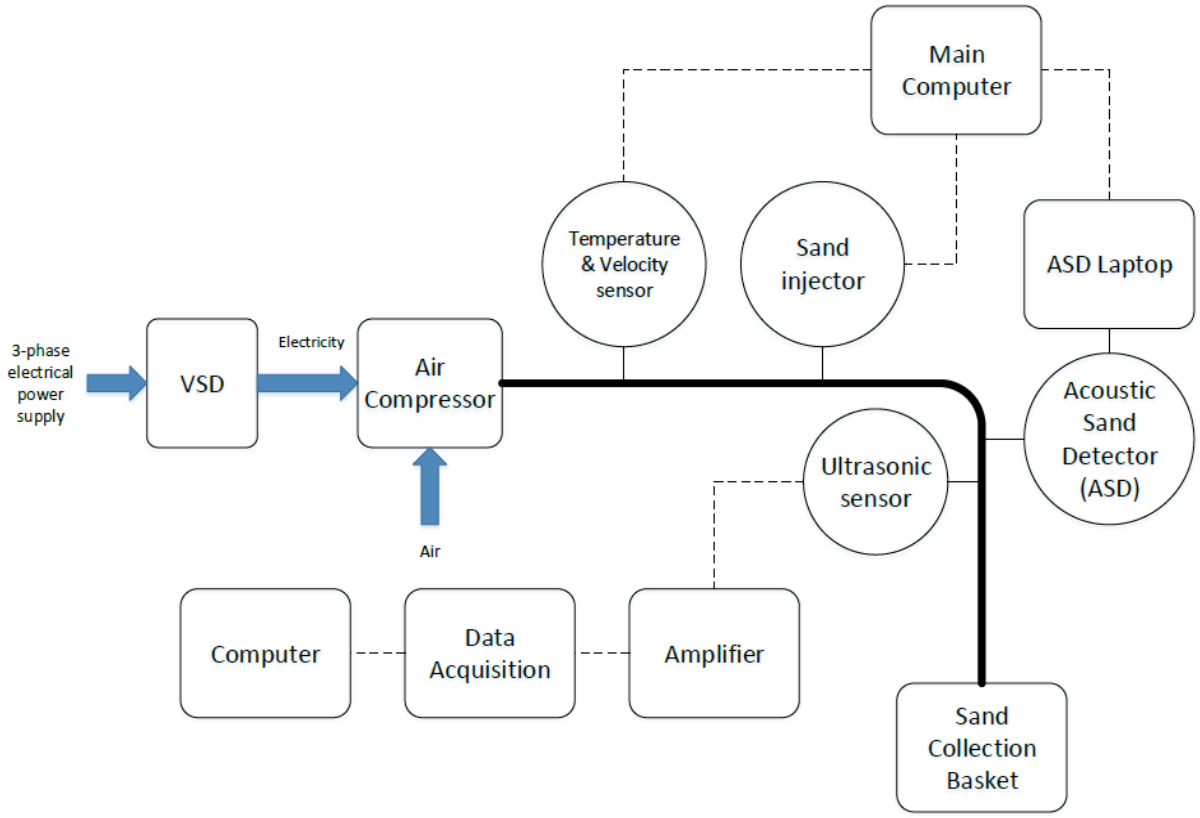

Figure 4-1: Schematic diagram of the flow loop facility after adding the ultrasonic measuring technique

As shown in the above schematic, the ultrasonic sensors were installed after the pipe bend near the ASD. The ultrasonic sensor output was connected to an amplifier, and the amplified ultrasonic signal was then connected to the data acquisition unit (which took samples of the amplified signal). These samples were transferred to a PC for collection and data analysis. In the following sections, various components of the ultrasonic measuring technique is explained in more detail.

4.2 Using an acoustic sensor to read the information about sand flow rate

In order to investigate the various hypotheses for sand flow rate measurement, ultrasonic sensors were selected for measuring the acoustic signals generated by sand particles passing through a pipe. After obtaining the ultrasonic signals generated by the sand particles hitting the pipe wall, various signal processing techniques can be applied to these raw signals. In order to have a good ultrasonic signal measurement, it is necessary to select a suitable ultrasonic sensor, in this case *Olympus*. *Olympus* is a well-known supplier of ultrasonic sensors, and have a range of ultrasonic sensors used for various applications. This company produces several types of ultrasonic sensors for

Non-Destructive Testing (NDT), for example, where ultrasonic signal is used to find any imperfections in different materials (e.g. metals). Also, NDT using ultrasonic sensors might be used to find whether the weld of any two metals has been performed without making any crack in the welding.

A high level of technology is needed for producing an ultrasonic sensor. Several factors such as reducing the natural noise of a sensor and having good signal to noise ratio is of prime importance. Also the frequency band of the sensor is another important factor.

Figure 4-2 shows the ultrasonic sensor used for this study.

Figure 4-2: A picture of the 1/2 inch diameter Olympus ultrasonic sensor used in this research

A contact-type ultrasonic sensor which can measure longitudinal acoustic waves propagated in the metal was used. These contact-type sensors must be installed in direct contact with the equipment under test (i.e., the pipe wall in this experiment). The surface of this sensor is coated with ASTM A217 grade WC5 material. The acoustic impedance of this material matches that of most metals [86], allowing acoustic signal across it. The pipe used in this experiment where sand particles pass through was made from a metal (Carbon steel), similar to most gas pipes in oil and gas applications. As the acoustic impedance of the sensor surface matched the acoustic impedance of the carbon steel pipe, this sensor allowed correct measurement of the ultrasonic signal derived from vibration of this metallic pipe (e.g. by being impacted by sand particles).

4.3 Amplifiers

In order to amplify the signal obtained from such sensors, an amplifier from a German company called *Femto* was selected. The model number of the selected amplifier was DHPCA-100. This amplifier had a very wide bandwidth of amplification. It could amplify signals from 0 Hz (DC current) to 200 M Hz.

Since ultrasonic signals are typically in the frequency range of less than 1 MHZ, this amplifier could pick up and amplify the ultrasonic signals expected.

It had an adjustable gain, which could be adjusted from 10^2 to 10^8. Using adjustable gain, the data acquisition (DAQ) system could have the best measurement accuracy. This was achieved by adjusting the gain in such a way that the maximum value of the input signal to the data acquisition was near to the maximum acceptable range of acquisition. In this way, the whole range of the DAQ system measuring scale was used without saturation of the DAQ hardware (which happens when the input to the DAQ is larger than the maximum scale value of the DAQ). For instance, if the DAQ can measure a signal in the range of -2 V to 2 V, the gain of the amplifier is adjusted in such a way that the maximum value of the amplified ultrasonic signal was also less than 2 volts, but not too much smaller than 2 V. Figure 4-3 shows the amplifier used in this research.

Figure 4-3: Amplifier used in this research

According to the manufacturer catalogue, to power up these amplifiers, both a +15 V DC and -15 VDC power source were needed. The power source should be connected to the amplifier through a special connector on the side of the amplifier. This special connector was from a company called *Lemo*. The counterpart connector on the cable which carried the power source to this amplifier was also from the same company (i.e., the counterpart connector should have a model number which matched the connector on the amplifier).

To provide an electrical power source the amplifier, a connector from same company was required. After procuring this connector, a cable is soldered to this connector. Considering the small size of the connector, special attention was made to solder these connectors to the cable in order to prevent short circuit between the leading pins. Figure 4-4 shows the procured connector before and after the cable soldering.

Figure 4-4: The connector for powering the amplifier

Figure 4-5 also shows the amplifiers after the power cables were connected to them.

Figure 4-5: Amplifiers with power cord and input/output signal connected

In this figure, the black cable connected on the left side is the input signal to the amplifier, which was connected to the output connection of the ultrasonic sensor. This cable used a BNC connector to connect to the amplifier.

In addition, the black cable on the right side of the amplifier in Figure 4-5 is the output of the amplifier. The output of the amplifier was connected to the Data Acquisition (DAQ) unit which is described in section 4.3 below. This cable also used BNC connectors at both amplifier and DAQ ends. The white cable on the right side of the amplifier carried the power to the amplifier.

Since a power source of ±15 VDC was required for powering up the amplifier, a separate power supply unit with ±15 VDC output was needed. I selected a power supply unit from a Company called *Delvin Power*. Since such a power supply with ±15 VDC output was not commonly used in Australia, the local distributor imported it.

Figure 4-6 shows the power supply unit with two power outputs connected in series. That means that the "+" port of one power source was connected to the "-" port of the other power source to make a common port, which was considered as ground. Consequently, I create +15 VDC and -15 V DC compared with the ground. The two power outputs were isolated from each other, which made it possible to connect them in series.

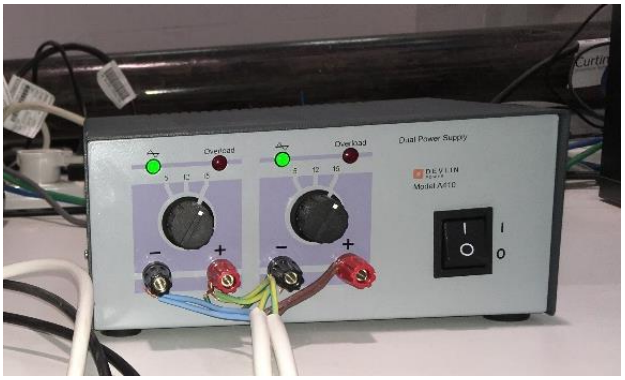

Figure 4-6: Power supply unit for powering the amplifiers

4.4 Reading the data using *National Instrument* Data Acquisition Unit

National Instruments Company manufactures a series of Data Acquisition (DAQ) systems. DAQ system from *National Instruments* model number PXI-1033 was used in this research for collecting the signal from the ultrasonic sensor, and Figure 4-7 shows this PXI-1033 DAQ system.

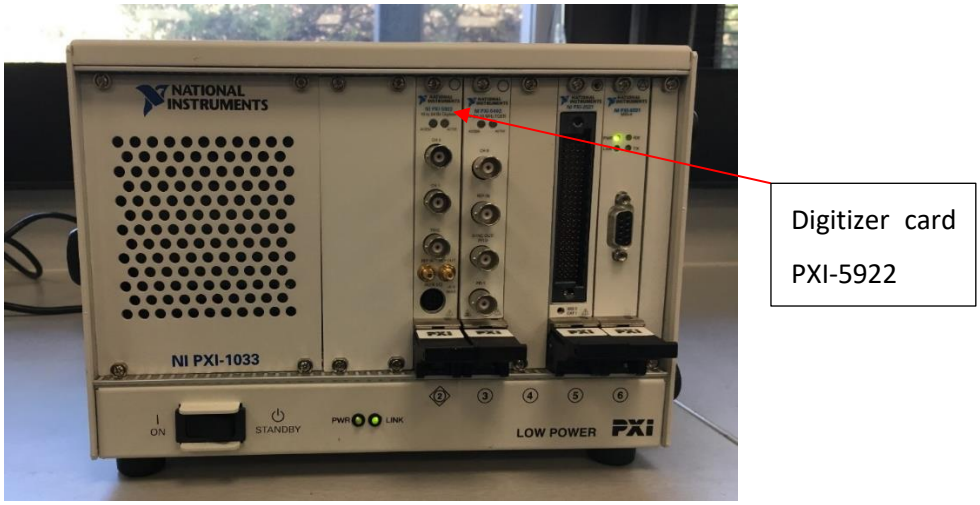

Figure 4-7: Data acquisition system (DAQ) from National instruments

As shown in this figure, a digitizer card type PXI-5922 was installed on the DAQ. This card could take samples with the speed of up to 15 MS/sec (Mega Samples per Second). Table 4-1 shows the resolution versus sampling rate of the PXI-5922 card [87]. This table shows that the PXI-5922 digitizer can take samples with a high sample rate and high resolution, taking samples of ultrasonic signals with very high accuracy.

Table 4-1: Sampling rate versus resolution of PXI-5922 card

Sample Rate	Resolution
50 kS/s	24 bits
500 kS/s	24 bits
1 MS/s	22 bits
5 MS/s	20 bits
10 MS/s	18 bits
15 MS/s	16 bits

As per the Nyquist law, the sampling rate should be at least two times the maximum frequency content of the signal. To have good sampling, it is recommended that the sampling rate be 5-10 times the maximum frequency content of the signal. In this research, in order to make sure that all frequency ranges were properly investigated, a sample rate of 2 MHz was selected. Consequently, frequencies of up to 1 MHz could be studied in this research. From Table 4-1, it can be seen that at sampling rates up to of 2 MHz, the resolution of measurement using PXI-5922 was 20 bits.

In order to see the effect of resolution on a measurement, a parameter called the "code width" can be used. "Code width" is a terminology frequently used in digitizers referring to the smallest detectable change of the digitizer which is defined as follows [88]:

$$code\ width = \frac{meaurement\ range}{2^{resolution}} \tag{4.1}$$

With this digitizer card, the measurement range was 2 Volts Peak-to-Peak for the first channel (as it measured from -1 V DC to +1 V DC in the first channel) [87].

Therefore the code width of measurement of an ultrasonic signal for sand measurement using a PXI-5922 in channel 1 was as follows:

$$code\ width = \frac{meaurement\ range}{2^{resolution}} = \frac{2}{2^{20}} \approx 1.9\ \mu\ V \tag{4.2}$$

Therefore, the PXI-5922 could measure minimum detectable changes of 1.9 µV for this application (with sampling frequency of 2 MS/s, 20 bit resolution for frequencies up to 5 MS/s). As the ultrasonic signal was amplified by the amplifier before getting connected to the DAQ, this 1.9 µV was the minimum detectable change of the amplified ultrasonic signal.

The gain of the amplifier was 1000, and the smallest detectable change in the ultrasonic sensor output in this research (using amplification gain of 1000 and sampling rate with PXI-5922 of 2MHz) was 1.9 nV (1.9 nano Volt). This value (1.9 nV) was obtained by dividing the minimum detectable signal by of the DAQ (1.9 µV) by the amplifier gain (1000). Consequently this high resolution PXI-5922 led to a very small minimum detectable value of 1.9 nV.

4.5 Signal generator

In order to perform tests with digitizer card, the Arbitrary Function Generator (AFG) card available in the DAQ system was used. This AFG card was model PXI-5402 from *National Instruments*. This card could generate any required signal shape (e.g., sine wave, square wave, etc.) at the output of this card, and so this card was used to test the signal measured by the digitizer. For example, to check whether the digitizer could measure the signal properly and the information from the DAQ device transferred to the PC correctly, a known signal (e.g., a sine wave with 10 kHz frequency) was generated by the AFG card. Then the output of this AFG was connected to the digitizer card. Since the signal measured by the digitizer (and transferred to the PC) was of the same shape (e.g., sine wave with frequency of 10 kHz), then it was understood that the digitizer communication with the PC was working correctly.

4.6 Associated software

Labview is the main software used by *National Instruments* to monitor the information provided by their hardware as well as other third-party hardware. Labview was therefore used to read the signal from the PXI-5922 hardware. MAX (Measurement and Automation Explorer) software from *National instruments* was used to identify the hardware and to establish communication with the DAQ system.

Labview stored the ultrasonic sensor data in a specially structured data format called “Hierarchical Waveform Storage (HWS)”. In order to read the signal using the HWS data format, suitable scripting was performed in Matlab Software. Since HWS has a sophisticated data format, a lot of time and effort was made to extract data from its structure.

Moreover, in order to analyse the responses obtained from ultrasonic sensors, the MATLAB program was then used. Various scripting was performed in MATLAB to analyse the response and to find a relationship between the data collected from the ultrasonic sensors and the sand flow rate.

4.7 Rectifying a Communication Issue with DAQ Hardware

In order to transfer the digitizer signal of the DAQ to the PC where Labview software was installed, an interface card was installed in the PC. This interface card was provided by *National Instruments* and installed in the PCIe (PCI Express) slot of the PC. The output port of the interface card was connected to the DAQ. One of the issues with this DAQ was that it could not communicate with the PC using the communication port at the back of this DAQ.

In the first trials, the interface card and DAQ was not recognizable in the MAX software. One of the issues with the interface card was that it did not have the bracket to install the card in the small size desktop PC. The available interface card could only be installed on the older PCs which had a large case. *National Instruments* offered the bracket for installing the interface card. This bracket is then installed on the PC. This was the first step to solve communication issue. Then suitable driver is installed on the PC to communicate with the interface card. After installing the bracket and a suitable driver, the MAX software was able to recognize the digitizer and DAQ system and communication between the DAQ hardware and the PC was established. I tried to then transfer the data from the DAQ to LabVIEW software. After a lot of attempts, it was possible to transfer the data from DAQ to Labview software and to record the results of the ultrasonic sensors.

4.8 Propagation of sound signal through metal

Since the vibration created by the sand particles hitting the pipe are conducted along the metallic pipe wall to the ultrasonic sensor, in this section I now explain how sound propagates in metal. Acoustic signals travel in metal by two primary methods which are 'longitudinal' and 'transverse' directions [89]. The amplitude of an acoustic signal attenuates (dampens) according to the formula [89]:

$$Attenuation\ in\ amplitude\ of\ acoustic\ signal\ = e^{-\delta x} \tag{4.3}$$

where δ is the dampening coefficient of the acoustic signal and x is the length acoustic signal travels in the metal. The smaller the dampening coefficient, the smaller the attenuation of the acoustic signal in the media will be.

Reduced attenuation of the signal means that the signal propagates better through the media. For instance, in sand rate measurement applications using an ultrasonic sensor, the sand particles hit the internal side of the pipe while the ultrasonic sensor contacts the outer side of the pipe. Therefore the acoustic signal should travel through the pipe wall to reach the ultrasonic sensor. The smaller the attenuation of the signal in the pipe wall, the better the acoustic signal propagates through the pipe wall to reach the ultrasonic sensor.

For instance, the dampening coefficient of aluminium is about 0.4. This means that the acoustic signal will dampen about 2.7 times every 2.5 metres. The dampening coefficient of metals are typically much less than the dampening coefficient of the other media. Therefore when we put the ultrasonic sensor on the pipe wall to measure the acoustic signal, we need to make sure that there is proper contact

between the sensor and the pipe. Otherwise any gap between ultrasonic sensor and pipe wall will cause reduced output of the ultrasonic sensor. The acoustic signal attenuates much faster in an air gap (i.e., the ultrasonic signal is unable to properly propagate through an air gap).

As shown in Figure 4-2, the ultrasonic sensor has a flat surface face. The pipe where the ultrasonic sensor was installed had a curved shape. In this research, first the ultrasonic sensor was directly fixed onto the curved pipe wall. But due to not having a good contact and weakness of ultrasonic signal, it was decided to make a contact wedge to improve the contact between the pipe and the ultrasonic sensor. To do that, a piece of aluminium was used for creating the contact between the pipe and the ultrasonic sensor. This piece of aluminium was machined to have a flat face on one side which is in contact with the ultrasonic sensor. Also it was machined to have the curved shape of the pipe on the other side which is in contact with the pipe. Since the length of this metal piece was about 7 cm (±0.1 m) as average, the dampening of the acoustic signal was around 3% in this 7 cm of aluminium. Considering this low attenuation of the signal, using this metal for creating an acoustic path to the ultrasonic sensor was acceptable.

4.9 Installing the ultrasonic sensor on the pipe

In order to measure the sand flow rates and obtain the relationship between the sand flow rate and the ultrasonic signal, the sensor must be installed on the external surface of the flow loop. It should be installed after a bend in the pipe where sand particles are passing through. When there is a bend in the pipe, then due to the momentum of the passing sand particles, they impact the pipe wall after the bend causing an ultrasonic signal vibration. As a result, by installing the ultrasonic sensor after the bend, the maximum ultrasonic signal can be obtained from such an ultrasonic sensor. During the first trials of the sensor on flow loop test pipe, the sensor was installed after the pipe bend with a clamp and without any metallic bracket. Figure 4-8 shows how the ultrasonic sensor was installed on the pipe during first trials.

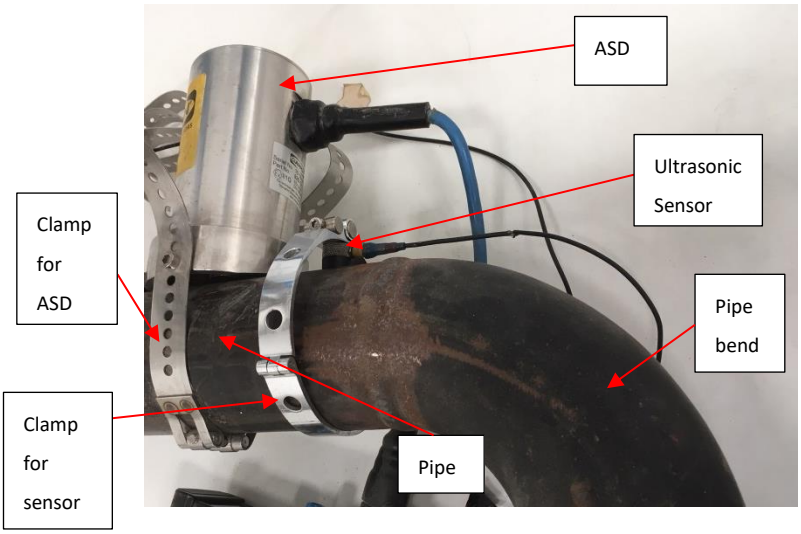

Figure 4-8: First trial for installing the ultrasonic sensor after a pipe bend

As can be seen, the ultrasonic sensor was installed on the outside bend of the pipe wall. This was the point where the probability of the sand particles hitting the pipe wall was maximum and therefore higher strength of ultrasonic signal would occur. As can be seen, the Clamp-On Acoustic Sand Detector (ASD) was also installed adjacent to the ultrasonic sensor.

After installing the sensor at this location, it was observed that the ultrasonic signal was weak. In order to increase the contact surface, it was tried to use a metal fitting having a curved surface (as explained in section 4.8). The curved surface of this metal fitting was made to match the pipe surface. The other side of this fitting had a flat surface where the sensor could be placed.

Since the clamp-On ASD should also be installed after the bend, a small space was allowed between the welding zone of the bend and the clamp-on ASD. Considering the space was small between the weld zone and the ASD, it was decided to cut the fitting into two pieces, so that each piece could be fitted in this space. Figure 4-9 shows the metal pieces after cutting.

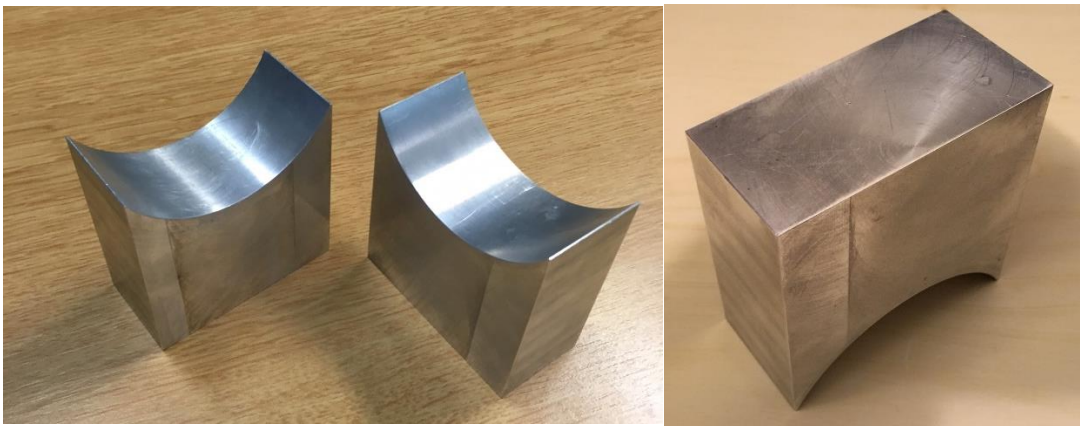

Figure 4-9: Picture of the metal pieces for creating contact between the pipe and ultrasonic sensor

Then, one of the fittings was placed on the pipe wall after the bend and before the ASD. Two ultrasonic sensors were installed on top of this metal piece. Figure 4-10 shows the picture of the ultrasonic sensor and the metal piece.

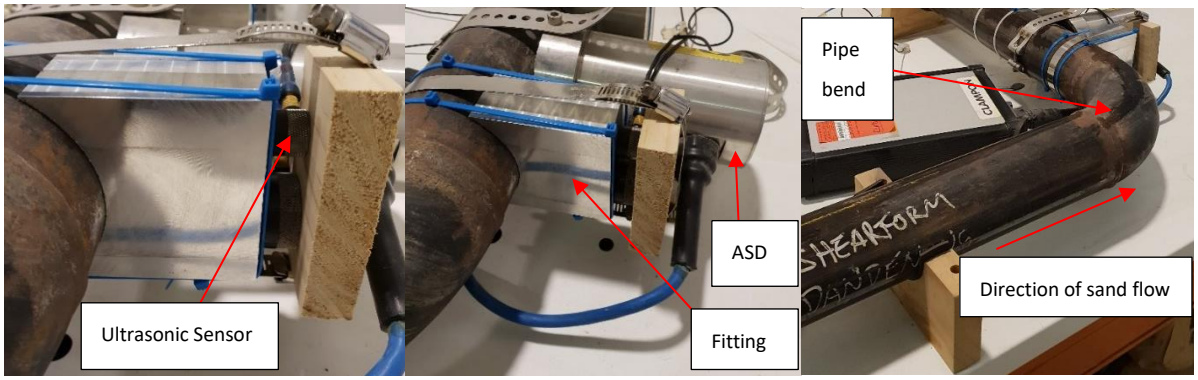

Figure 4-10: Pictures of the installation of the fitting and ultrasonic sensor after the pipe bend

After installing the ultrasonic sensor on the pipe, it was connected to the amplifier, which in turn was connected to the power supply unit. The output of amplifiers were also connected to the DAQ system and the output of the DAQ was transferred to the PC where Labview software was installed.

In the following section, the method for analysing the ultrasonic signals obtained in the flow loop test is explained. First, an explanation of the applied signal processing methods used in this research is provided.

4.10 Selecting the frequency range and sampling rate

One of the important factors in selecting ultrasonic sensors was the frequency range of these sensors and the sampling frequency of the data acquisition system. This research would use frequency domain analysis to investigate the effect of sand production in gas pipelines. In order to be able to investigate the effect of sand particles at various frequencies, an ultrasonic sensor which could measure frequencies up to 1 MHz was chosen. As mentioned in previous sections, the data acquisition system (DAQ) and the amplifier used for this experiment were also able to handle higher frequency ranges. As per Nyquist theory, the sampling frequency should be at least twice the frequency of the sampled signal. Therefore in this research, a sampling frequency of 2 MHz was chosen.

Since the data acquisition system had very high resolution (20 bit at sampling rate of 2 MHz), therefore as explained in section 4.4, the code width (minimum debatable signal at the input of DAQ) was very small (1.9 μV). Considering the amplification of 1000 in this research, the minimum detectable ultrasonic signal (resolution) was 1.9 nV. Having good resolution (1.9 nV) and wide frequency range of measurement (up to 1 MHz) enabled me to apply various data analysis methods in the frequency domain (i.e., FFT, wavelet transform and Welch methods which are explained later in this chapter).

4.11 Discrete Fourier transform

In order to perform signal processing using digital processors, typically samples are taken from continuous signals using analogue to digital convertors (e.g. DAQs). This results in a discrete version of the same signal which can be processed by digital processors (e.g. computers, etc.). Similar to the concept of the Fourier transform for continuous signals, discrete signals can also be transferred to the frequency domain. The Discrete Fourier Transform (DFT) may be used to convert a discrete signal from the time domain to the frequency domain, which is defined as follows [90]:

$$X_k = \sum_{i=0}^{N-1} x_i e^{-\frac{j2\pi ki}{N}} \qquad (4.4)$$

where x_i is a series of discrete signals, the length of this discrete signal is N, and output of the DFT is a number series of values, X_k .

The Fast Fourier Transform (FFT) is a computational way to perform the DFT algorithm. Basically, the FFT output is the same as the DFT output, but it provides a more efficient way to compute the DFT which requires less amount of computation. In this research, the sampling of the ultrasonic signals was performed by the DAQ and the results were stored in a structured format. Then this data was

transferred to MATLAB using suitable scripting. Then, the FFT of the ultrasonic signal for each test could be obtained using MATLAB signal processing capabilities.

4.12 Savitzky-Golay filter

In order to smooth the power spectra obtained from the FFT, the Savitzky-Golay filtering method was used. Savitzky–Golay filtering is a method to remove the noise in a signal. This method uses a weighting factor as shown in the following formula to obtain the estimated value at each point [91]:

$$Y_j^* = \sum_{i=-(M-1)/2}^{(M-1)/2} C_i Y_{j+i} \qquad \frac{M+1}{2} \leq j \leq n - \frac{M-1}{2} \tag{4.5}$$

where Y_j^* is the estimated value at time j. Also the Y_{j+i} is the value of any adjacent signals in a window around the j time instant. C_i is the weighting factor for each of the adjacent signals. To obtain this weighting factor, this method assumes number series has a polynomial structure [91]. The polynomial structure has the following form [92]:

$$p(n) = \sum_{k=0}^{N} a_n n^k \tag{4.6}$$

where N is the order of the polynomial, which is fit to the data set. At any given point, n, the value of the signal, $p(n)$, is obtained by this polynomial value. To obtain the coefficients of this value, $2M + 1$ samples around $n = 0$ are considered. Then, the polynomial coefficients are estimated using a least squares approach [93]. This method identifies the coefficient in the above polynomial so that the error in the following relationship is minimized [92]:

$$\varepsilon_n = \sum_{n=-M}^{M} (P(n) - x[n])^2 = \sum_{n=-M}^{M} \left(\sum_{k=0}^{N} a_n n^k - x[n] \right)^2 \tag{4.7}$$

where M is the number of adjacent points which are considered when estimating the polynomial coefficients. Once the coefficients of the polynomial, a_n, are obtained by minimizing the error in this relationship, then the estimated value at point $n = 0$ is obtained in the polynomial relationship. Therefore, the estimated value at point $n = 0$ is equal to:

$$y[0] = p(0) = a_0 \tag{4.8}$$

This process is repeated for every sample point. To apply the Savitzky-Golay filter, the order of the polynomial, N, is selected as well as the number of adjacent points, M. Figure 4-11 shows the response time of the Savitzky-Golay filter in the frequency domain [92]. In this graph, the frequency response is shown as normalized and M is selected as 16. This means that the frequency is divided by the sampling

frequency. It can be seen that the bigger the value of N, the bigger the frequency band of the Savitzky-Golay filter.

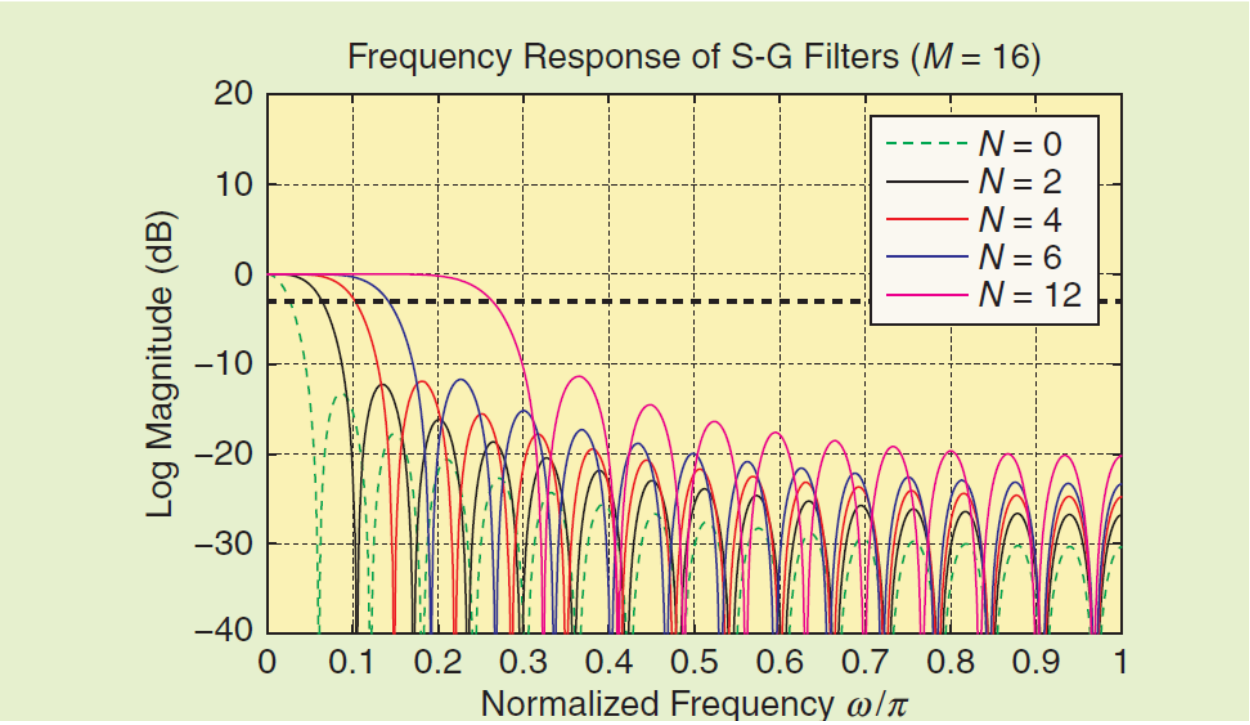

Figure 4-11: Frequency response of the Savitzky-Golay filter

The number of points considered for Savitzky-Golay estimation $(2M + 1)$ is larger than the number of coefficients in a polynomial estimation $(N + 1)$, while the order of polynomial (N) should not be too large to obtain good results [92].

The other important factor in selecting the number of points for Savitzky-Golay estimation $(2M + 1)$ and the order of polynomial estimation (N), is the passband frequency of the Savitzky-Golay. The passband cut-off frequency is the frequency where the gain of the Savitzky-Golay filter is 3 dB less than the gain of Savitzky-Golay filter at zero frequency. Amplitude gain of the filter is defined as $20\ Log_{10}|H(e^{jw})|$ where $H(e^{jw})$ is the frequency response of the Savitzky-Golay filter. Figure 4-12 shows the normalized bandpass frequency of the Savitzky-Golay filter for various values for M and N [92]. In this research, the Savitzky-Golay filter is used to smooth any FFT response. Applying the Savitzky-Golay filter is performed in MATLAB.

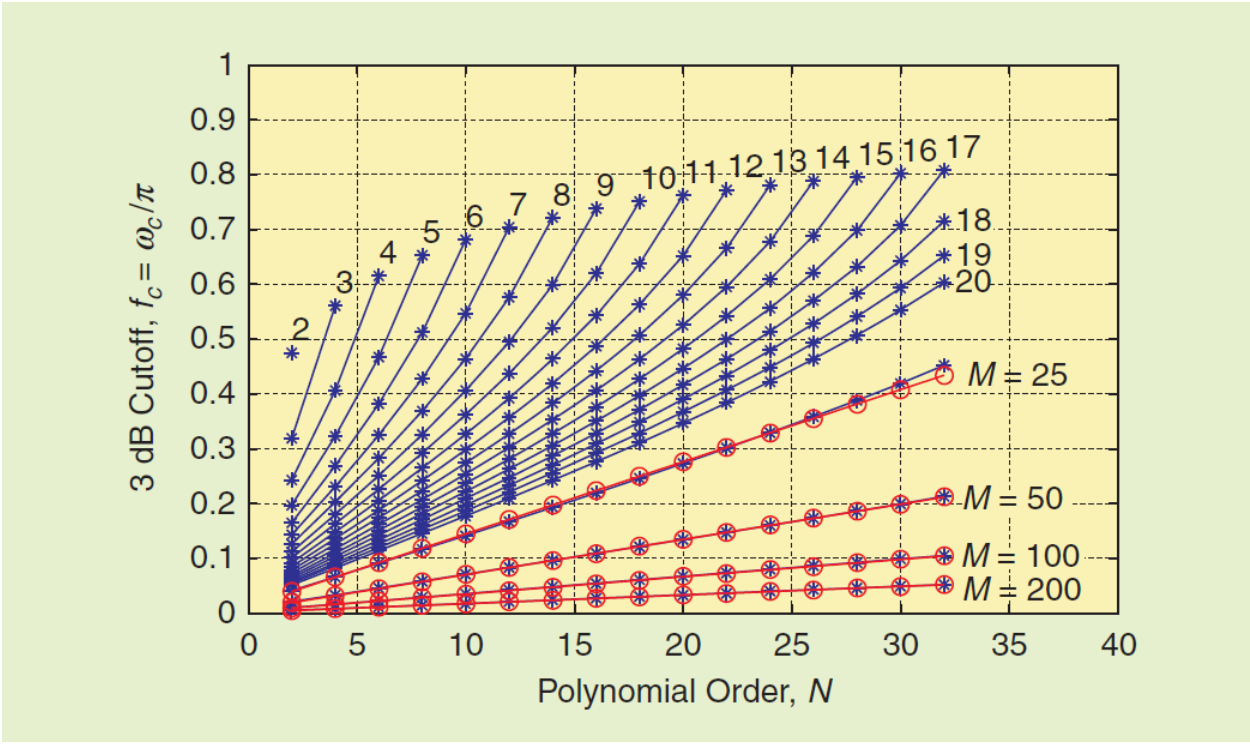

Figure 4-12: Relationship between cut-off frequency, the polynomial order (N) and number of adjacent points (M)

4.13 Analysing the ultrasonic sensor signal using FFT method

The first method chosen to analyse the signals obtained from the ultrasonic sensor was the FFT, and this section explains the analysis performed using the FFT method. After setting up the ultrasonic sensors, the amplifier and the signal conditioning unit, various tests had been performed to collect the data from the ultrasonic sensors under various experimental conditions. In these tests, different sand flow rates and air velocities were tested. Different sand flow rates were obtained by giving appropriate commands to the sand hopper. Also various air velocities were obtained by giving suitable commands to the Variable Speed Drive (VSD) for the air blower. Figure 4-3 shows the test matrix for these experiments.

Table 4-2: Test Matrix for ultrasonic sensor

Sand flow rate versus fluid velocity	0 m/s	1 m/s	3 m/s	5 m/s	7 m/s	9 m/s	11 m/s	13 m/s	15 m/s	17 m/s	20 m/s	24 m/s	27 m/s
0	X	X	X	X	X	X	X	X	X	X	X	X	X
5 g/s		X	X	X	X	X	X	X	X	X	X	X	X
15 g/s		X	X	X	X	X	X	X	X	X	X	X	X
25 g/s		X	X	X	X	X	X	X	X	X	X	X	X
35 g/s		X	X	X	X	X	X	X	X	X	X	X	X
45 g/s		X	X	X	X	X	X	X	X	X	X	X	X

In this table, the rows show sand flow rate in grams per second (g/s), and the columns show the air velocity in metres per second (m/s). Various experiments were performed using 60 different conditions (plus the one at zero velocity and zero sand rate). The results from these tests were collected, and a MATLAB program was used to read the results from these sensors for comparison purposes. Figure 4-13 shows the average frequency response (FFT) of the ultrasonic signals at various fluid velocities. This FFT was obtained over a wide range of frequencies (up to 1 MHz).

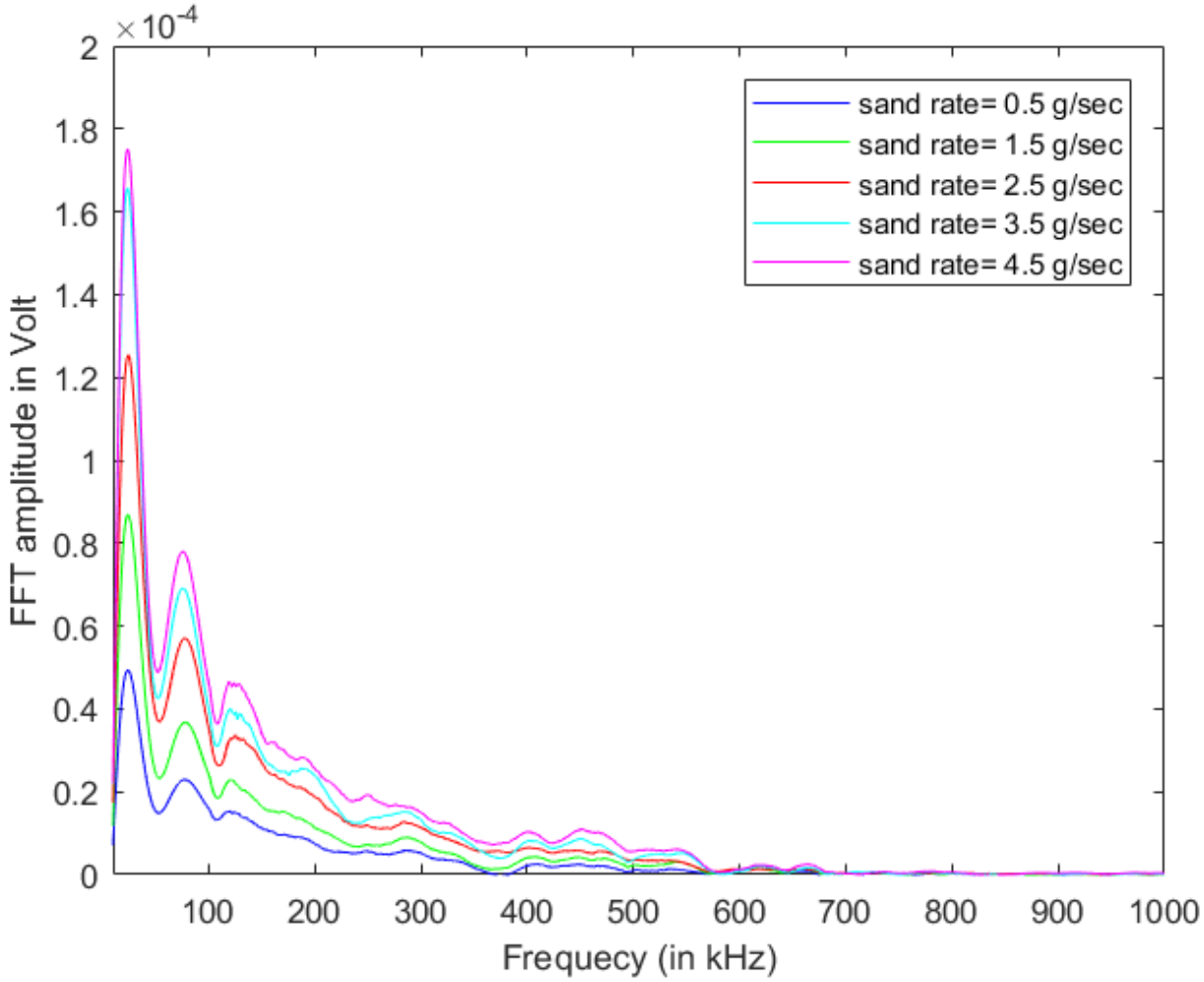

Figure 4-13: Average of FFT signal from ultrasonic sensors collected at various sand flow rates

In this Figure, the FFT of the ultrasonic signal was obtained at various sand flow rates. Each colour in this graph shows the average FFT signal for a particular sand flow rate. For instance, the purple colour in this graph shows the average of FFT signals at various fluid velocities when the sand flow rate was 4.5 g/sec.

As can be seen, the amplitude of the FFT curve is greater when the sand flow rate is higher. For instance, the sand flow rate at 0.5 g/s shown by the blue colour is the lowest amplitude. In addition, the sand flow rate of 4.5 g/s shown with a purple colour is generally greater in amplitude than the other curves.

The difference in amplitude between the curves for various sand flow rates are greater at the lower frequencies. At frequencies above 550 kHz, the difference between the curves is so small that they cannot be distinguished from each other. That is, when using the FFT method to identify the sand flow

rate using the ultrasonic sensors, it is advisable to look in the lower range frequencies (e.g. below 550 kHz).

Figure 4-4 shows the FFT in the lower range of the spectrum. In this case, the FFT of the ultrasonic response is depicted when the sand flow rate is zero (i.e., no sand is injected into the pipe). As mentioned, the FFT of the ultrasonic response is more dependent on sand flow rate in frequency ranges less than 550 kHz.

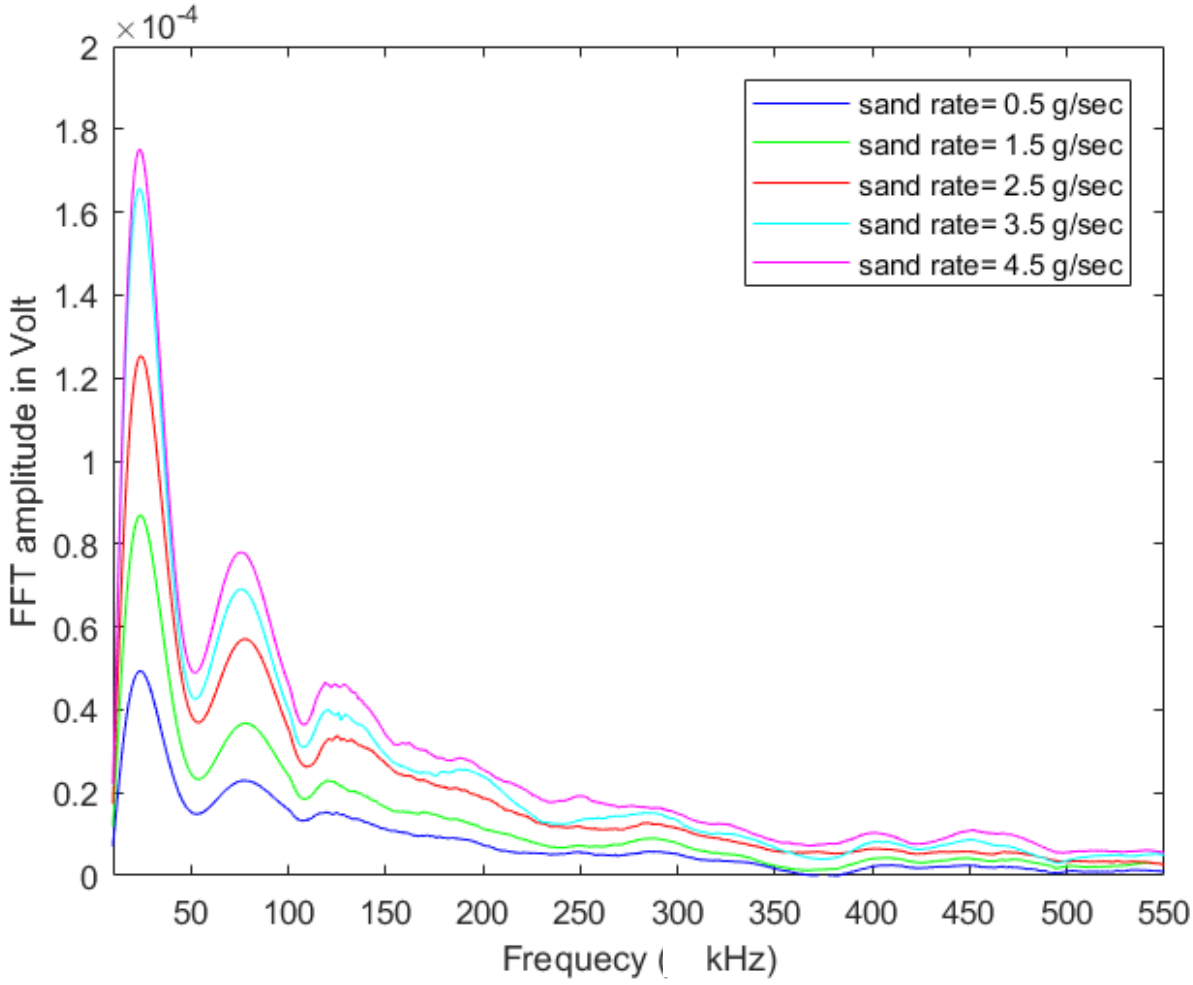

Figure 4-14: FFT of Ultrasonic signal in the selected frequency range

The FFT signal is very sensitive to sand flow rate in the frequency range from 0 to 50 kHz. Therefore, the frequency range below 50 kHz is considered in further detail. Figure 4-15 shows the FFT range in the frequency range of 10-50 kHz.

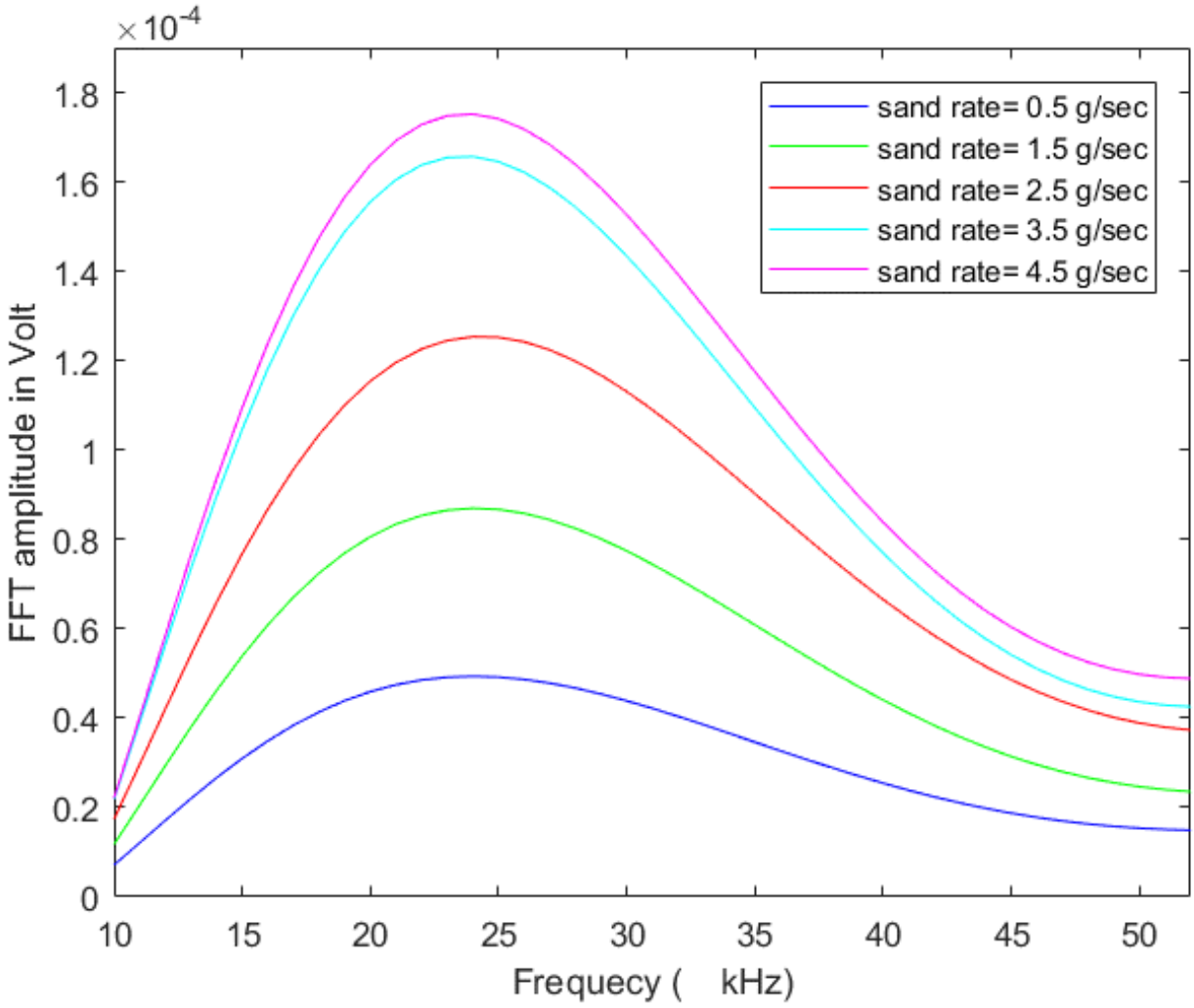

Figure 4-15: FFT of the ultrasonic signals for different sand flow rates at 10 - 50 kHz frequency range

It can be seen in this figure that the FFT signal has a peak around a frequency of 25 kHz for all sand flow rates. Also it can be seen that the maximum peak of the FFT is getting bigger as the sand flow rate increases. This observation was the basis of the idea of relating the sand flow rate to the peak value of the FFT signal in the frequency range of 10-50 kHz. This idea was tested after trying to relate various features of the FFT signal with sand flow rates. While many other features of the FFT signal did not show as good a relationship with the sand flow rate, the peak value of the FFT was best. To evaluate this idea further, the peak value of the FFT signal was plotted against the sand flow rate. Figure 4-16 shows the FFT signal peak value versus the sand flow rate.

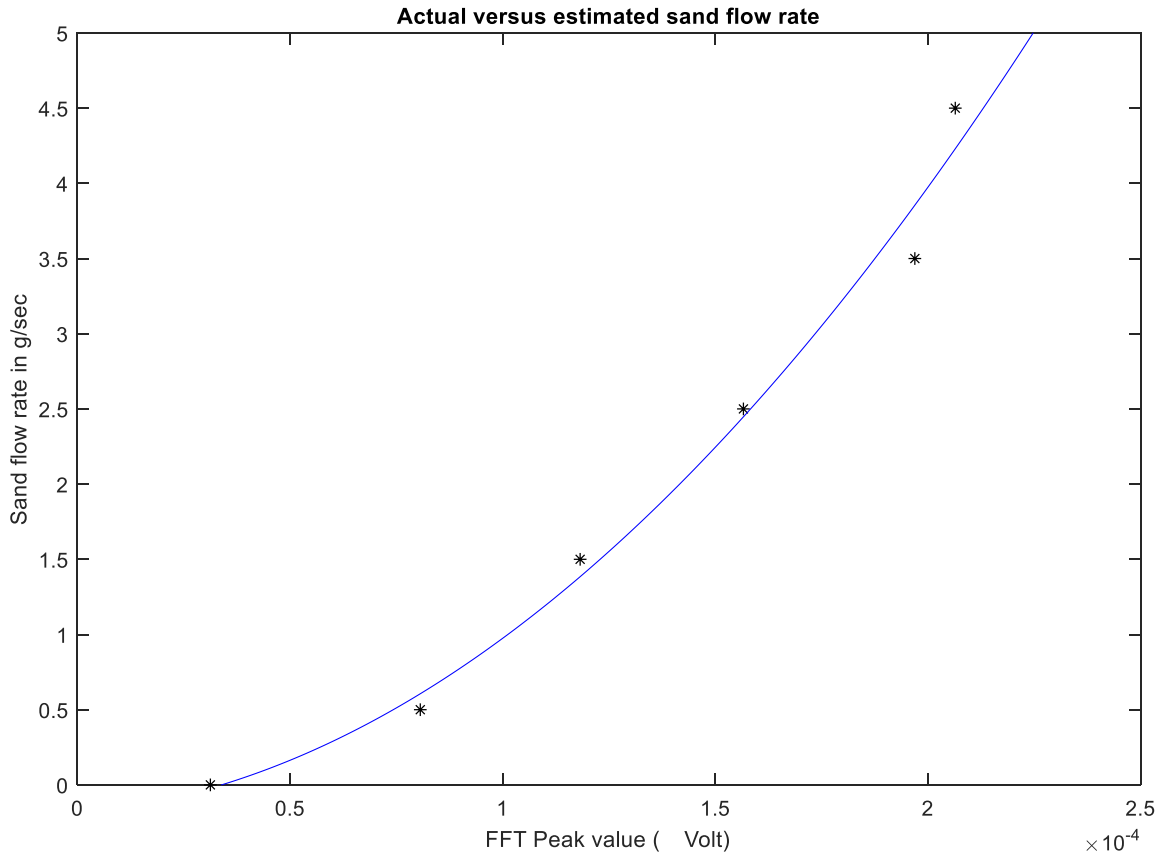

Figure 4-16: Peak value of FFT signal versus sand flow rate

The asterisks in this figure shows the actual sand flow rate versus the FFT representation, and the solid line in this figure shows the two-degree polynomial fit to these points. It can be seen that the two-degree polynomial is a very close approximation to actual sand flow rate. The only issue with this polynomial is that at zero flow rate, the peak value of the FFT matrix is not zero. The reason for this is that at zero flow rate, there could be some ultrasonic signal which is generated from other sources rather than sand particles vibrating the pipe wall.

In order to reduce the bias produced by reading a noise value at zero sand flow rate, the FFT peak value at zero flow rate was deducted from the FFT peak value at other sand flow rates. Figure 4-17 shows the FFT peak value minus the FFT peak value at zero flow rate, at various sand flow rates. The asterisks shows the points representing the FFT of the actual sand flow rates minus the FFT at zero sand flow rate, and the solid line shows a new second-degree polynomial fit to these points.

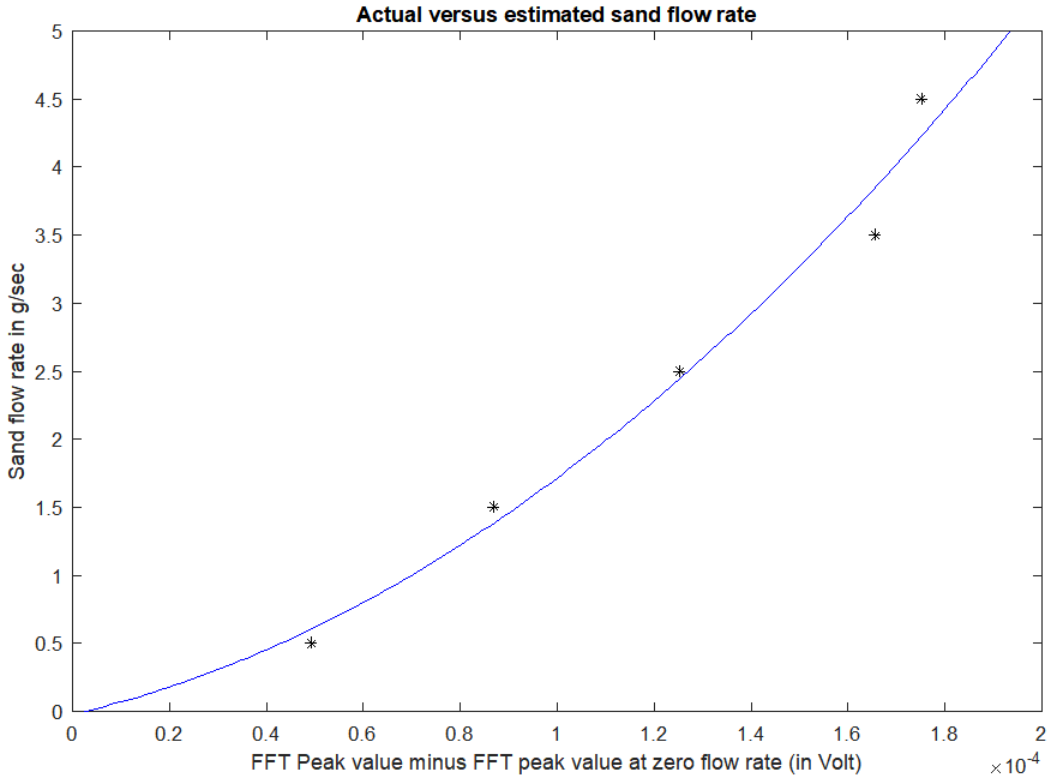

Figure 4-17: Actual versus sand flow rate estimation

As can be seen in the Figure 4-17, this second degree polynomial provides a good estimation of the sand flow rate. Also this polynomial can be extrapolated back to the vicinity of a zero value on the X axis. This second-degree polynomial then passes very close to the reference point (coordinate [0, 0]). This indicates that if this second-degree polynomial is used for sand flow rate calculation, then it can predict very small amounts of sand flow rate (near zero sand flow rate) with reasonable accuracy.

I provide the second-degree polynomial obtained in this research. This polynomial correlates the peak value of the FFT signal to the sand flow rate:

$$Q = a\,(F - F_0)^2 + b(F - F_0) + c \quad \text{where } a=9.1823*10^7,\ b=8.1929\text{x}10^3,\ c=-0.0221 \qquad (4.9)$$

In this relationship, Q is the sand flow rate, F is the peak value of FFT signal between 10 kHz and 50 kHz, and F_0 is the peak value of FFT signal at zero flow rate in this frequency range.

A similar second-degree polynomial can be used in other applications where an ultrasonic sensor is installed. Then the calibration must be performed to obtain the parameters a, b , c for that application. The calibration must be performed in a way the experiments were performed in this research, and in order to obtain these parameters for each application, a few experiments need to be

performed. In each experiment, ultrasonic signals must be obtained when a known amount of sand flow rate is injected into the pipe. After obtaining the ultrasonic signals and getting the FFT value for each case, the maximum value must be determined for each case. Then the curve fitting needs to be performed to correlate the maximum value of FFT signal to the sand flow rate. The parameters obtained from this curve fitting can then be used replacing the parameters in the previously mentioned relationship.

Since the second-degree polynomial is obtained for an average value of the FFT signals over various air velocities, the question may arise whether the same second-degree polynomial works well for each individual velocity. Figure 4-18 [85] shows the sand estimation using the FFT amplitude method compared with the actual sand injection rate for various air velocities.

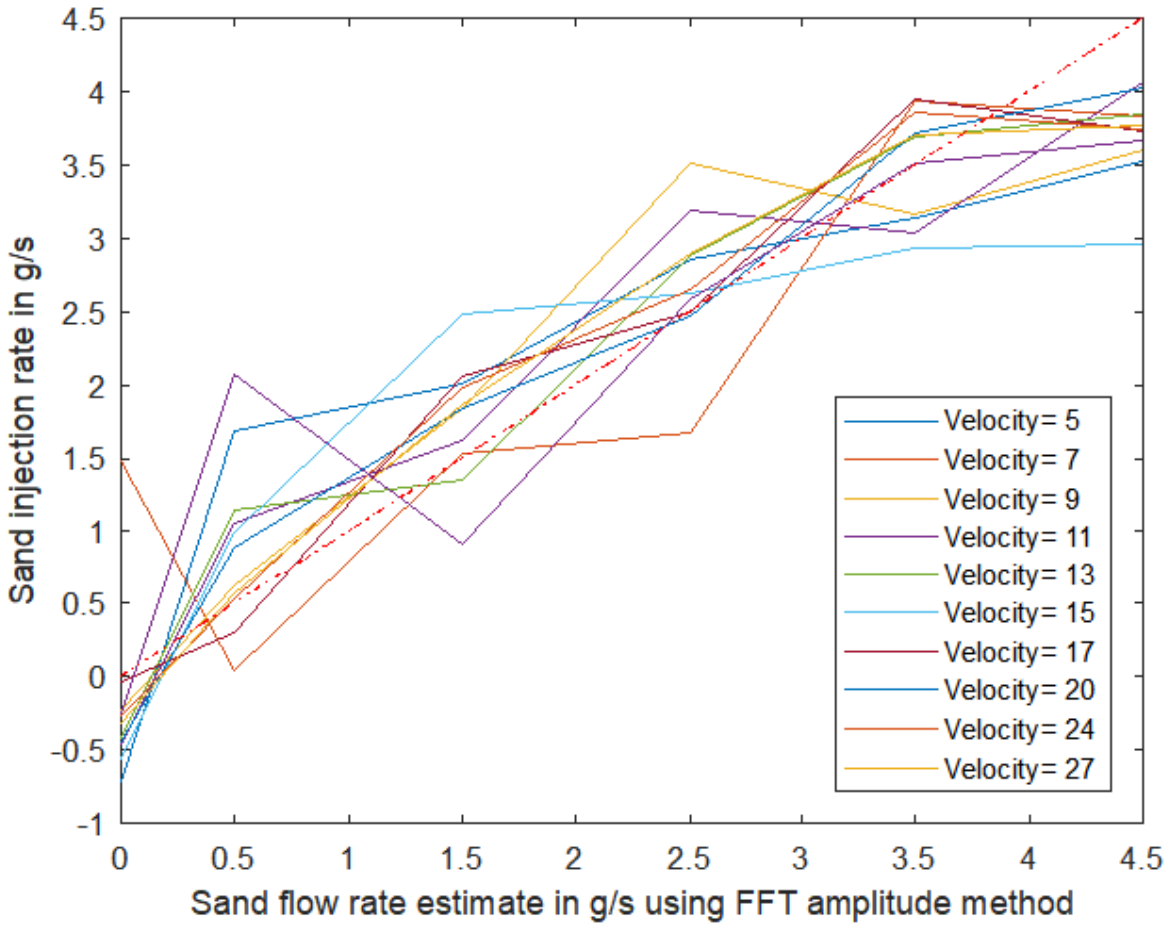

Figure 4-18: Prediction of sand flow rate at various air velocities using two-degree polynomial

As can be seen in this figure, the FFT method can measure the sand flow rate at various air velocities quite accurately. The dotted line in this figure shows the ideal case where the estimated flow rate exactly matches with the actual sand injection rate. The closer the estimation curves are to this dotted line, the more accurate is the estimation of sand flow rate. From this figure it can be seen that the estimation curves at various velocities are generally close to the dotted line for various fluid velocities and sand flow rate. Also it can be seen that the closeness of the estimation at different velocities does not depend on the sand flow rate (i.e., the estimation at higher and lower velocities are showing similar patterns around the dotted line). This is a proof that the sand flow rate estimation using an FFT signal eliminates the necessity of measuring fluid velocity.

In many applications, the velocity of the gas phase is not known. Therefore having a method to predict the sand flow rate without the need for knowing the velocity of the gas is a good achievement. For instance in many typical subsea wellheads, flow meters may not be available. In such cases, a knowledge of gas velocity cannot be easily obtained. In these cases, if the ASD is to be installed on the wellhead, then there may be difficulty to use the sand flow rate calculation methods which need the gas velocity. Typically in these applications where a flow meter is not available, some indirect method to estimate fluid velocity is used. For instance, in subsea wellhead applications where an actual flow meter is not available, the differential pressure across the choke and the opening percentage of the choke might potentially be used to estimate the fluid velocity. Using such methods substantially increase the uncertainty in sand flow rate estimation. In this case, this velocity estimation is easily affected by changes in fluid property (e.g. viscosity), non-linear behaviour of differential pressure versus choke opening, etc. So the proposal provided in this research for using a two-degree polynomial and FFT signal greatly simplifies the calculation of the sand flow rates, as this method does not need the gas velocity.

When conventional methods are used in such applications, sometimes a more sophisticated method may be used for predicting fluid velocity. For instance, virtual flow metering software may be used for such applications and the velocity is estimated from the virtual metering, and so estimated velocity is used for sand flow measurement [94]. Using virtual flow metering needs extra measurement from various pressure and temperature sensors as well as a simulation model to predict flow rates. The model must be calibrated using well testing data [95]. Finally the accuracy of the velocity estimation using virtual flow metering software is not as accurate as the velocity estimated by physical flow meters, and this results in further uncertainty of sand flow rate estimation. Furthermore, it increases the complexity and capital cost of a project. Therefore the method suggested in this research simplifies the control system design by eliminating the need to use various methods to predict the gas velocity.

4.14 Analysing the ultrasonic sensor signal using wavelet transform method

In this section, the wavelet transform method which was used in this research as an alternative approach to analyse the data obtained from the flow loop, is explained. A wavelet is a rapidly decaying wave like an oscillation with a zero mean. Figure 4-19 shows a typical Morlet wavelet [96].

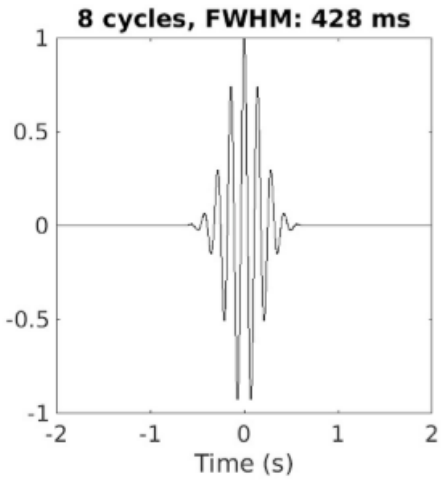

Figure 4-19: A typical Morlet Wavelet

As can be seen in this figure, the wave shape is over a certain time period and is zero outside this period. In the wavelet transform method, a signal can be represented by a series of wavelets, in similar manner to the FFT method where a signal is represented by a series of sinusoidal signals.

As mentioned in Chapter 2, the wavelet transform is a more advanced analytical method compared with the FFT method. While the FFT transforms a signal from the time domain to the frequency domain, the wavelet transform method converts a signal from the time domain to the time-frequency domain. Converting the signal to the time-frequency domain helps to identify the frequency component of a signal at various time periods. To better illustrate this issue, Figure 4-20 shows a typical "scalogram" of the wavelet transform of an ultrasonic signal collected from the ultrasonic sensor at a fluid velocity of 7 m/sec and sand rate of 3.5 g/sec. This scalogram shows the strength of signal using different colours, and in this case, the strength is in the unit of V^2 (Volt to the power of 2).

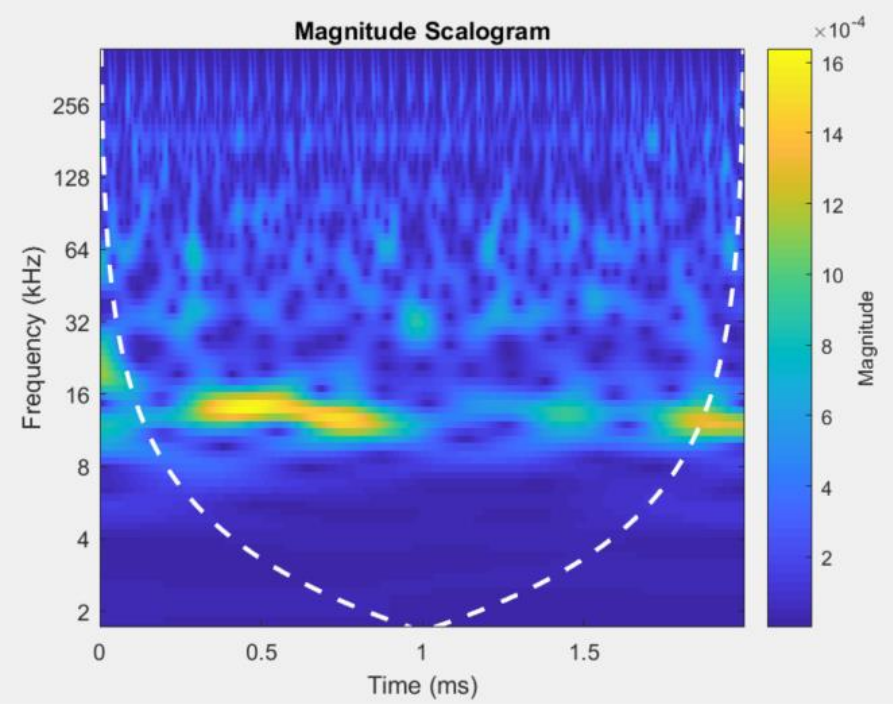

Figure 4-20: Scalogram of wavelet transform for ultrasonic signal at fluid velocity of 7 m/sec and sand rate of 3.5 g/sec

The dotted cone shape is the “cone of influence”. The data inside the cone (above the dotted line) is trust worthy, and free of computational edge effect, also known as “Boundary Effects”. The information near the cone (near dotted line) and outside the cone (below the dotted line) is not trustworthy due to “Boundary Effects”. This is due to the fact that the signal is finite (with a limited amount of sampling). Therefore when a wavelet transform is applied to the data, when the wavelet reaches the end of the data set, the wavelet spills over from the edge of the data set. Figure 4-20 shows the boundary effect for a finite data set [97].

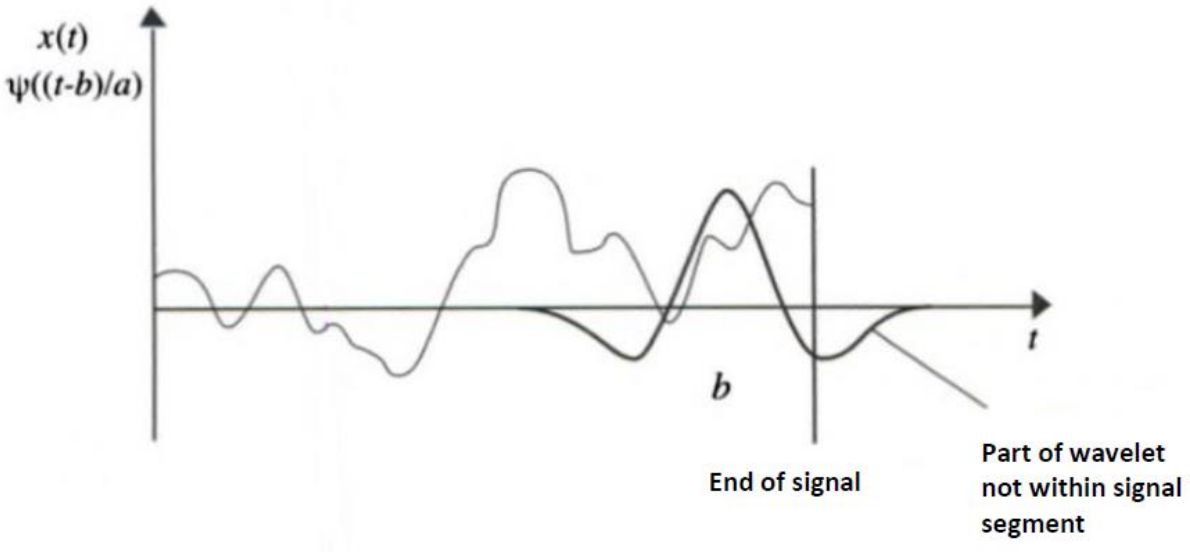

Figure 4-21: An example of boundary effects in wavelet transform for a finite data set [97]

In this figure, a typical signal is shown by the lighter line. The wavelet is represented by the darker line. During calculation of the wavelet transform, the wavelet is shifted in time. As can be seen, when the wavelet is close to the end of the signal, then part of the wavelet is not within the signal segment, and instead data is zero. Therefore the results of the wavelet transform near the end of the signal are erroneous compared with when the wavelet is within the signal segment.

As can be seen from this figure, the magnitude of the signal has higher strength in frequencies around 15 kHz. Also it can be seen that the strength of the signal at frequency of 15 kHz changes over time. For instance, the strength of signal at 15 kHz is more in the time domain around 0.5 sec compared with 1.5 sec. Note that in this experiment, the ultrasonic signal was recorded for 2 seconds. Therefore the wavelet transform is a suitable tool for analysis of the signals which varies over time (non-stationary signal). Figure 4-22 shows the Scalogram of the wavelet transform of an ultrasonic signal at a fluid velocity of 17 m/sec and sand rate of 35 g/sec.

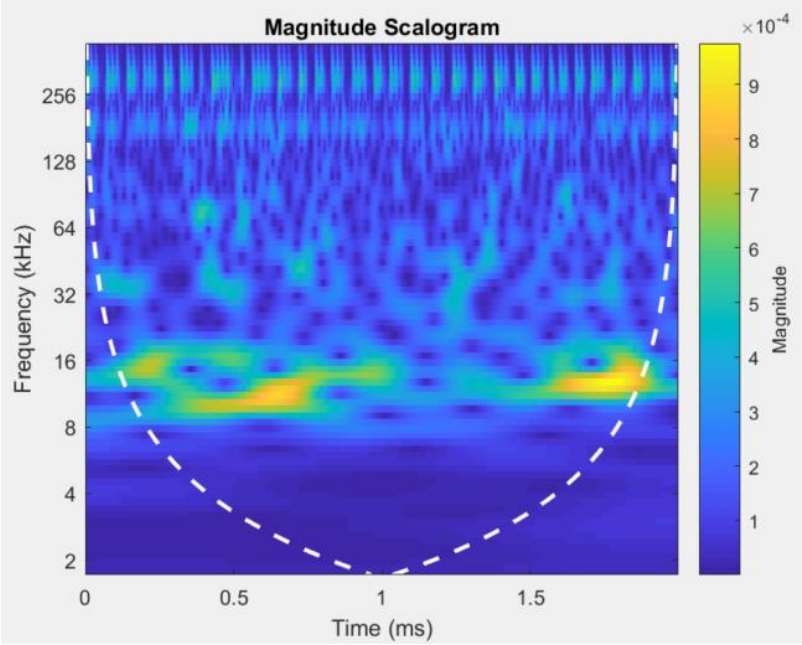

Figure 4-22: Scalogram of wavelet transform for ultrasonic signal at fluid velocity of 17 m/sec and sand rate of 35 g/sec

Figure 4-23 shows the Scalogram of the wavelet transform of an ultrasonic signal at a fluid velocity of 17 m/sec and sand rate of 15 g/sec. As can be seen in Figures 4-22 and 4-23, the wavelet frequency shows strong output at frequencies around 15 kHz. This is in line with the results obtained from FFT analysis.

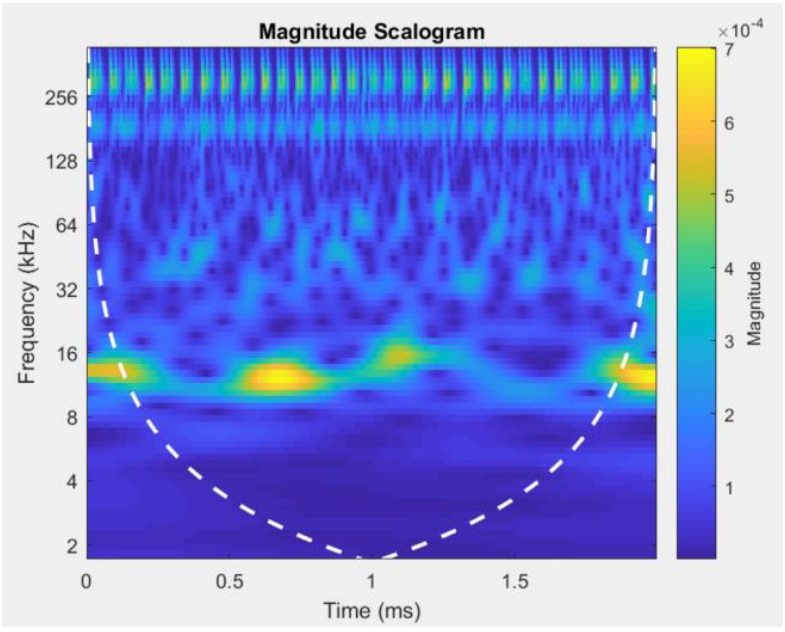

Figure 4-23: Scalogram of wavelet transform for ultrasonic signal at fluid velocity of 17 m/sec and sand rate of 15 g/sec

In the wavelet transform, the frequency domain is divided into various intervals. For example, in this application where the maximum frequency for sampling was set to 1 MHz, the frequency intervals were defined as follows in Table 4-3:

Interval 1	500 kHz to 1 MHz
Interval 2	250 kHz to 500 kHz
Interval 3	125 kHz to 250 kHz
Interval 4	62.5 kHz to 125 kHz
Interval 5	31.25 kHz to 62.5 kHz
Interval 6	15.625 kHz to 31.25 kHz
Interval 7	7.8125 kHz to 15.625 kHz
Interval 8	3.90625 kHz to 7.8125 kHz
Interval 9	1.953125 to 3.90625 kHz

Table 4-3: Frequency intervals of wavelet transform used in this study

As can be seen above, in each division, the frequency range is divided by two. The same can also be seen in Figure 4-24. Note that in this Figure, for each frequency interval, the strength of the wavelet coefficients (sum of the squares of wavelet transform coefficients) are calculated.

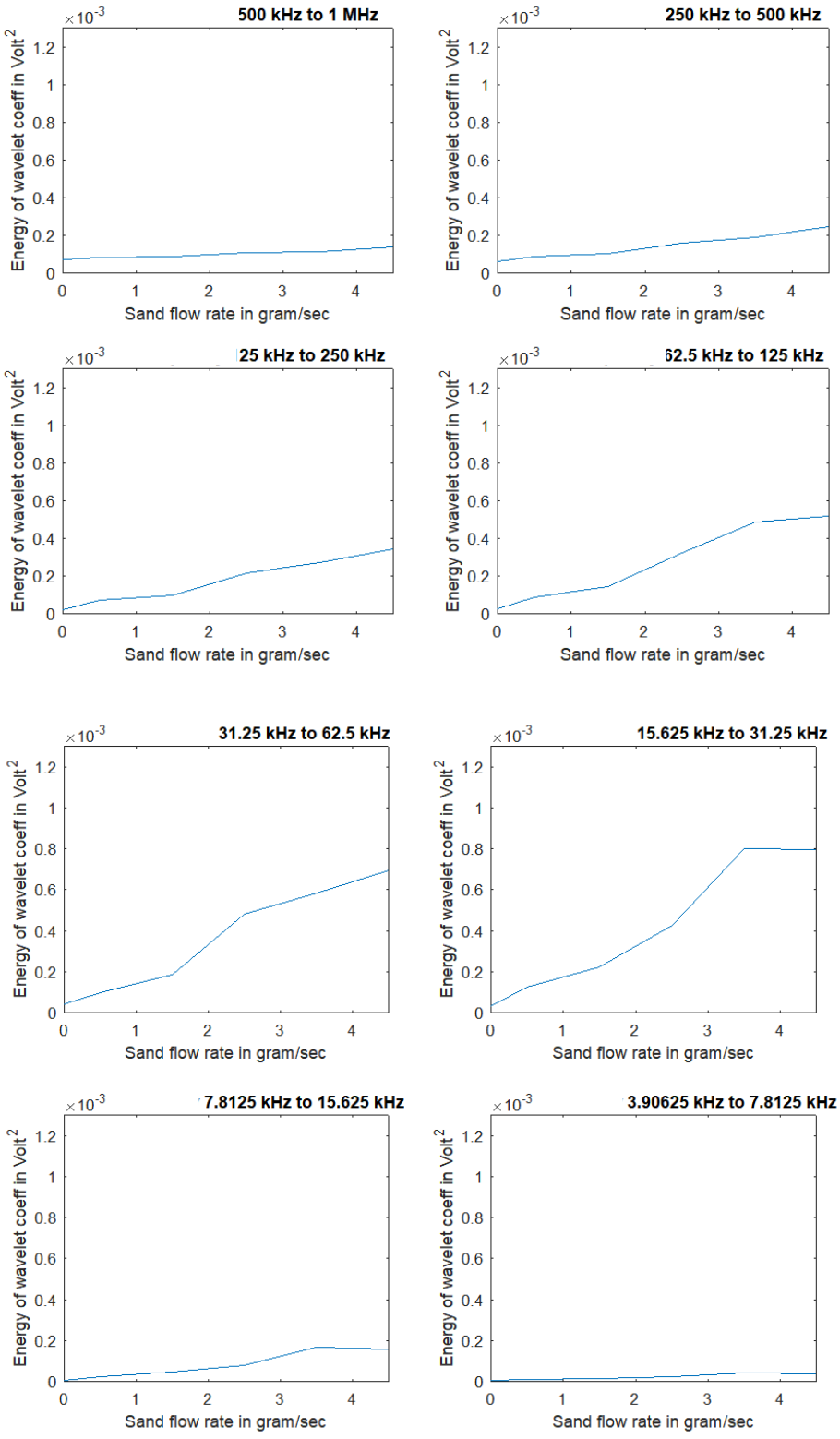

Figure 4-24: Wavelet transform of Ultrasonic signal at various frequency ranges

X-axis in Figure 4-24 shows the sand flow rate in gram per second. The Y-axis in this figure shows the sum of the wavelet coefficient at that frequency interval (what is referred to as “strength of wavelet

transform"). As can be seen in this figure, the wavelet response is much stronger at two frequency intervals (i.e., frequency range 31.25 kHz to 62.5 kHz and frequency range 15.625 kHz to 31.25 kHz).

In order to get the best response in these two frequency ranges, I add the strength of wavelet coefficients in both of these frequency ranges. Figure 4-25 shows the sum of strength of wavelet coefficients in these two frequency ranges against the sand flow rate.

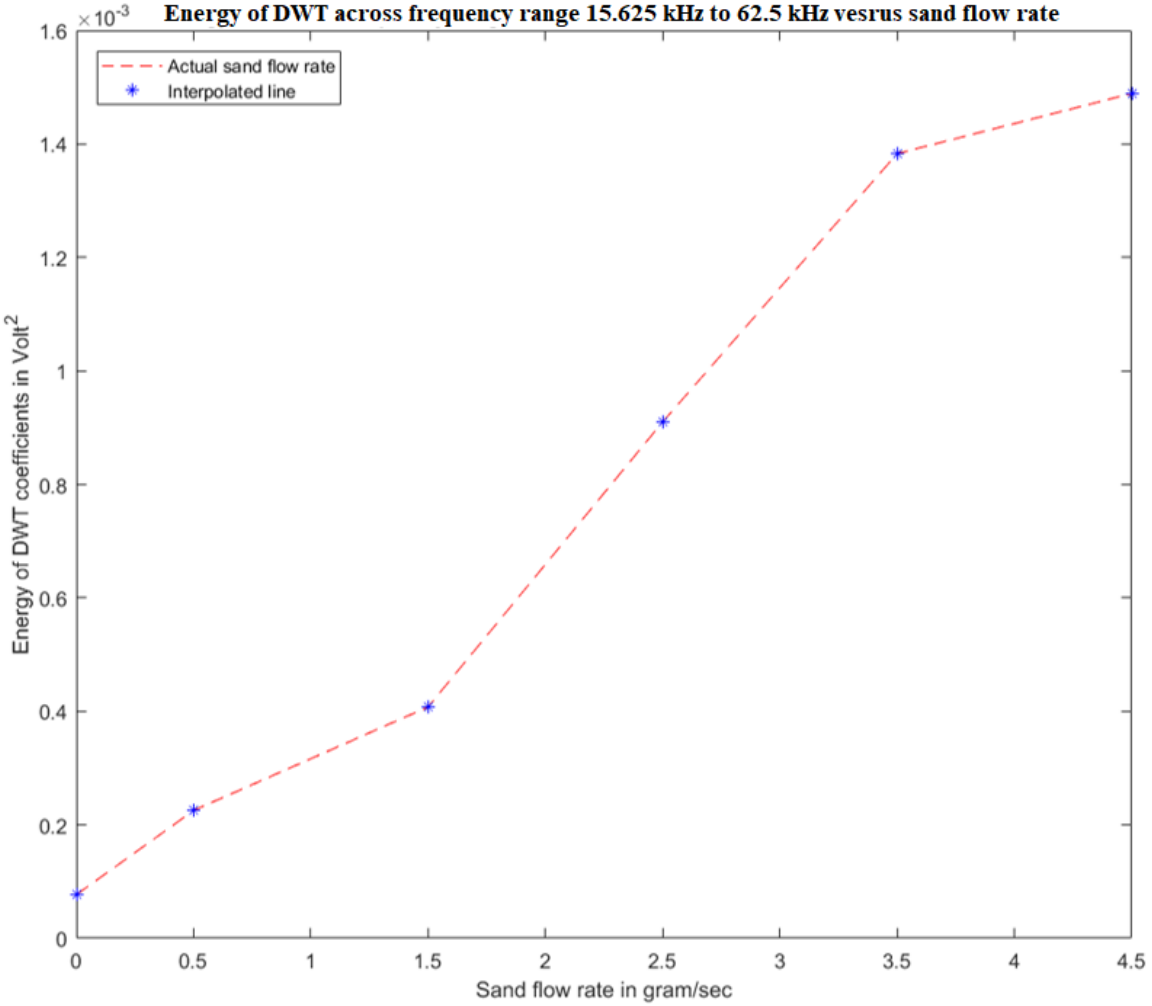

Figure 4-25: Sum of wavelet coefficients across two frequency ranges versus the sand flow rate

In this Figure, the values shown indicate the Energy of DWT coefficients and the dashed line is showing the interpolation between these values. As can be seen in Figure 4-25, the energy of the wavelet coefficient in the frequency range 15.625 kHz to 62.5 kHz is increasing in almost a linear fashion with the increase in sand flow rate. Considering this approximate linear relationship, a linear curve can be fit to the strength of the wavelet coefficient in the frequency range 15.625 kHz to 62.5 kHz, and Figure 4-26 shows this:

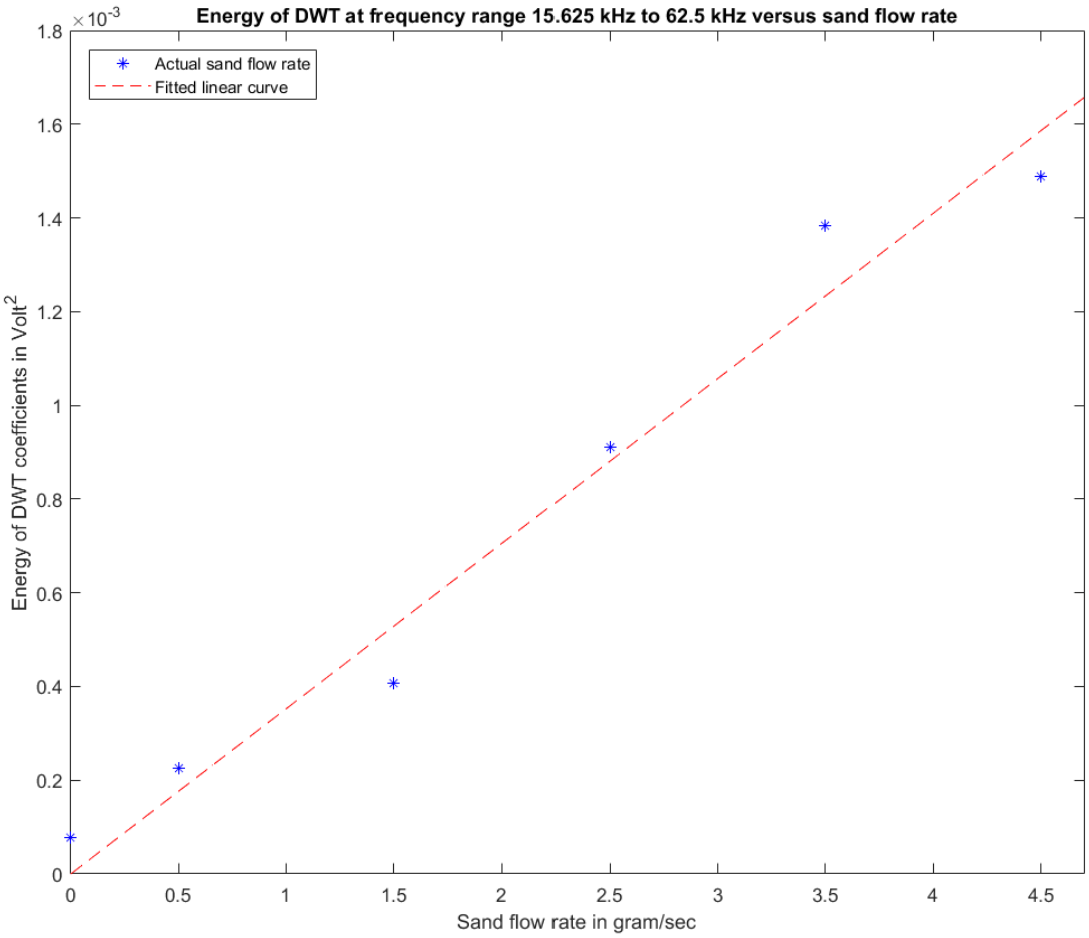

Figure 4-26: Linear curve fit to the DWT point in frequency range from 15.625 kHz to 62.5 kHz

In Figure 4-26, the dashed line shows the best linear curve fit to the data. Also each asterisk shows the actual data collected from the wavelet transform. It should be noted that in order to have a good estimation at small sand flow rate, the linear curve was fit with the constraint that it should pass through the origin (coordinate 0, 0) in this figure. It can be seen that the line is a good approximation to the actual data.

This linear relationship between the strength of the wavelet coefficient (sum of squares of wavelet coefficient) over a frequency range from 15.625 kHz to 62.5 kHz is provided as a new relationship:

$$Q = a\,P \quad \text{where} \tag{4.10}$$

$$a = 2837$$

In this relationship, Q is the sand flow rate (in g/s), and P is the sum of the squares of wavelet coefficients of an ultrasonic signal in the frequency range 15.625 kHz to 62.5 kHz (in Volt^2).

Equation 4.10 provides a very easy way to estimate sand flow rate using an ultrasonic sensor and the discrete wavelet transform. It should be noted that in industry, it is preferred to have a simple relationship due to the resulting simplicity of implementing it in the control system.

Also it should be noted that parameter a in equation 4.10 must be obtained for each application during the calibration process. Since there is only one parameter to be estimated during calibration, therefore calibrating sand flow rate using the wavelet method is an easy task for the operator comparing to the calibration procedure for typical sand detectors in the market where few parameters need to be obtained at various velocities. In this case, fewer tests are required to obtain enough data for the calibration of this one parameter.

To examine how much the strength of the wavelet transform coefficients over a frequency range of 15.625 to 62.5 kHz depends on the velocity, MATLAB analysis was used. Figure 4-27 shows this strength at various velocities.

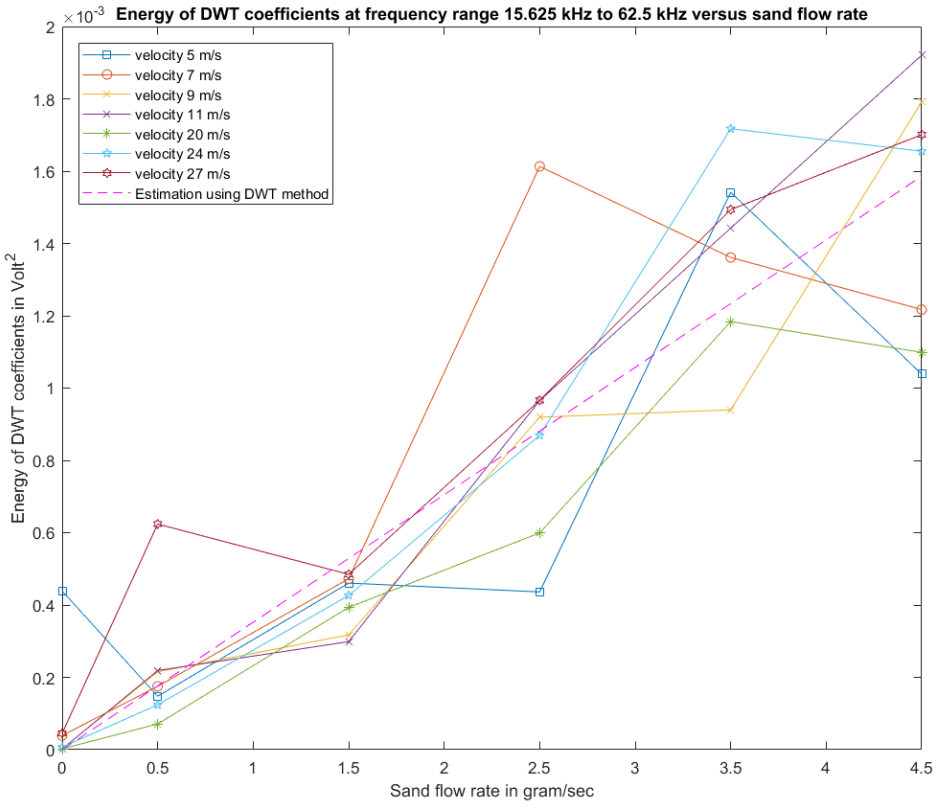

Figure 4-27: Energy of DWT coefficients over frequency range 15.625 to 62.5 kHz at various velocities

It can be seen in Figure 4-27 that DWT curves for various fluid velocities are located around the dashed line (represented by equation 4-10). Therefore the linear equation 4.10 provides a good estimation of the sand flow rate at various velocities.

4.15 Analysing the ultrasonic sensor signal using the Welch method

Welch [98] proposed a technique for estimating the spectral density of the signal (PSD). Similar to a Fourier transform, the Welch method transforms the signal from the time domain to the frequency domain. PSD is generally used for analysis of a stochastic signal. The ultrasonic signal created by sand particles hitting the pipe wall shows stochastic (non-deterministic) behaviour due to the large number of sand particles and also various characteristic of sand particles (e.g. shape, size, density, velocity, etc.). Therefore the Welch method is a good nominee to perform further analysis of the ultrasonic signal in this application.

One of the advantages of the Welch method is that it has good noise cancelling features compared with the Fourier Transform. In contrast, the frequency resolution of the Welch method is less than the Fourier transform. Since the signal from an ultrasonic sensor used in sand measurement is often accompanied by various noises, therefore the Welch method may be a suitable technique for this application.

As explained in section 2.7.4, in the Welch technique, first the signal is divided into various segments in time. These segments have some overlaps. Then the DFT method is applied to each segment. Then the DFT for various segments are squared and averaged to obtain the Welch spectral density. Due to the sudden change at the edge of each segment, there could be some unwanted introduction of high frequency components after the DFT is calculated for each segment. In order to avoid such unwanted high frequencies, a tapering window is applied to each segment before taking the DFT.

Figure 4-28 shows the sum of power spectral density (PSD) over a frequency range from 1 to 200 kHz for various fluid velocities. It can be seen that the sum of the PSD at various velocities generally follow a linear pattern with the sand flow rate (i.e., increase in the sand flow rate leads to increase in PSD in almost a linear fashion).

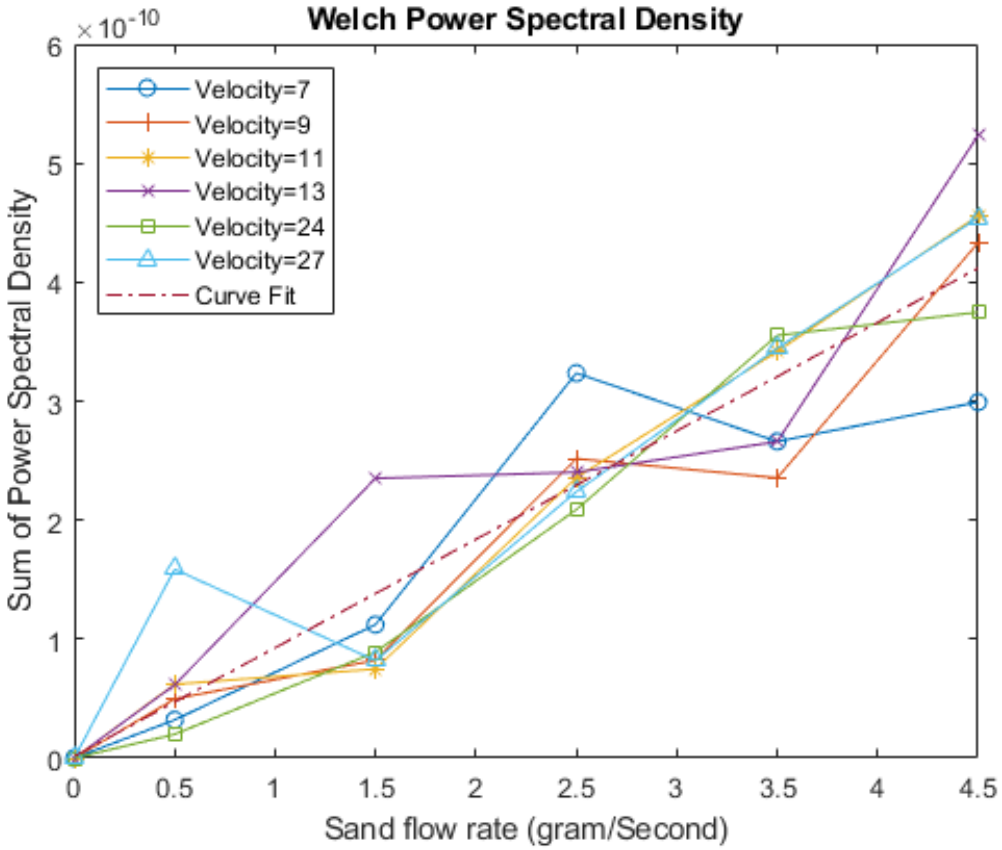

Figure 4-28: Sum of Power Spectral Density for various velocities

In Figure 4-28, the dotted line is the linear relationship fit to the average of the sum of the PSD at various velocities. It can be seen that the PSD values at various velocities are close to this linear relationship, and so this shows that the PSD signal is not dependent on the fluid velocity.

The following shows the method to estimate the sand flow rate from the PSD of the signal from an ultrasonic sensor.

$$Q = a\,P \qquad (4.11)$$

$$\text{where} \quad a = 0.9115 \; x \; 10^{-10}$$

Q is the sand flow rate. P is the PSD of the signal obtained using the Welch method. This relationship provides a simple method for estimating the sand flow rate from the PSD signal of any ultrasonic sensor obtained using the Welch method.

4.16 Summary of the chapter

This section presents an overview of experiments performed and summarizes the results obtained from applying various signal processing techniques to ultrasonic data to measure sand flow rate. First, the details of the installation of ultrasonic sensors and ultrasonic circuit were explained. These details included various hardware and software equipment/activities. On the hardware side, it has been mentioned that there were several issues with setting up the data acquisition system available in the lab. For instance, a few accessories were missing in the available data acquisition system. Also to power up the ultrasonic amplifier, a new power supply unit was ordered. Special connectors were procured to provide power supply to the amplifier. Also to have a good contact between the ultrasonic sensor and the pipe, a metallic support fitting was machined. Finally all the equipment (the metallic support, ultrasonic sensor, the amplifier, power supply and data acquisition system) were installed on the flow loop.

On the software side, it has been mentioned that various options for reading the signal from the sensor were investigated. Then Labview software was installed on the computer. There were many issues with the interface between the data acquisition system and the Labview software. For resolving the interface between the DAQ and Labview of the PC, a lot of investigation was performed. It was found that the supplier had another specific software (NI MAX) which helped to identify the hardware pieces and establish communications. Therefore this software (NI MAX) was installed. After many trials, the interface between the DAQ and Labview was established. Also it took a lot of effort to be able to read the data in LabVIEW software and to record the data provided by the ultrasonic sensor.

Afterward, many experiments were performed to obtain an ultrasonic response at various loop-operating conditions. These conditions included various fluid velocities and sand flow rates. Then the results of these experiments were stored in a special structured format.

The readings from these experiments are input into the MATLAB software using suitable scripting. Then the FFTs of the signals for various tests were calculated in MATLAB. Afterwards, the analysis of the FFT signals was performed to find a relationship between the FFT signals and the sand flow rate. After various analyses and testing various hypotheses, it was observed that the peak value of FFT signal in a range of 10 kHz to 50 kHz had a relationship with the sand flow rate. This observation was further investigated. After the investigations, a second-degree polynomial was obtained to correlate the signal from the ultrasonic sensor with the sand flow rate.

It was then explained how the DWT method would be used to analyse the signal from the sensor. For doing this analysis, the strength of the DWT signal was obtained at various frequency bands. It was noted that the DWT signal is stronger in a frequency interval from 31.25 kHz to 62.5 kHz and frequency

interval from 15.625 kHz to 31.25 kHz. The DWT signals in these two frequency response were then added. It was then found that there was a linear relationship between the sum of the DWT signal in these two frequency ranges and the sand flow rate. This linear relationship is therefore suggested as a useful estimate for sand flow rate using ultrasonic signals and the DWT analysis technique.

Finally in this chapter, it was explained how the Welch method was used to analyse the ultrasonic signal. After applying the Welch method, the PSD of the signal was calculated in the frequency range from 1 to 200 kHz. It was found that the sum of the PSD signals in the frequency range from 1 to 200 kHz has a linear relationship with sand flow rate. Therefore this linear relationship was suggested as an estimate of the sand flow rate using an ultrasonic sensor and the Welch analysis technique.

In conclusion, it was explained how three different techniques (i.e., FFT, DWT and Welch) were applied to analyse the signals from an ultrasonic sensor. For each of these techniques, a relationship was found to estimate the sand flow rate using the ultrasonic sensor. This new knowledge later resulted in the publication of two peer-reviewed papers.

5 Results and discussions

5.1 Overview

In chapter 3 of this thesis, the flow loop used for testing the Acoustic Sand Detector (ASD) was explained. Also various test conditions where an ASD was tested were explained. In this chapter, first I review the various hypotheses used to correlate an ASD's output with the sand flow rate. Then I provide the results for each hypothesis and compare these hypotheses based on these results. Finally I introduce the best hypothesis for predicting sand flow rate from an ASD output.

5.2 Analysis of the output of the ASD

One of the aims of this research was to improve the measurement of sand flow rate using an ASD. To perform this activity, a flow loop test facility was used where a mixture of sand and air was passing through. An ASD was installed on this flow loop and the reading of this ASD was stored in the computer. The velocity of the air, sand particle size and sand flow rate could be adjusted by the operator.

To understand the behaviour of the ASD in response to various parameters such as air velocity, sand particle size and sand flow rate, several tests were performed. During these tests, the following parameters were changed:

- Velocity of the air
- Sand particle size
- Sand injection rate

After performing several tests on an ASD under various conditions, I tried to find the relationship between the ASD output and various parameters such as sand flow rate, fluid velocity and sand particle size, all of which are useful information when sand is an issue in gas pipelines.

In order to use these parameters to estimate sand flow rate, the results of various tests were read in Matlab software using suitable scripting. By importing the results of various tests into the MATLAB environment, its data analysis and programming capabilities could be used.

Afterwards, it was necessary to find the relationship between ASD output and other parameters. Various types of relationship were considered for predicting the sand rate. These relationships would relate the sand flow rate to the ASD output and other physical parameters (e.g., air velocity, and sand particle size). In each of these relationships, it was possible to change different coefficients. The optimum coefficients in each relationship were obtained by minimising the error between the actual sand flow rate and the estimated sand flow rate. In order to obtain optimum coefficients in each relationship, a lot of effort was made in scripting in MATLAB. Various features of MATLAB such as the capability to work with multi-dimensional matrices were used during this scripting.

Then the best associations were selected between these relationships. The criteria for the selection of the best relationship (among those nominated in this research) was to minimize the mean error and standard deviation when predicting sand flow rate. In the following sections, various relationships were used for estimating the sand flow rate.

5.2.1 Relationship with velocity and particle size exponent factors

The first relationship for estimating the sand flow rate was as follows:

$$Q = \frac{M-Z}{dV^{b}(1+aD^{c})} \tag{5.1}$$

In this relationship, Q is the estimated sand flow rate, M is the ASD output, Z is the ASD output when there is no sand flow rate and was created by the background noise, V is the velocity of the fluid, D is the average diameter of the particle size. In addition, a, b, c, and d are the coefficients in this relationship. In this relationship, it was assumed that the estimated sand flow rate is dependent on the ASD output, background noise, fluid velocity and average diameter of particles. This relationship is similar to the Gao et al. [35] proposal for sand flow rate measurement, but it is more generalised than the Gao et al. relationship in the sense that it would consider the effect of sand particle size. Also it does not consider a fixed exponent of two for fluid velocity, rather it considers a parametric exponent factor for fluid velocity.

5.2.2 Relationship with velocity exponent factor and particle size polynomial form

The second relationship for estimating the sand flow rate was as follows:

$$Q = \frac{M-Z}{dV^{b}(1+aD+cD^{2})} \tag{5.2}$$

In this relationship, Q is the estimated sand flow rate, M is the ASD output, Z is the ASD output when there is no sand flow rate and was created by the background noise, V is the velocity of the fluid, and D is the average diameter of the sand particles. Furthermore, a, b, c, and d are the coefficients. In this relationship it was assumed that the estimated sand flow rate was dependent on the ASD output, the ASD output due to background noise, fluid velocity and average diameter of particles.

In this relationship, it was assumed that sand flow rate has an inverse relationship with an exponent factor of fluid velocity. Also, it was assumed that the sand flow rate has an inverse relationship with a polynomial of sand particle size. This relationship is also similar to the Gao et al. [35] version for sand flow rate measurement. But it is more generalised than that of the Gao et al. as it considered the effect of sand particle size. Also it does not consider a fixed exponent of two for fluid velocity, rather it considers a parametric exponent for fluid velocity. The difference between this relationship and the one specified in section 5.2.1 is that the one specified in this section considers a second degree polynomial for the particle size while that one in section 5.2.1, considers a parametric exponent for particle size.

5.2.3 Relationship with velocity polynomial form

The third relationship for estimating the sand flow rate is as follows:

$$Q = \frac{M-Z}{d(1+bV+cV^{2})} \tag{5.3}$$

In this relationship, Q is the estimated sand flow rate, M is the ASD output, Z is the ASD output when there is no sand flow rate and created due to background noise, V is the velocity of the fluid. Moreover, b, c, and d are the coefficients in the relationship. In this relationship, it is assumed that the estimated sand flow rate is dependent on the ASD output, ASD output due to background noise, fluid velocity and average diameter of particles.

In this relationship, it was assumed that sand flow rate has an inverse relationship with a polynomial of fluid velocity. This relationship was also similar to the Gao et al. [35] version for sand flow rate measurement. However, it is more generalised than the Gao et al. relationship, as it considered a second degree polynomial for fluid velocity rather than a square of fluid velocity.

5.2.4 Relationship with particle size polynomial form

The fourth relationship for estimating the sand flow rate was as follows:

$$Q = \frac{M-Z}{d(1+aD+cD^2)} \tag{5.4}$$

In this relationship, Q is the estimated sand flow rate, M is the ASD output, Z is the ASD output when there is no sand flow rate and was created by the background noise, and D is the average diameter of the sand particles. Furthermore, a, c, and d are the coefficients in above mentioned relationship. In this relationship, it was assumed that the estimated sand flow rate was dependent on the ASD output, ASD output due to background noise and the average diameter of particles.

In this relationship, it was assumed that the sand rate had an inverse relationship with a polynomial of sand particle size. This relationship is similar to that of Ibrahim et al. [6], but it is more generalized as it considered sand particle effect in measuring sand flow rate.

5.2.5 Relationship with velocity exponential form

The fifth relationship for estimating the sand flow rate was as follows:

$$Q = \frac{M-Z}{dV^b} \tag{5.5}$$

In this relationship, Q is the estimated sand flow rate, M is the ASD output, Z is the ASD output when there is no sand flow rate and was created by the background noise, while V is the velocity of the fluid. Moreover, b and d are the coefficients in the relationship, in which it was assumed that the estimated sand flow rate was dependent on the ASD output, the ASD output background noise and the fluid velocity.

In this relationship, it was assumed that the sand flow rate has an inverse relationship with an exponent factor of fluid velocity. This relationship is also similar to the Gao et al. [35] version for sand flow rate measurement. However, it is more generalised than that of Gao et al., as it has considered a parametric exponent instead of a fixed exponent of two.

5.2.6 Relationship with ASD exponential form

The sixth relationship for estimating the sand flow rate was as follows:

$$Q = \frac{M^2 - Z^2}{d(d + 2 * Z)} \tag{5.6}$$

In this relationship, Q is the estimated sand flow rate, M is the ASD output, Z is the ASD output when there is no sand flow rate and was created by the background noise, while V is the velocity of the fluid. Moreover, d is the coefficient in the relationship. In this relationship, it was assumed that the estimated sand flow rate was dependent on the ASD output, the ASD output due to background noise and the fluid velocity. This relationship was proposed by Odigies et al. [43].

5.2.7 Relationship with ASD exponential and velocity polynomial form

The seventh relationship for estimating the sand flow rate was as follows:

$$Q = \frac{M^2 - Z^2}{d(d + 2 * Z)(1 + bV + cV^2)} \tag{5.7}$$

In this relationship, Q is the estimated sand flow rate, M is the ASD output, Z is the ASD output when there is no sand flow rate and was created by the background noise, while V is the velocity of the fluid. Moreover, b, c, and d are the coefficients in the relationship, in which it was assumed that the estimated sand flow rate was dependent on the ASD output, the ASD output background noise as well as the fluid velocity. This relationship is a generalised form of the Odigies et al. [43] version in which the effects of sand particle size is added to the relationship.

5.3 Finding the optimum relationship for calculating sand flow rate using an ASD

In this section, the results of using various relationships for measuring sand flow rate using an ASD (as mentioned in section 5.2) are specified. The results for applying the repetitive process to find the optimum parameters in each relationship are shown in the tables provided in this section. Each row of these tables shows one case of running a MATLAB program in order to find the optimum point. Also, the case number for each row shows the sequence number when running the MATLAB program. For instance, case 1 was a first trial of testing the program.

As can be seen, the range of the parameters chosen is much wider for the earlier cases compared to the later cases. Then the range was adjusted to cover a smaller range around the optimum value found

in the previous case. Once the optimum range was found for that parameter, then a smaller range was selected around the optimum case found in the earlier stage.

Using this method for optimization helped reduce the computation time for finding the optimum case because to check the optimum case with a wide range for parameters and with small increment, the number of iterations was excessive. Running a Matlab program for such a large number of iterations needed more time for computation and a much stronger processor.

5.3.1 Results for Relationship with velocity and particle size exponent factors

In this sub-section, the results for finding the optimum parameters in the following relationship (which was described in section 5.2.1) is provided:

$$Q = \frac{M-Z}{dV^b(1+aD^c)} \tag{5.8}$$

Table 5-1: Table of Results for Relationship with velocity and particle size exponent factors

Case No	a range (No of intervals)	b range (No of intervals)	c range (No of intervals)	d range (No of intervals)	Mean error	Standard deviation	Optimum a	Optimum b	Optimum c	Optimum d
1	0-50 (10)	0-2 (10)	0-2 (10)	1-3000 (10)	-0.0043	1.3457	25	1.8	0	1200.6
2	20-30 (10)	1.6-2.4 (10)	0-0.2 (10)	900-1500 (10)	5.5817e-05	1.9938	23	2.24	0.06	1140
3	21-25 (10)	2-2.4 (10)	0-0.1 (10)	1000-1280 (10)	-4.4788e-06	2.1687	23.8	2.3	0.07	1028
4	23-24.5 (10)	2.2-2.5 (10)	0-0.1 (10)	960-1100 (10)	-8.6350e-05	2.0235	23.6	2.26	0.06	1086

In this table, the values in parenthesis were the number of intervals for each range. For instance, if the “a range” was specified as 0-50 (10), this means that 10 intervals were considered between 0 and 50. Therefore the values considered for parameter “a” were 0, 5, 10, 15, ..., 45, 50 for this raw data. In this example, there are 11 points (i.e., 0, 5, 10, …, 50) and 10 intervals (i.e., 0-5, 5-10, …, 45-50). The way optimisation was performed is that I checked the error for all the points around these intervals. For instance, I have checked the mean errors when the parameter "a" is 0, 5, 10, .. or 50. Then I checked which point provided the smaller mean error (which is 25 in this example). In the second round of optimisation (shown by the second row of table 5.1), I considered a range around this optimized point from the first round of optimisation (i.e., I selected range 20-30 around the optimized point of 25). Then I considered a smaller interval for this case (e.g., 2 in second round while the interval was 5 for the first round), so the points considered for second round of optimisation are 20, 22, ..., 30.

Then I calculated the mean error for these new points and found that 23 is the optimum point. I repeated this process of choosing the smaller range around the optimum case from the previous point for all 4 iterations. It should be noted that the mean error is reduced in each round of optimisation compared with the previous round of optimisation.

5.3.2 Results for relationship with velocity exponent factor and particle size polynomial form

In this sub-section, the results for finding optimum parameters in the following relationship (which was described in section 5.2.2) is provided:

$$Q = \frac{M-Z}{dV^b(1+aD+cD^2)} \tag{5.9}$$

Table 5-2: Table of results for relationship with velocity exponent factor and particle size polynomial form

Case No	a range (No of intervals)	b range (No of intervals)	c range (No of intervals)	d range (No of intervals)	Mean error	Standard deviation	Optimum a	Optimum b	Optimum c	Optimum d
1	0-20 (10)	0-3 (15)	0-20 (10)	100-3000 (20)	-4.1243	9.6897	18	2.8	18	2855
2	15-25 (10)	2.5-3.5 (10)	15-25 (10)	2500-3500 (10)	-0.9714	5.3800	24	3.4	24	3400
3	22-27 (10)	3.1-3.7 (10)	22-27 (10)	3200-3700 (10)	-0.2828	4.2328	26.5	3.64	26.5	3650
4	25-28 (10)	3.4-3.9 (10)	25-28 (10)	3500-3800 (10)	5.6612e-06	3.7585	27.4	3.8	25	3680

In this table, the values in parenthesis were the number of intervals for each range. For instance, if the “a range” was specified as 0-20 (10), this means that 10 intervals were considered between 0 and 20. Therefore the values considered for parameter “a” were 0, 2, 4, 6, ..., 18, 20 for this raw data.

5.3.3 Results for relationship with velocity polynomial form

In this sub-section, the results for finding the optimum parameters in the following relationship (which was described in section 5.2.3) is provided:

$$Q = \frac{M-Z}{d(1+bV+cV^2)} \qquad (5.10)$$

Table 5-3: Table of results for relationship with velocity polynomial form

Case No	b range (No of intervals)	c range (No of intervals)	d range (No of intervals)	Mean error	Standard deviation	Optimum b	Optimum c	Optimum d
1	0-200 (20)	0-200 (20)	100-3000 (20)	-5.7494e-04	0.4690	70	0	1550
2	50-90 (20)	0-20 (20)	1300-1700 (20)	1.0554e-04	0.4931	66	1	1500
3	60-75 (20)	0-4 (20)	1400- 1600 (20)	-5.6615e-06	0.5273	64.5	2	1410
4	61-68 (20)	0-3 (30)	1400- 1500 (30)	-5.6615e-06	0.5273	64.5	2	1410

In this table, the values in parenthesis were the number of intervals for each range. For instance, if the “b range” was specified as 0-200 (20), this means that 10 intervals were considered between 0 and 200. Therefore the values considered for parameter “b” were 0, 10, 20, ..., 190, 200 for this raw data.

5.3.4 Results for relationship with particle size polynomial form

In this sub-section, the results for finding the optimum parameters in the following relationship (which was described in section 5.2.4) is provided:

$$Q = \frac{M-Z}{d(1+aD+cD^2)} \tag{5.11}$$

Table 5-4: Table of results for relationship with particle size polynomial form

Case No	a range (No of intervals)	c range (No of intervals)	d range (No of intervals)	Mean error	Standard deviation	Optimum a	Optimum c	Optimum d
1	0-100 (20)	0-100 (20)	100-6000 (20)	-214.8129	101.7092	95	95	5705
2	60-140 (20)	60-140 (20)	4000-8000 (20)	-153.8264	72.6051	136	136	7800
3	100-200 (25)	100-200 (25)	7000-10000 (25)	-117.9731	55.3989	196	196	9880
4	180-400 (25)	180-400 (25)	9000-15000 (25)	-72.3640	33.4859	391	391	14760
5	380-600 (25)	380 600 (25)	14000 20000 (25)	-49.6912	22.7779	591.2	591.2	19760
6	500-2000 (25)	500-2000 (25)	18000-50000 (25)	-12.4810	5.8789	1940	1940	48720
7	1900-5000 (25)	1900-5000 (25)	45000-100000 (25)	-2.4589	1.8006	4876	4876	97800

In this table, the values in parenthesis were the number of intervals for each range. For instance, if the “a range” was specified as 0-100 (20), this means that 10 intervals were considered between 0 and 100. Therefore the values considered for parameter “a” were 0, 5, 10, 15, .., 95, 100 for this raw data.

5.3.5 Results for relationship with velocity exponential factor

In this sub-section, the results for finding the optimum parameters in the following relationship (which was described in section 5.2.5) is provided:

$$Q = \frac{M-Z}{dV^b} \qquad (5.12)$$

Table 5-5: Table of results for relationship with velocity exponential factor

Case No	b range (No of intervals)	d range	Mean error	Standard deviation	Optimum b	Optimum d
1	0-4 (40)	100-4000 (40)	-0.0079	3.8475	3.9	3415
2	2-5 (50)	3000-4500 (40)	6.4472e-04	3.8422	3.92	3375
3	3.5-4.5 (50)	3500-4000 (40)	-5.2003e-04	3.7611	3.8	3725
4	3.6-3.85 (50)	3650-3800 (50)	-4.5334e-05	3.7492	3.785	3773

In this table, the values in parenthesis were the number of intervals for each range. For instance, if the "b range" was specified as 0-4 (40), this means that 10 intervals were considered between 0 and 4. Therefore the values considered for parameter "b" were 0, 0.1, 0.2, 0.3, .., 3.9, 4 for this raw data.

5.3.6 Results for relationship with ASD output square form

In this sub-section, the results for finding the optimum parameters in the following relationship (which was described in section 5.2.6) is provided:

$$Q = \frac{M^2 - Z^2}{d(d+2*Z)} \tag{5.13}$$

Table 5-6: Table of results for relationship with ASD output square form

Case No	d range (No of intervals)	Mean error	Standard deviation	Optimum d
1	100-100000000 (1000)	0.1375	1.4043	1.1001e+06
2	500000-1500000 (1000)	5.0451e-04	1.4981	1058000
3	900000-1100000 (1000)	-1.8576e-04	1.4986	1057800
4	1040000-1080000 (1000)	-4.7671e-05	1.4985	1057840
5	1055000-1059000 (1000)	-6.2484e-06	1.4985	1057852

In this table, the values in parenthesis were the number of intervals for each range. For instance, if the "d range" was specified as 500000-1500000 (1000), this means that 10 intervals were considered between 500000 and 1500000. Therefore the values considered for parameter "d" were 500000, 501000, 502000, ..., 14990000, 1500000 for this raw data.

5.3.7 Results for relationship with ASD output square and velocity polynomial form

In this sub-section, the results for finding the optimum parameters in the following relationship (which was described in section 5.2.7) is provided:

$$Q = \frac{M^2 - Z^2}{d(d+2*Z)(1+bV+cV^2)} \quad (5.14)$$

Table 5-7: Table of results for relationship with ASD output square and velocity polynomial form

Case No	b range (No of intervals)	c range (No of intervals)	d range (No of intervals)	Mean error	Standard deviation	Optimum b	Optimum c	Optimum d
1	1 -25 (25)	1 -15 (25)	20000 - 100000 (25)	2.1117e-04	0.7865	17.3200	7.1600	48800
2	5 -15 (25)	2 -10 (25)	40000 - 80000 (25)	-9.0981e-05	0.8082	9.4000	6.1600	56000
3	8 -12 (25)	3 -7 (25)	55000 - 66000 (25)	3.3288e-05	0.8071	9.1200	5.8800	57200
4	9.7 -10.3 (25)	4.6 -5.5 (25)	59000- 62000 (25)	-2.3567e-07	0.7929	9.7720	4.7800	61160

In this table, the values in parenthesis were the number of intervals for each range. For instance, if the “d range” was specified as 20000-100000 (25), this means that 25 intervals were considered between 20000 and 100000. Therefore the values considered for parameter “d” were 20000, 23200, 26400, ..., 96800, 100000 for this raw data.

5.3.8 Comparing the results from various relationships with ASD data

In this section, the results of various relationships (relating the reading from an ASD to the sand flow rate) are compared with each other. First of all, the results for various relationships are summarized in the table below. In this table, each relationship is specified in a separate row, where the mean error and standard deviation of sand flow rate estimation using that relationship is specified in this row.

Table 5-8: Comparison of various relationships for sand flow rate measurement

Case no	relation	Mean error	Standard deviation
1	$Q = \frac{M - Z}{dV^b(1 + aD^c)}$	-8.6350e-05	2.0235
2	$Q = \frac{M - Z}{dV^b(1 + aD + cD^2)}$	5.6612e-06	3.7585
3	$Q = \frac{M - Z}{d(1 + bV + cV^2)}$	-5.6615e-06	0.5273
4	$Q = \frac{M - Z}{d(1 + aD + cD^2)}$	-2.4589	1.8006
5	$Q = \frac{M - Z}{dV^b}$	-4.5334e-05	3.7492
6	$Q = \frac{M^2 - Z^2}{d(d + 2 * Z)}$	-6.2484e-06	1.4985
7	$Q = \frac{M^2 - Z^2}{d(d + 2 * Z)(1 + bV + cV^2)}$	-2.3567e-07	0.7929

By comparing the results obtained in this table, it can be seen that the mean error of relationship 7 is much smaller than the other relationships (i.e., the mean error is about 10% or less than the mean error of the other relationships). Also the standard deviation of this relationship is relatively small compared with other relationships (i.e., the standard deviation is the second smallest standard deviation in this table). This means that this relationship improves the accuracy of the sand flow measurement at least 10 times more than the other relationships. Therefore, equation 7 is recommended as the optimum in this study.

The other relationships are generalised forms of various relationships suggested by other researchers. Since the mean error of predicting sand flow rate using relationship 7 is at least 10% of the mean error for the other relationships, therefore this relationship substantially improves the accuracy of sand flow rate measurement in the field. This is a major achievement in this research considering several site operators are concerned most about the accuracy of existing sand flow measurements in various gas field developments. Since the input to this relationship is the raw signal of the commonly used ASD in gas fields, therefore this relationship can be used in various gas fields around the world without any hardware modification.

One of the advantages of using relationship 7 is that it does not need the sand particle average diameter for sand flow rate calculation. Typically measuring sand particle size is not a convenient task, as a sample of the sand particle must be collected and then submitted to a laboratory for average sand particle measurement. So using relationship 7 provides a simple way to measure the sand flow rate, as it does not require a sample of sand particles to be measured for the average size of sand particles.

5.4 Summary of the results obtained using an Ultrasonic sensor and the FFT method

As mentioned in Chapter 4, as part of this research, the ultrasonic sensing method was used for measuring the sand flow rate. In this study, a data acquisition unit from *National Instruments* and an ultrasonic sensor from *Olympus* were used.

First the ultrasonic circuit was established, where various activities such as the below-mentioned tasks were performed:

- Machining of the support for an ultrasonic sensor
- Procurement of the ±15 VDC power supply unit for powering the amplifier
- Obtaining of the missing accessories of the data acquisition unit from the supplier
- Installing the ultrasonic sensor, amplifiers, and data acquisition unit on the flow loop
- Resolving the hardware interface issue between the data acquisition unit and the computer
- Establishing the interface between Labview software on the computer and the data acquisition unit
- Performing experiments at various conditions (e.g., various sand flow rate and air velocities) and collecting the results in a structured data format
- Scripting in MATLAB to read the results of various experiments in a structured data format
- Scripting in MATLAB to perform an FFT of the ultrasonic signals for various tests
- Testing various hypothesis to find a relationship between the FFT of ultrasonic signals and the sand flow rate by writing suitable script in MATLAB
- Obtaining a relationship between the sand flow rate and the maximum value of FFT signal in the signal range of 10 kHz to 50 kHz
- Further investigation of this relationship and establish a two degree polynomial to correlate the maximum value of FFT signal and the sand flow rate
- Propose a procedure for obtaining the parameters of this two-degree polynomial in various installation cases.

In summary, the above mentioned activities led to finding a new relationship to estimate the sand flow rate data using the frequency domain (FFT) of the ultrasonic response. This was a major achievement since most researchers have previously focused on the time domain. Finding a relationship between the peak value of the FFT curve and the sand flow rate is new knowledge in this research, and resulted in a paper [85] (which is also mentioned in the list of publications).

5.5 Summary of the results obtained using an Ultrasonic sensor and Discrete Wavelet Transform

In this section, the results of using a wavelet transform for analysis of ultrasonic sensor data was examined. As was discussed in section 2.7.3, the wavelet transform provides a few series of coefficients. Each series represents the strength of the signal at certain frequency bands.

After analysis of the ultrasonic signal obtained from various test points, it was found that the strength of the wavelet coefficients was greater in two frequency bands (i.e., frequency ranges from 31.25 kHz to 62.5 kHz, and from 15.625 kHz to 31.25 kHz).

Then I calculated the strength of signal (sum of the squares of the wavelet coefficients) in these two frequency bands. It was noticed that the strength of the signal in these frequency bands had a linear relationship with the sand flow rate. Therefore a method was obtained to estimate the sand flow rate from the discrete wavelet coefficient.

Since the relationship between the wavelet transform strength and the sand flow rate was linear, calibration of the ultrasonic sensor for measuring sand flow rate using a wavelet transform was an easy task. The reason for this was that there is a need to obtain only one parameter during calibration (i.e., the multiplier factor to convert the strength of the wavelet transform to the sand flow rate). So with a small number of tests during calibration, this multiplication factor can be estimated for each particular installation.

Finally, this method could estimate the sand flow rate without needing the fluid velocity. Most commercial sand detectors need fluid velocity for sand measurement and in various applications. Fluid velocity cannot easily be estimated in various applications (due to the lack of a flow measuring device). Therefore using the wavelet transform method to measure sand flow rate was simpler than using most of the commercial sand detectors, since it does not need fluid velocity for estimating sand flow rate. This alone is new knowledge important to the sand monitoring/measurement application in gas industry.

5.6 Summary of the results obtained using an Ultrasonic sensor and the Welch method

In this section, the results of using the Welch method for analysing the output of an ultrasonic sensor are explained. As was elaborated in section 2.7.4, the Welch method provides the Power Spectral Density (PSD) of the signal in the frequency domain. The Welch method is a good technique for analysing non-deterministic signal. Due to the non-deterministic nature of sand flow rate measurement, this method was tested in this research for analysis of the signal from the ultrasonic sensor. It was shown that the PSD of the signal has a good correlation with the sand flow rate. Also it was demonstrated that there was a linear relationship which could be used to estimate the sand flow rate. This linear relationship provides a simple way to estimate the sand flow rate. Since the proposed relationship uses only one parameter to correlate the PSD to the sand flow rate, calibration of the sand measuring device is an easy task to obtain this parameter for each application. Using limited data, this parameter can be estimated. In a gas field, it is usually not possible to change the operating conditions over a wide range for calibration purposes (as there could be some restrictions from a reservoir point of view, etc.), so using this proposed Welch method to calculate sand flow rate is advantageous, as it needs minimum data for calibration.

Finally this method can estimate the sand flow rate without needing the fluid velocity. Most commercial sand detectors need fluid velocity for sand measurement and in various applications. Fluid velocity cannot easily be estimated in various applications due to the lack of a flow measuring device. Therefore, using the Welch method to measure the sand flow rate is simpler that using most of the commercial sand detectors, since it does not need fluid velocity for estimating sand flow rate. And again, it is a new knowledge.

5.7 Comparing the results obtained from FFT, DWT and Welch methods

In this section, the uncertainty of sand flow measurement using various signal processing techniques (i.e., FFT. Welch and DWT) are compared. This comparison was performed by calculating the one-standard deviation for each sand flow rate measuring method. Table 5-9 shows the one-standard deviation result of each method:

Table 5-9: Comparing the uncertainty of sand flow rate measurement using various methods

Method	One-standard deviation in sand flow measurement	Full scale accuracy
Welch method	0.6923 g/sec	15.3%
FFT method	0.2126 g/sec	4.7%
DWT method	0.7696 g/sec	17.1%

As can be seen, the FFT method has the lowest one-standard deviation, and so provides the most accurate estimation of sand flow rate among these three options. Comparison between the accuracy of various methods is shown in Figure 5-1.

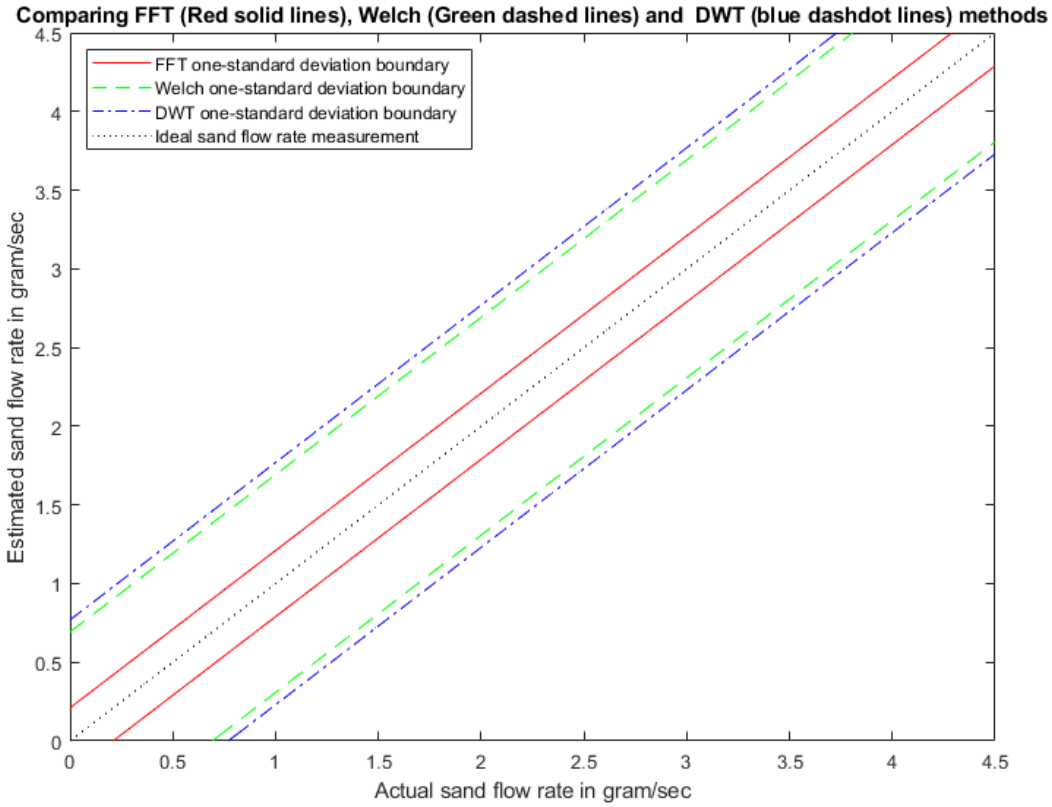

Figure 5-1: Accuracy of FFT, Welch and DWT methods

In this figure, the actual sand flow rate is shown along the X axis and the estimated sand flow rate is specified along the Y axis. The ideal case (shown with a dotted black line) is when the estimated flow rate is exactly equal to actual flow rate. The narrower the boundary that the one–standard deviation is, the more accurate the sand flow rate measurement. Therefore the FFT method shown by a solid red line provided the most accurate sand flow rate measurement according to this figure. After the FFT method, the Welch method provided the second most accurate measurement followed by the DWT method.

To summarize, a relationship to calculate sand flow rate was obtained for all of these methods. This relationship is provided as a general format:

$$Y=f(X) \qquad (5.15)$$

where X is a parameter which is extracted from the frequency domain (after the ultrasonic signal is converted from time domain to frequency domain). For instance, in the FFT method, X is the peak value of the FFT curve (which is smoothed by the Savitzky–Golay filter). Also for the case of the DWT method, X is the sum of the squared values of DWT coefficients over a frequency range of 15.625 to 62.5 kHz. In the case of the Welch method, X is the sum of the Power Spectral Density in the frequency range of 1 to 200 kHz. Y is the estimated sand flow rate. In the case of the Welch and the DWT methods, f(X) is a first-order polynomial as mentioned earlier in the relationships 4.10 and 4.11. In the case of the FFT method, f(X) is a second-order polynomial as mentioned earlier for relationship 4.9.

5.8 Summary of the chapter

In this chapter, the results of using various methods for measuring sand flow rate were established. First the results of using an ASD for sand flow rate was explained. The relationships used to correlate the ASD output to the sand flow rate were examined. Then the results of using MATLAB to optimise the parameters in each relationship were provided. The mean error and standard deviation in measuring sand flow rate were tabulated for various relationships. Finally the relationship which provided the minimum mean deviation was selected. This relationship is the optimum method proposed for estimating the sand flow rate using the signal obtained from an ASD.

Then, the results of using the FFT method to analyse the ultrasonic sensor signal were provided. Various activities to set-up the ultrasonic sensor were summarized. Also it was mentioned that as part of this research, a second-degree polynomial was found to correlate the peak value of the FFT curve with the sand flow rate.

Then, the results of using the DWT method to measure the sand flow rate were explained. It was mentioned that as part of this research, a linear relationship was found to correlate the strength of DWT coefficients with the sand flow rate.

Moreover, the results of using the Welch method to measure sand flow rate were discussed. It was explained that as part of this research, a linear relationship was found to correlate the sum of the PSD calculated using the Welch method with the sand flow rate.

Finally, the uncertainty of sand flow rate measurement using various signal analysis methods used in this research (i.e., FFT, DWT and Welch) were compared. It was concluded that the FFT method provided the most accurate sand flow rate measurement, and this method has advantages over the commercial method commonly used.

6 Conclusions and recommendations

6.1 Conclusions

This research focuses on sand measurement in gas pipelines. As mentioned in the first chapter of the thesis, typically gas reservoirs produce sand particles along with the gas. Sand production introduces various issues such as the erosion of pipes and other downstream devices. In extreme cases, such erosion can endanger the integrity of the pipe which might lead to explosion and causing harm to the personnel and plant facilities. Also sand production has other negative effects such as reservoir collapse and sand accumulation in the downstream facility causing interruption to the gas process flow.

To minimize/prevent these side effects of sand production, sand control and sand management techniques are typically used. To properly apply sand control/management techniques, it is necessary to accurately measure the sand flow rate. As mentioned in Chapter 1, currently there are many concerns about the accuracy of sand flow rate measurement [7]. Not having accurate sand flow rate measurement can potentially cause various issues in operation such as not noticing sudden sand flow rate (which prevents the operator from taking necessary action to minimise the side effects of sand production), giving false alarms to the operators, etc. Therefore this research was focussed on the subject of sand flow measurement to address such concerns.

In this research, two main methods were considered for sand flow measurement. One method was to use Acoustic Sand Detectors (ASDs) and the other method was to use ultrasonic sensors to measure sand flow rate.

Chapter 1 is the introduction section of this thesis. It defined the problem statement for this research. Then, it mentioned the objectives of this research in more detail. Also the significance of performing this study was mentioned in this chapter.

In Chapter 2 of this thesis, I reviewed the background of sand flow measurement. Various sand control techniques to prevent sand production were explained, and the sand management technique was discussed. Various sand measuring devices were then explained, after which the benefits of accurate sand measurement was mentioned. Moreover, the ultrasonic sensing method and various signal

processing techniques used in this research were discussed. This chapter provided the fundamental knowledge used in the following chapters of the thesis.

In Chapter 3 of the thesis, the existing but dismantled flow loop test facility used in this research was explained. I have explained various activities performed in this research to restore this flow loop to normal operation. These activities included the procurement/refurbishment of various pieces of hardware and installation/setup/programming of various software. I have also explained how sand particles were segregated into different sizes. Also the test matrix used to test the Acoustic Sand Detector (ASD) was explained.

In Chapter 4 of this thesis, I explained the application of the ultrasonic circuit used in this research to measure sand flow rate. I elaborated on the various hardware equipment used in the ultrasonic circuit such as the ultrasonic sensor, amplifier, data acquisition unit, and PC. Also various activities to procure the required hardware and rectify the issues using the existing hardware, were explained, as well as the software used to collect the data from the ultrasonic sensor and its analysis, were explained. This involved a test matrix for checking an ultrasonic sensor and also signal processing techniques used to analyse the ultrasonic signal. The results of applying these signal processing techniques were then provided. Based on the test methodology, I found three different techniques to measure sand flow rate using an ultrasonic sensor. These three different techniques (as explained in Chapter 4) were:

1. I obtained a new method to calculate sand flow rate using ultrasonic sensors and FFT signal analysis. In this method, an off-the-shelf ultrasonic sensor was installed on the pipe after a bend. Then the signal from the ultrasonic sensor was amplified, and sampled using a data acquisition system. FFT signal processing was then applied to the ultrasonic signal, and the FFT curve was smoothed using a Savitzky–Golay filter. I found that there was a correlation between the peak value of the smoothed FFT curve in the frequency range of 10 kHz to 50 kHz and the sand flow rate. The same method provided sand flow rate measurement with a full scale accuracy of 4.7% (i.e., this method provides sand flow rate measurement with a 4.7% error). Obtaining such accuracy of sand flow rate measurement is a valuable achievement for this research, as the operators have a lot of concerns about accuracy of existing sand flow measuring devices and therefore having a new method which provides them with a sand measurement with 4.7% error is considered as a trustworthy source of information. This result is published in a paper [85].
2. I also propose a new method to calculate the sand flow rate using ultrasonic sensors and the DWT signal processing method. Using this method, I demonstrated that the strength of DWT signals in the frequency range of 15.625 kHz to 62.5 kHz had a linear relationship with sand flow rate. Therefore an ultrasonic sensor and the DWT method can be used to estimate sand flow rate using this linear relationship. The same result was published in another paper [99].

3. I also propose a method to measure sand flow rate using an ultrasonic sensor and the Welch signal processing technique. Using this method, I found that the strength of the Welch signal over the frequency range of 1 to 200 kHz has a linear relationship with sand flow rate. Therefore an ultrasonic sensor and the Welch method can be used to measure sand flow rate using this linear relationship.

In Chapter 5 of this thesis, the data analysis used to analyse the signal from the ASD was discussed. It was explained that seven different parametric relationships were considered to correlate the reading from the ASD and the sand flow rate. Then the parameters in each relationship were optimised to get the most accurate sand flow rate. Finally the optimised relationships were compared to select the relationship which provided the most accurate sand flow rate measurement using the raw signal obtained from the ASD. Based on this data analysis, I obtained a method to improve the accuracy of sand flow rate measurement using one type of commonly used commercial ASD. This type of commercial ASD has been widely used in various gas fields around the world and there have been some concerns about the accuracy of sand flow rate measurement using this type of ASD (as suggested by Chevron supporting this project). The interesting feature of the proposed method is that it does not need any change in the hardware of the ASD. Therefore in applying this method, there was no need to change existing commercial ASDs in the current facilities to achieve a more accurate sand flow rate measurement. Only some changes need to be performed in the way the sand flow rate was calculated in the control system using the raw signal provided by the ASD. The same can be done by a relatively easy change in the logic for sand flow rate calculation.

In Chapter 5 of this thesis, three different techniques proposed in this research for measuring sand rate using an ultrasonic sensor (i.e., FFT, DWT and Welch) were also compared. It was found that the FFT method along with a Savitzky–Golay filter provided the most accurate sand flow rate measurement followed by the Welch method. It should be noted that all of these methods can be applied in real-time. The same real-time calculation can be used to provide real-time monitoring of sand flow rate based on which the operator can take necessary actions (e.g., in case of a sudden increase in the sand flow rate or prolonged production of sand).

Considering the concerns about the accuracy of commercial ASDs, this thesis has provided a way to improve the reading from these ASDs. Also this thesis has provided alternative methods for measuring sand flow rate instead of using commercial ASDs. The accuracy of these alternative methods (e.g., full scale accuracy of 4.7% of FFT peak detection method) is very promising, as several operators do not have much trust in the accuracy of commercial ASDs. The accuracy of the commercial ASDs varies in different cases depending on various satiations such as how often these ASDs are calibrated, the installation location, the background noise, etc. Also the suppliers of these ASDs claim that they are

continuously improving their products. Taking into account the above mentioned factors and commercial nature of this subject, I have not mentioned any specific accuracy figure for such commercial ASDs in this thesis. The accuracy of ASDs is site dependent, changing from one site to the next. Therefore we can say that the proposed methods developed herein will generally be far superior to the commercial ASDs, dependant on site.

By having more accurate sand flow rate measurement using the proposed methods in this research (either the improved method for sand flow rate calculation using commercial ASDs or by using ultrasonic sensor and various signal processing methods such as FFT, DWT or Welch), operators can apply sand control and sand management strategies more efficiently. For instance, they can identify any failure in the sand screen downhole (where a sand screen is used as a sand control technique) faster and with more certainty than when using commercial ASDs. Also they can control the side effects of sand production such as erosion (where sand management techniques are used) more accurately than when they use commercial ASDs. By applying accurate sand control and sand management using the proposed sand measurement methods, the operator can minimise any side effects of sand production, prevent catastrophic events, and protect their valuable assets.

6.2 Recommendations

I have the following recommendations to continue this research and perform further developments in the area of sand flow measurement. It should be noted that the following suggestions are not necessarily the only methods or the best methods to perform further research in the area of sand flow measurement. They are based on my understanding of the facilities in Curtin University and the knowledge I gathered during my research.

- The flow loop test facility at Curtin University simulates the production from a gas well which produces a dry gas (i.e., gas without condensate or water) and sand particles. Although several gas wells produce dry gas or a gas which is very close to dry gas (e.g., the gas volume ratio is more than 99%), some of the gas wells do produce wet gas (i.e., gas with some condensate or water). To perform research on sand flow rate measurement in a wet gas situation, a flow loop test facility which simulates wet gas conditions is needed. Therefore one of the recommendations for further research in this area is to enhance the flow loop facility at Curtin University to simulate wet gas conditions. After such improvement, it is possible to investigate sand flow measurement using an ASD and an ultrasonic sensor in gas wells which produce wet gas and then obtain ways to improve sand flow rate measurement under wet gas conditions. To apply this recommendation, a liquid (e.g., water) should also be injected into the flow loop where gas and sand particles are passing through. Such liquid can simulate the water/condensate in the wet gas extracted from gas wells. Then, the ASD and ultrasonic sensor can be tested in various percentages of the sand and liquid in total fluid. Specifically the liquid droplets might impact the pipe wall and create ultrasonic signals and as a result, the liquid can wrongly be reported as sand particles by sand measuring instruments. Therefore one can investigate difference between the characteristics (e.g., frequency band) of the ultrasonic signals generated by liquid droplets and the sand particles. Based on such characteristic, one may propose a way to predict sand flow rate in wet gas condition with minimal error due to the presence of liquid droplets.
- In this research, I have investigated several signal processing techniques and found that three different signal processing techniques (i.e., FFT, DWT and Welch) can be used to analyse the data using off-the-shelf ultrasonic sensors and correlate it to the sand flow rate. Also I investigated which method provides more accurate sand flow rate measurement among these three techniques. Since there are many signal processing techniques and new signal processing techniques may become available, it is recommended that other signal processing techniques should be tested to check whether those techniques can be used for sand flow rate measurement. If any other method is found, then comparison can be performed to find which

signal processing method can provide more accurate sand flow rate measurement. For instance, it is well worthy to check below points:

a) See if there is an absolute phase relationship of the FFT curve with sand flow rate.
b) See if there may be a relationship of instantaneous phase or instantaneous frequency relationship, such as is used in seismic attribute analysis.

- The flow loop test in Curtin University is an open loop system. This means that once the sand is injected in the fluid, it accumulates in the basket at the end of the flow loop. Also the air which is taken at the inlet of flow loop test is expelled to the atmosphere. To repeat the test, a new batch of sand (which can be the one collected from the basket) has to be manually placed in the container of the sand hopper. As a recommendation for further research, this flow loop test can be converted to a closed loop system. In this case, the same air and sand can circulate in the system. Having a closed flow loop simplifies the experiment to a large extent. Therefore, there is no need to put a new supply of sand for every new test. Also the duration of each test can be extended, as in the case of the open flow loop, in which the test finishes when the sand container in the sand hopper is emptied, while in the close flow loop, the sand is still circulating in the system.
- The DAS method can be used in the flow loop test facility. To apply DAS, fibre optic cable can be installed along the flow loop. Then the possibility of using DAS to measure sand flow rate can be investigated and the accuracy of DAS in measuring sand flow rate can be compared with the accuracy of sand measurement using ASD and ultrasonic sensor. Since DAS have a lot of other features such as the ability to identify the location of sand production in a gas well, several research methods can be conducted using DAS to find/improve various features. Considering the distributed nature of measurement by DAS, using this technique necessitates handling large amounts of data and applying sophisticated signal processing techniques.

References

1. MacKinnon, A., J. Brown, and G.K. Brown, *Keeping Acoustic Sand Monitoring Simple*, in *Corrosion 2011*. 2011, NACE International: Houston, USA.
2. Allahar, I.A., *Acoustic Signal Analysis for Sand Detection in Wells with Changing Fluid Profiles*, in *Society of Petroleum Engineers Annual Conference*. 2003, Society of Petroleum Engineers: Port-of-Spain, Trinidad and Tobago.
3. Brown, G.K. and R. Davies, *Solids and Sand Monitoring - An Overview*, in *CORROSION 2000*. 2000, NACE International: Orlando, USA.
4. Jaimes Plata, M., et al., *Sand Exclusion or Management: Multidisciplinary Approach in Decision Making*, in *SPE Latin America and Caribbean Petroleum Engineering Conference*. 2012, Society of Petroleum Engineers: Mexico City, Mexico.
5. Nisbet, *Implementation of a Robust Deepwater Sand Monitoring Strategy*, in *Society of Petroleum Engineers Annual Conference*. 2003, Society of Petroleum Engineers: Denver, USA.
6. Ibrahim, M. and T. Haugsdal, *Optimum Procedures for Calibrating Acoustic Sand Detector, Gas Field Case*, in *Canadian International Petroleum Conference/SPE Gas Technology Symposium 2008 Joint Conference*. 2008, Petroleum Society of Canada: Alberta, Canada.
7. Emiliani, C.N., et al., *Improved Sand Management Strategy: Testing of Sand Monitors under Controlled Conditions*. 2011, Society of Petroleum Engineers.
8. Benipal, N., *Sand Control and Manangement - Development of a Sand Control Strategy*. 2004, The University of Texas at Austin.
9. Mansouri, A., *A Combined CFD-Experimental Method for Developing an Erosion Equation for Both Gas-Sand and Liquid-Sand Flows*, in *Mechanical Engineering*. 2016, The University of Tulsa.
10. Syltøy, C., *New generation expandable sand screens*. 2014, University of Stavanger, Norway.
11. Gang, W., et al., *Vibration Sensor Approaches for the Monitoring of Sand Production in Bohai Bay.* Journal of Shock and Vibration, 2015: p. 1-16.
12. Burke, C., *Why acoustic sand detectors don't work*, in *6th European Sand management forum*. 2014.
13. Avent, M., *Investigation into Sand Deposition and Transportation in Multiphase Pipelines – Phase 2*. 2012, CEED: CEED Seminar Proceedings 2012.
14. Ranjith, P.G., et al., *Sand production during the extrusion of hydrocarbons from geological formations: A review.* Journal of Petroleum Science and Engineering, 2014. **124**: p. 72-82.
15. Carlson, J., D. Gurley, and G. King, *Sand Control: Why and How.* Oilfield Review, 1993. **4**(4): p. 41-53.
16. Ahad, N.A., M. Jami, and S. Tyson, *A review of experimental studies on sand screen selection for unconsolidated sandstone reservoirs.* Journal of Petroleum Exploration and Production Technology, 2020. **10**(4): p. 1675-1688.
17. Perrier, S. and L. Martins, *Subsea Sand Detection in Digital Oil Age: Case Study of An Innovative Virtual Erosion Probe Technique*, in *SPE annual technical conference*. 2017, Society of Petroleum Engineers: San Antonio, Texas, USA.
18. Fucheng, D., et al., *Simulation Research on the Erosion of Slotted Screen for the Unconsolidated Sand Formation.* Arabian Journal for Science and Engineering, 2014. **39**(6): p. 5237-5243.

19. Ruslan, M. and P.Y. Lee, *Integrated Approach to Sand Management in Matured Field Operations*, in *SPE European Formation Damage Conference*. 2015, Society of Petroleum Engineers: Budapest. Hungary.
20. Tiffin, D.L., M.H. Stein, and X. Wang, *Drawdown Guidelines for Sand Control Completions*, in *SPE annual technical conference*. 2003, Society of Petroleum Engineers: Colorado, USA.
21. Hedges, B., *A Comparison of Monitoring Techniques for Improved Erosion Control: a Field Study*, in *Corrosion 2004 conference*. 2004: New Orleans, USA.
22. Dees, J.M. and P.J. Handren, *A New Method of Overbalanced Perforating and Surging of Resin for Sand Control.* Journal of Petroleum Technology, 1994.
23. Mohyaldinn, M.E., R. Hamzah, and M.C. Ismail, *Prediction of Sand Erosion in Elbows and Tees Using Direct Impingement Model*, in *NACE Asia Pacific Conference*. 2009: Kuala Lumpur, Malaysia.
24. Sukotrihadiyono, T., et al., *Sand Control and Gas Well Production Optimisation in a Multilayer Reservoir Gas Field*, in *SPE Asia Pacific Oil & Gas Conference*. 2013, Society of Petroleum Engineers: Jakarta, Indonesia.
25. Zainal Abidin, S.A., Z. Harun, and A. Jothy, *Effective Slug Handling and Sand Separation Using Innovative Separator System*, in *Offshore Technology Conference Asia*. 2014: Kuala Lumpur, Malaysia.
26. Matanovic, D., M. Cikes, and B. Moslavac, *Sand Control in Well Construction and Operation*. 2012, Berlin, Heidelberg: Springer Berlin Heidelberg.
27. Ben Mahmud, H., V.H. Leong, and Y. Lestariono, *Sand production: A smart control framework for risk mitigation.* Petroleum, 2019.
28. Kalgaonkar, R., et al., *New Advancements in Mitigating Sand Production in Unconsolidated Formations*, in *SPE Kingdom of Saudi Arabia Annual Technical Symposium and Exhibition*. 2017, Society of Petroleum Engineers: Dammam, Saudi Arabia. p. 11.
29. Stein, M.H., et al., *Integrated Sand and Erosion Alarming on NaKika, Deepwater Gulf of Mexico*, in *SPE Annual Technical Conference and Exhibition*. 2005, Society of Petroleum Engineers: Dallas, Texas.
30. Andrews, J., H. Kjorholt, and H. Joranson, *Production enhancement from sand management philosophy. A Case Study from Statfjord and Gullfaks*. 2005.
31. Al-Lababidi, S., W. Yan, and H. Yeung, *Sand Transportations and Deposition Characteristics in Multiphase Flows in Pipelines.* Journal of Energy Resources Technology, 2012. **134**(3): p. 034501.
32. Selfridge, F., et al., *Safely Improving Production Performance through Improved Sand Management*, in *Offshore Europe*. 2003, Society of Petroleum Engineers: Aberdeen, United Kingdom.
33. Salama, M.M., *Sand Production Management*, in *Offshore Technology Conference*. 1998, Offshore Technology Conference: Houston, Texas.
34. Oyeneyin, B., *Introduction to Sand and Condition Monitoring Strategies for Asset Integrity*. Developments in Petroleum Science: Integrated Sand Management For Effective Hydrocarbon Flow Assurance. Vol. 63. 2015. 173-189.
35. Gao, D., Nouri,, et al., *Sand rate model and data processing method for non-intrusive ultrasonic sand monitoring in flow pipeline.* Journal of Petroleum Science and Engineering, 2015. **134**(Supplement C): p. 30-39.
36. Nabipour, A., et al., *Methods for Measurement of Solid Particles in Hydrocarbon Flow Streams*, in *SPE Asia Pacific Oil and Gas Conference*. 2012, Society of Petroleum Engineers: Perth, Australia.

37. Briongos, J.V., et al., *Characterization of flow-induced vibrations in gas–solid fluidized beds: Elements of the theory.* Chemical Engineering Science, 2013. **93**(C): p. 181-196.
38. Barton, *Erosion in elbows in hydrocarbon production systems: Review document*, T.N. Limited, Editor. 2003: Glasgow, UK.
39. Haugen, S., et al. *Clamp on ultrasonic instruments in subsea applications*. in *Offshore Technology Conference*. 1995. Houston, USA.
40. Emiliani, C.N., et al., *Improved Sand Management Strategy: Testing of Sand Monitors under Controlled Conditions*, in *SPE Annual Technical Conference*. 2011, Society of Petroleum Engineers: Denver, USA.
41. Sampson, M., B.S. McLaury, and S.A. Shirazi, *A Method for Relating Acoustic Sand Monitor Output to Sand Rate and Particle Kinetic Energy*, in *CORROSION 2002*. 2002: Denver, USA.
42. Salama, M.M., *Performance of sand monitors*, in *Corrosion 2000*. 2000: Orlando, USA.
43. Odigie, M., et al., *Acoustic Monitor Threshold Limits for Sand Detection in Multiphase Flow Production System*, in *SPE International Conference and Exhibition on Oilfield Corrosion*. 2012, Society of Petroleum Engineers: Aberdeen, UK.
44. Time, W., *Improved pulsed broadband ultrasonic spectroscopy for analysis of liquid-particle flow.* Applied Acoustics, 2011. **72**: p. 324–335.
45. Braaten, N.A., et al., *Field Experience with a Subsea Erosion Based Sand Monitoring System*. 1996, Society of Petroleum Engineers.
46. Nabipour, A., et al., *Methods for Measurement of Solid Particles in Hydrocarbon Flow Streams*. 2012, Society of Petroleum Engineers.
47. Fan, C., B.S. McLaury, and S.A. Shirazi, *Evaluation of Electrical Resistance Probes To Detect Pipeline Erosion and Sand Production in Low Liquid Loading Flow Conditions*, in *SPE Eastern Regional Meeting*. 2011, Society of Petroleum Engineers: Columbus, USA.
48. Leong, M. and A. Sanchis, *Intrusive erosion Probes on Subsea Equipment - Design and Placement Considerations*, in *Offshore Technology Conference*. 2016: Kuala Lumpur, Malaysia.
49. Kesana, N.R., et al., *Effect of Particle Size and Liquid Viscosity on Erosion in Annular and Slug Flow.* Journal of Energy Resources Technology, 2014. **136**(1): p. 012901.
50. Han, G., et al., *A Comprehensive Study of Sanding Rate From Gas Field From Reservoir, Completion, Production, to Surface Facilities*, in *2009 Annual Technical Conference*. 2009, Society of Petroleum Engineers: New Orleans, Louisiana, USA.
51. Shirazi, S.A., B.S. McLaury, and M.M. Ali, *Sand Monitor Evaluation in Multiphase Flow*, in *Corrosion 2000*. 2000: Orlando, USA.
52. Bakku, S.K., et al., *Vertical Seismic Profiling Using Distributed Acoustic Sensing in a Hydrofrac Treatment Well*. 2014, Society of Exploration Geophysicists.
53. Thiruvenkatanathan, P., et al., *Downhole Sand Ingress Detection Using Fibre-Optic Distributed Acoustic Sensors*. 2016, Society of Petroleum Engineers.
54. Cannon, R.T. and F. Aminzadeh, *Distributed Acoustic Sensing: State of the Art*, in *SPE Digital Energy Conference* 2013, Society of Petroleum Engineers: Woodlands, USA.
55. Denney, D., *Distributed Acoustic Sensing for Hydraulic- Fracturing Monitoring and Diagnostics.* Journal of Petroleum Technology, 2012.
56. Carpenter, C., *Distributed Acoustic Sensing for Downhole Production and Injection Profiling.* Journal of Petroleum Technology, 2016.
57. Mullens, S., G. Lees, and G. Duvivier, *Fiber-Optic Distributed Vibration Sensing Provides Technique for Detecting Sand Production*, in *Offshore Technology Conference*. 2010: Texas, USA.

58. Thiruvenkatanathan, P., et al., *Downhole Sand Ingress Detection Using Fibre-Optic Distributed Acoustic Sensors*, in *Abu Dhabi International Petroleum Exhibition & Conference*. 2016, Society of Petroleum Engineers: Abu Dhabi, UAE.

59. Paleja, R., et al., *Velocity Tracking for Flow Monitoring and Production Profiling Using Distributed Acoustic Sensing*, in *SPE Annual Technical Conference and Exhibition*. 2015, Society of Petroleum Engineers: Houston, USA.

60. Allanic, C., et al., *Distributed Acoustic Sensing For ESP Understanding And Surveillance*, in *SPE Middle East Intelligent Energy Conference*. 2013, Society of Petroleum Engineers: Dubai, UAE.

61. van der Horst, J., et al., *Fibre Optic Sensing for Improved Wellbore Surveillance*, in *International Petroleum Technology Conference*. 2013, International Petroleum Technology Conference: Beijing, China.

62. Patni, S. and D. Dria, *In-well monitoring for Deepwater Wells - Operator's View*, in *Offshore Technology Conference*. 2014, Offshore Technology Conference: Houston, USA.

63. Gardner, N., F. Hveding, and R. Sambrook, *Technology Update: Distributed Fiber-Optic Technologies Drive New Intervention Applications.* Journal of Petroleum Technology, 2015.

64. Siebenaler, S., et al., *Evaluation of Distributed Acoustic Sensing Leak Detection Technology for Offshore Pipelines*, in *The Twenty-fifth International Ocean and Polar Engineering Conference*. 2015, International Society of Offshore and Polar Engineers: Kona, USA.

65. Bertola, V.e. and SpringerLink, *Modelling and Experimentation in Two-Phase Flow / edited by Volfango Bertola*. 2003: Vienna : Springer Vienna : Imprint: Springer.

66. Warnken, D., et al., *Sand Management in Tangguh Big Gas Wells*. 2013, Society of Petroleum Engineers.

67. Brown, G.K., *External Acoustic Sensors and Instruments for the Detection of Sand in Oil and Gas Wells*, in *Offshore Technology Conference*. 1997: Houston. USA.

68. Balgobin, C.J., *Sand Management of Ultra-High-Rate Gas Wells*, in *SPE Latin American and Caribbean Petroleum Engineering Conference*. 2005, Society of Petroleum Engineers: Rio de Janeiro, Brazil. p. 7.

69. Stein, N., A.S. Odeh, and L.G. Jones, *Estimating Maximum Sand-Free Production Rates From Friable Sands for Different Well Completion Geometries.* Journal of Petroleum Technology, 1974. **26**(10): p. 1156-1158.

70. Kinsler, L., et al., *Fundamentals of Acoustics*. Fundamentals of Acoustics. 1999: John Wiley & Sons.

71. Boyd, J.W.R. and J. Varley, *The uses of passive measurement of acoustic emissions from chemical engineering processes.* Chem. Eng. Sci., 2001. **56**: p. 1749.

72. Asher, R.C., *Ultrasonic sensors for chemical and process plant*. Ultrasonic sensors. 1997.

73. Sinclair, A.N. and R. Malkin, *Sensors for Ultrasonic NDT in Harsh Environments*. 2020: MDPI - Multidisciplinary Digital Publishing Institute.

74. Instrument, T., *Ultrasonic Sensing Basics*. 2020.

75. Wang, K., et al., *Non-intrusive characterization of sand particles dispersed in gas–water bubbly flow using straight and bent pipes with vibration sensing.* Powder Technology, 2019. **344**: p. 598-610.

76. Kumar, B.P., *Digital Signal Processing Laboratory*. 2016.

77. Wang, Y., S. Ji, and H. Xu, *Non-stationary Signals Processing Based on STFT*. 2007. p. 3-301-3-304.

78. Polikar, R., *The Wavelet Tutorial.* 2006.

79. Burt, P. and E. Adelson, *The Laplacian Pyramid as a Compact Image Code.* IEEE Transactions on Communications, 1983. **31**(4): p. 532-540.

80. Shukla, K.K., *Efficient Algorithms for Discrete Wavelet Transform : With Applications to Denoising and Fuzzy Inference Systems*. 2013, London: Springer London.
81. Brandt, A., *Noise and Vibration Analysis: Signal Analysis and Experimental Procedures*. 1. Aufl. ed. 2011, Bognor Regis: Bognor Regis: Wiley.
82. M., O. and S. Jr., *PSD computation using Welch's method*. 1991.
83. Suhnat, E., *New solution: Operational Field Control of Pipelines Corrosion Rate*, in *SPE Russian Oil and Gas Conference and Exhibition*. 2010, Society of Petroleum Engineers: Moscow, Russia. p. 3.
84. Ibrahim, M. and T. Haugsdal, *Optimum Procedures for Calibrating Acoustic Sand Detector, Gas Field Case*. 2008, Petroleum Society of Canada.
85. Seraj, H. and B. Evans, *Improving sand flow rate measurement of commercial ASDs and comparison with ultrasonic spectral analysis and filtering.* IET Science, Measurement & Technology, 2020. **14**(9): p. 746-752.
86. *Ultrasonic Transducers for Nondestructive Testing*. Available from: https://www.olympus-ims.com/en/ultrasonic-transducers/contact-transducers/.
87. *SPECIFICATIONS PXI-5922*. Available from: http://www.ni.com/pdf/manuals/374033b.pdf.
88. Stamps, D., *Learn Labview 2013/2014 Fast: A Primer for Automatic Data Acquisition*. 2015: SDC Publications.
89. Nazarchuk, Z., V. Skalskyi, and O. Serhiyenko, *Acoustic Emission, Methodology and Application*. 2017, Cham, Germany: Springer.
90. Parker, M., *Digital Signal Processing, Everything you need to know to get started*. 2017: Elsevier.
91. Candan, Ç. and H. Inan, *A unified framework for derivation and implementation of Savitzky–Golay filters.* Signal Processing, 2014. **104**: p. 203-211.
92. *What Is a Savitzky-Golay Filter? [Lecture Notes].* IEEE Signal Processing Magazine, 2011. **28**(4).
93. Acharya, D., et al., *Application of adaptive Savitzky–Golay filter for EEG signal processing.* Perspectives in Science, 2016. **8**: p. 677-679.
94. Haldipur, P. and G.D. Metcalf, *Virtual Metering Technology Field Experience Examples*, in *Offshore Technology Conference*. 2008, Offshore Technology Conference: Houston, Texas, USA. p. 23.
95. Petukhov, A.Y., et al., *Virtual Metering System Application in the Ceiba Field, Offshore Equatorial Guinea*, in *SPE Digital Energy Conference and Exhibition*. 2011, Society of Petroleum Engineers: The Woodlands, Texas, USA. p. 21.
96. Cohen, M.X., *A better way to define and describe Morlet wavelets for time-frequency analysis.* NeuroImage, 2019. **199**: p. 81-86.
97. Addison, P.S.A., *The illustrated wavelet transform handbook : introductory theory and applications in science, engineering, medicine, and finance*. 2002: Institute of Physics Pub.
98. Welch, P., *The use of fast Fourier transform for the estimation of power spectra: A method based on time averaging over short, modified periodograms.* IEEE Transactions on Audio and Electroacoustics, 1967. **15**(2): p. 70-73.
99. Seraj, H., B. Evans, and M. Sarmadivaleh, *Improving sand flow rate measurement using the wavelet transform and ultrasonic sensors.* International Journal on Smart Sensing and Intelligent Systems, 2021. **14**: p. 1-13.